SYNTHESIS, CHARACTERIZATION AND MODIFICATION OF QUANTUM DOTS FOR ANALYTICAL AND BIOMEDICAL APPLICATIONS

THESIS

SUBMITTED TO

BABASAHEB BHIMRAO AMBEDKAR UNIVERSITY

(A CENTRAL UNIVERSITY)

LUCKNOW

BABASAHEB
BHIMRAO
AMBEDKAR
UNIVERSITY

LUCKNOW

प्रज्ञा शील करूणा

ESTABLISHED 1996

FOR THE DEGREE OF

Doctor of Philosophy

IN

APPLIED CHEMISTRY

Submitted by

VIVEK PANDEY

ENROLMENT NUMBER 857/12

CO-SUPERVISOR

Dr. MOHANA KRISHNA REDDY MUDIAM

Principal Scientist, Analytical Chemistry
Laboratory & Scientist Incharge,
Pesticide Toxicology Laboratory
Regulatory Toxicology Group
CSIR-Indian Institute of Toxicology
Research Lucknow- 226001, INDIA.

SUPERVISOR

Dr. GAJANAN PANDEY

Associate Professor & Head,
Department of Applied Chemistry
School for Physical Sciences
Babasaheb Bhimrao Ambedkar University
Lucknow, 226025, INDIA.

2015

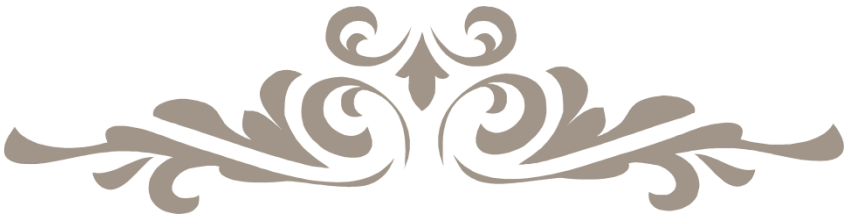

Dedicated to my

Father

& Mentor

BABASAHEB BHIMRAO AMBEDKAR UNIVERSITY
LUCKNOW
प्रज्ञा शील करुणा
ESTABLISHED 1996

बाबासाहेब भीमराव अम्बेडकर विश्वविद्यालय
विद्या विहार, रायबरेली रोड, लखनऊ–226 025
Babasaheb Bhimrao Ambedkar University
(A Central University)
Vidya Vihar, Raebareli Road, Lucknow-226 025

Letter No. .....
Date .....

Gajanan Pandey, Ph.D.,
Associate Professor & Head
Department of Applied Chemistry
E-mail: pandeygajanan26@gmail.com

October 30, 2015

CERTIFICATE

This is to certify that the thesis entitled ""**Synthesis, Characterization and Modification of Quantum Dots for Analytical and Biomedical Applications"** submitted to **Department of Applied Chemistry, Babasaheb Bhimrao Ambedkar University, Lucknow**, in fulfillment of the requirements for the award of degree of **Doctor of Philosophy in Applied Chemistry** embodies the original research work carried out by **Mr. Vivek Pandey** under my supervision and has not been submitted in part or full for any degree or diploma to any other University. It is further certified that the scholar fulfils all the requirements as laid down by the University for the purpose of submission of Ph.D. thesis.

(Gajanan Pandey)

Mohana Krishna Reddy Mudiam, Ph.D.,
Principal Scientist, Analytical Chemistry Laboratory,
Scientist-Incharge, Pesticide Toxicology Laboratory,
Academic Editor, PLOSONE
Co-coordinator, AcSIR (Chemical Sciences)@CSIR-IITR
E-mail: mohanitrc@hotmail.com; mohanitrc@gmail.com

October 27, 2015

CERTIFICATE

This is to certify that the thesis entitled ""**Synthesis, Characterization and Modification of Quantum Dots for Analytical and Biomedical Applications"** submitted to **Department of Applied Chemistry, Babasaheb Bhimrao Ambedkar University, Lucknow**, in fulfillment of the requirements for the award of degree of **Doctor of Philosophy in Applied Chemistry** embodies the original research work carried out by **Mr. Vivek Pandey** under my co-supervision and has not been submitted in part or full for any degree or diploma to any other University. It is further certified that the scholar fulfils all the requirements as laid down by the University for the purpose of submission of Ph.D. thesis.

(Mohana Krishna Reddy Mudiam)

DECLARATION

I hereby declare that this thesis entitled *"**Synthesis, Characterization and Modification of Quantum Dots for Analytical and Biomedical Applications**"* is my own work carried out by me under the supervision of **Dr. Gajanan Pandey**, Associate Professor and Head, Department of Applied Chemistry, Babasaheb Bhimrao Ambedkar University, Lucknow and co-supervision of **Dr. Mohana Krishna Reddy Mudiam**, Principal Scientist, Analytical Chemistry Laboratory & *Scientist- Incharge*, Pesticide Toxicology Laboratory, CSIR –Indian Institute of Toxicology Research, Lucknow. The work done in this regard is for the fulfillment of requirements with respect to Doctor of Philosophy degree. Here in any part of this work has not been submitted for any other degree of this or any other university or institution.

Date: Vivek Pandey, M.Sc.,

COPYRIGHT STATEMENT

Vivek Pandey, M.Sc.

Mohana Krishna Reddy Mudiam , Ph.D.,
(Co-Supervisor)

Dr. Gajanan Pandey, Ph.D.
(Supervisor)

Acknowledgement

It has been a long journey to finally reach the destination I aspired. I owe special thanks to my supervisors Dr. Mohana Krishna Reddy Mudiam, Principal Scientist, CSIR-Indian Institute of Toxicology Research, Lucknow and Dr. Gajanan Pandey, Associate Professor and Head, Department of Applied Chemistry, Babasaheb Bhimrao Ambedkar University, Lucknow without whom this arduous journey could not be possible. They always have been a great scientific advisors and mentors who supported me at every stage during the research.

I would like to pay my sincere thanks to The Vice-Chancellor of BBAU, Lucknow and Prof. Alok Dhawan, Director, CSIR-IITR, Lucknow for their sustained interest in my work and helped in providing the facilities to carry out my research work.

I would also like to express my appreciation and thanks to the members of Department of Applied Chemistry, Babasaheb Bhimrao Ambedkar University: Dr. Kaman Singh, Dr. Jyoti Pandey and Dr. Sailesh Kumar.

There always has been a significant support from the members of CSIR-IITR family viz., Drs. Devendra Parmar, VK Khanna, Prof. Ram Chandra, A.B Pant, R.C. Murthy, D.K. Patel, S.K. Patnaik, Rakesh Kuma, Mr. Pramod Kumar Srivastava, Mr. Satgur Prasad, Mr. Ramesh, Mr. G.N.V. Satyanarayana, Mr.Ajay and Mr. Shukla Ji throughout my work in the lab.

I also thank to Dr.LKS Chauhan, Dr. PN Saxena and Mr. Sanjeev Kumar Singh for their warm technical support that has been the key for my experimental work and designing.

I can never forget the precious and touching moments I spend with few people: Vandana Pandey, Dr.Vinay Kr. Tripathi, Mr. Amit Kumar Singh, Mr. Yatindra Nath Shukla, Er. Nitesh Kr. Upadhyay, Ms Smita Panchal and Ms Tejasvi Bhatia. They have always been there throughout my journey and provided me the emotional and intellectual support whenever I needed. I will be indebted to them.

Many thanks also go to my lab members and colleagues, viz., Ch. Ratnasekhar, Abhishek Chauhan, Rajeev Jain, Manoj Kumar Gupta, Gaurav Pal, Pratibha Singh, Pathya Pandey, Ritu Singh, Ankita Asati, Anshuman Srivastava, Abhishek Singh, Sapna Yadav and Satyjeet Rai.

Above all I would like to thank my Parents for their blessings, inspirations and their support for making and creating me a good human being which always motivated me. A special thanks to God who provided the path from destiny to destination.

I am grateful to UGC, New Delhi for providing research fellowship at BBAU, Lucknow.

The financial support from INDEPTH (BSC0111) and NanoSHE (BSC0112) to carry out my research work at CSIR-IITR, Lucknow are greatly acknowledged.

I would like to dedicate my thesis to my father who inspired me to reach here and to my mentor Dr. Mohana Krishna Reddy Mudiam who nurtured my career in research.

Vivek Pandey, M.Sc.

ABSTRACT

Quantum Dots (QDs) has revolutionized the field of nanotechnology with its leap towards all branches of natural science. Synthesis of the quantum dots for various applications is need of modern day material chemist. Small size of the material which is in the range of 2-10 nm makes it biologically efficient by easy uptaking of the cells and the strong quantum confinement paves the way of tuning size with optical and electronic properties. Photostability of the material and low background noise due to large stokes shift has been explored to use the QDs for bioimaging and sensing applications. The biological applications of the material can only be done if it proves itself non-toxic while the sensing applications of the material depend on sensitivity and selectivity. Quenching of photoluminescence intensity of QDs by interaction of surface of the material with external environment is the best mechanical property to obtain optical signal. These materials hence must be functionalized at surfaces to explore them for tailor made applications Thus prior to obtain the applications of QDs a lot of material pre-treatment at surface is needed which can be possible during synthesis by surface modification of the nanoparticle. These assumptions and hypothesis form the basis of this research work.

Metal chalcogenides are extensively studied and performed in the thesis. Manganese doped Zinc Sulphide crystal lattice is synthesized and modifications of the lattice at surface has been used to investigate optical and biological properties. Green synthetic approach was utilized to synthesize the Mn doped QDs at room temperature. Nucleation controlled synthesis was done at room temperature while Ostwald growth was controlled by suitable capping agent. The capping agents have thiol group (L-cysteine and MPTS) which binds specifically with the zinc metal ion. Imidazole as donor ligand has been developed as novel capping agent in the thesis

which has Nitrogen as binding site with metal ion. Low temperature and water as solvent employed in the synthesis has been a potent green synthetic route of nanoparticle synthesis. The synthesized QD was characterized by SEM for surface morphology, TEM for size determination and the crystal lattice was studied by XRD for composition and size calculations. The Braggs equation and Scherer calculation was derived to obtain the precise size of the synthesized material. The luminescence properties of the QDs were studied by PL spectrophotometer and UV Spectrometer. The band gap and excitation wavelength was calculated from the UV spectra.

The analytical applications of the QDs were done by fabricating the surface through imprinted polymer and surface defects. The optical properties were explored to develop optical sensors. In subsequent chapters, the sensing ability of Mn doped ZnS by surface modifications with molecularly imprinted polymer (MIP) has been explored for target analyte as 3-phenoxy benzoic acid (urinary metabolite for synthetic pyrethroids) and by creation of surface defects for methyl mercury (an organic form of mercury). The QD-MIP for 3-PBA was formed by imprinted polymers with aminopropyl trimethoxysilane (APTES) as monomer on Mn doped ZnS QDs. The methyl mercury based sensor was developed by creating defects on the QD surface through enriched sulphur. The defect decreases on binding the analyte to the synthesized Mn doped ZnS crystal lattice, as a result of this increase in intensity occurs with increase in concentration of the methyl mercury. The studies shown that, the surface modification not only improves optical sensitivity but also enhances the selectivity towards a desired analyte.

In subsequent later chapters biomedical applications of QDs were performed. The orange emission of the manganese doped zinc sulphide QDs has potential of non-invasive imaging applications. As part of biomedical applications imaging of the cells

by QD have been studied. The biological applications of nanoparticle are dependent on the toxicological tests. Here in various toxicity assessments have been done to evaluate and find the suitability of the material in biological environment of the cells. L-Cysteine and imidazole as capping agents lowers the toxicity of the QDs upto many fold. The toxicity evaluation of the as synthesized manganese doped zinc sulphide QDs is performed by *in-vitro* method.

Neuronal cell lines and human lung cell lines are used for uptaking the nanoparticles. The in-vitro toxicity assessment was performed by checking cell viability through MTT and NRU assays. The other parameters like oxidative degradation of lipids (LPO), reactive oxygen species, Lactate dehydrogenase activity, Glutathione, Oxidative stress and catalase assay was performed to determine oxidative stress in the cells by the entrance of QD in the cell. Genetic toxicology was performed by analysis of chromosomal aberration and micronucleus test. Through these analysis we can predict the biocompatibity of the as synthesized quantum dots and the usage of these materials in biomedical applications. The L-Cysteine and imidazole as capping has been used to synthesize small sized quantum dots and also to reduce toxicity. Both of the capping agents were tested with QD for its bio-applicability. The L-cysteine capped QD has shown toxicity above 1500 ppm and the as synthesized QD capped with L-Cysteine was also used as imaging probe. The red luminescence and its bright field contrast image confirm that QD has been uptake by cells without rupturing the cell membrane. The antioxidant property of L-cysteine was the key for its reduction in toxicity up to higher concentration. L-cysteine being a biomolecule which can be further functionalized for targeted applications as well. Imidazole capped Mn doped ZnS QDs were also prepared and passed through cytotoxic assessment. The toxicity at cellular, molecular and genetic level was done for

imidazole capped QDs. It was found that the synthesized Imidazole capped QD was non toxic upto 1000 ppm. Hence water soluble non-toxic Mn doped QDs was synthesized by various capping agents has shown that the synthesized QDs are biocompatible and can be used in biomedical sciences. Thus biomedical applications of the QDs were studied by toxicity assessment and imaging methods.

Table of contents

LIST OF ABBREVIATIONS

Abbreviation	Full form
$ZnSO_4.7H_2O$	Zinc sulphate heptahydrate
2, 5 DHBA	2,5-Dihydroxybenzoic acid
3-PBA	3-Phenoxybenzoic acid
4-VP	4-Vinylpyridine
AIBN	Azobis Iso Butyro Nitirile
APTES	3-Aminopropyl triethoxysilane
CA	Chromosomal Assay
CAT	Catalase level
DMSO	Dimethyl Sulphoxide
DVB	Divinylbenzene
EGDMA	Ethylene Glycol Dimethacrylate
FLD	Fluorescence detector
FM	Fluorescence microscope
FTIR	Fourier transformed infrared spectroscopy
FWHM	Full Width at Half Maximum
GC-MS-MS	Gas chromatography-tandem mass spectrometry
GC	Gas chromatography
GSH	Glutathione
HCHO	Formaldehyde
HPLC	High Performance Liquid Chromatography
IARC	International Agency for Research on Cancer
IPS	Injector port silylation
LC	L-Cysteine
LC-MS	Liquid chromatography-mass spectrometry
LDH	Lactate dehydrogenase
LOD	Limit of detection
LOQ	Limit of quantification
LPO	Lipid Peroxidation
MAA	Methacrylic acid
MIP	Molecularly Imprinted Polymer

MM	Methylmercury
MN	Micronucleus Assay
Mn:ZnS	Manganese doped zinc sulphide
$MnCl_2.4\ H_2O$	Manganese (II) chloride tetrahydrate
MPA	Mercapto propionic acid
MPTS	3-Mercaptopropyltriethoxysilane
MTT	3-(4, 5-dimethylthiazol-2-yl)-2, 5-diphenyl tetrazolium bromide)
$Na_2S.XH_2O$	Sodium sulphide
NIP	Non-imprinted Polymer
nMIP	Nano- molecularly imprinted polymer
NRU	Neutral Red Uptake
PBS	Phosphate buffer saline
PL	Photoluminescence
QD	Quantum dot
ROS	Reactive Oxygen Species
%RSD	Percent relative standard deviation
SEM	Scanning Electron Microscope
SH	Thiol group
SH-SY5Y	Human neuroblastoma cell line
t,t-MA	*t-t*-muconic acid
TEM	Transmission Electron Microscope
TEOS	Tetraethyl Ortho Silicate
THB	1, 2, 4-trihydroxybenxene
UBMs	Urinary Benzene Metabolites
UV	Ultra-violet spectrophotometer
XRD	X- Ray Diffraction
LC	Liquid chromatography
QD-MIP	Quantum dot-molecularly imprinted polymer
QD-NIP	Quantum dot-non imprinted polymer
ZnS	Zinc Sulphide
R^2	Regression coefficient

LIST OF FIGURES

LIST OF TABLES

Chapter-1

Chapter-1

Introduction

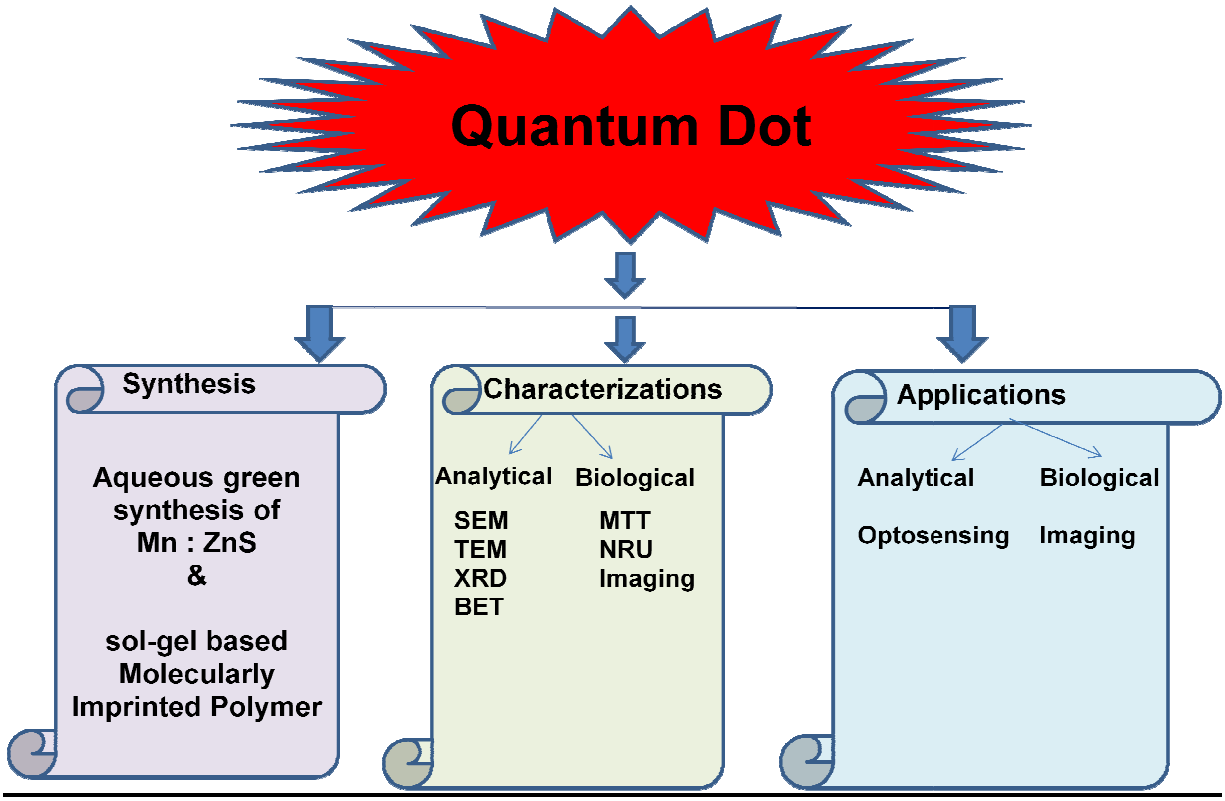

1.1. Background

In the beginning of twentieth century as part of his doctoral thesis the great scientist Albert Einstein using diffusion techniques [*Einstein et al 1905*] measured the size of a sugar molecule and found it to be 1 nm in diameter. The size of an H atom is about 0.1 nm in diameter thus it makes sense for chemists to think on the nanoscale which is nothing but atomic or molecular scale. Later in 1959 the statement of Feynman "there is plenty of room in bottom" made the researchers to think about exploring new area of science called nanoscience. The particles that have their size in the range of 1-100 nm along any dimension or axis is called nanoparticles. The most significant aspects of such particles is having a larger surface area to volume ratio than larger particles. The large surface to volume ratio of these nanoparticles affects the interaction of them to each other and with other particles as well. In general, it is calculated that, a 10 nm nanoparticle has about 15% of atoms on their surface while for bulk solids have only about 1% of atoms at the surface [*L.E Smart CRC Press*]. Since particles of nano dimension consist of very few number of particles so the energy level associated with each particle is very much similar to an individual atoms. This makes these materials to show strong quantization and hence follow principles of quantum mechanics. Application of quantum mechanical principles leads to the understanding of interaction of these particles with light and electromagnetism. The electronic energy level of these particles is like the arrangement of electrons in an atom which affects the conductivity and other optical properties that evolves due to the interaction with light. Royal society has defined Nanoscience as the study of phenomenon and manipulation of materials at atomic, molecular and macromolecular scales, where properties differ significantly from

those at larger scales. Various applications of nanotechnology has been obtained till date. Recently this technology at nano scale has been used for energy storage, drug delivery and sensor development. The nano size will enhance certain properties of the nano material like surface to volume ratio, quantized energy level and increased thermodynamic properties is the key for their success. The application in all fields of science *viz*. physics, medicine, chemistry and technology gives an example of interdisciplinary research in this area. The basic knowledge of physics, chemistry and biology is required to deal with nanoscience. Thus, this innovative area of science will be the key for emergence of combining multidisciplinary academics. Nanoparticles can be organic or inorganic, examples, include fullerenes [*Herald Kroto et al. 1985*], Bucky balls, carbon nanotube [*SumioLijima et al. 1991*], liposomes [*AD Bangham et al 1961*], nanoshells, dendrimers, supermagnetic gold, silver nanoparticles and quantum dots etc. A nano-crystal of a semiconductor having size in the nano-range of 2-10 nm and having only 10^2-10^4 atoms is called quantum dot. Metal nanoparticles of size 2-10 nm has evolved a highly profound material due to its size dependent property, dimensions similar to biological molecules like DNA, protein and some microorganisms. The ease of surface modification of these particles to form bioconjugates and nanohybrids make them potential area of research. The crystalline structure and forming colloidal solution in various dispersion medium add some more properties of surfaces.

Thus, the semiconductor nano crystallites arouse a smart material that can be tailor made for various applications in all major fields. These particles are not easy to synthesize due to indefinite and fast growth leading to a larger size. The physical property of these particles as electronic energy level, magnetic property, optical and

mechanical property are more promising than their chemical composition (*Alivisatos et al 2005*). The chemistry of these particles is only important for their synthesis. Broadly three factors govern the synthesis of such small nanocrystallite. Firstly the precursors, secondly the surfactant and thirdly the temperature (*Bawendi et al 1992*). Optical property of these materials is highly useful for biological and analytical applications. As now-a-days most of the sensors and imaging probes are made of quantum dots. The photo stability, nonbleaching property, external quenching, tunable optical property is the most recognizable characteristics of QDs which make them excellent material for sensor and imaging probes.

1.2.1 Theory and Principles: Consequences of the nanoscales

a. Effect on nanoparticle morphology

A diverse morphology of nanoparticles has been obtained based on their growth. These morphologies have been explored a lot for significant applications. Generally nanowires, nanorods, nanoflowers and nanobrushes have been synthesized based on growth mechanism of the material. Although there are many factors that contribute such specific morphology but surfactant controlled morphology have been routinely done.

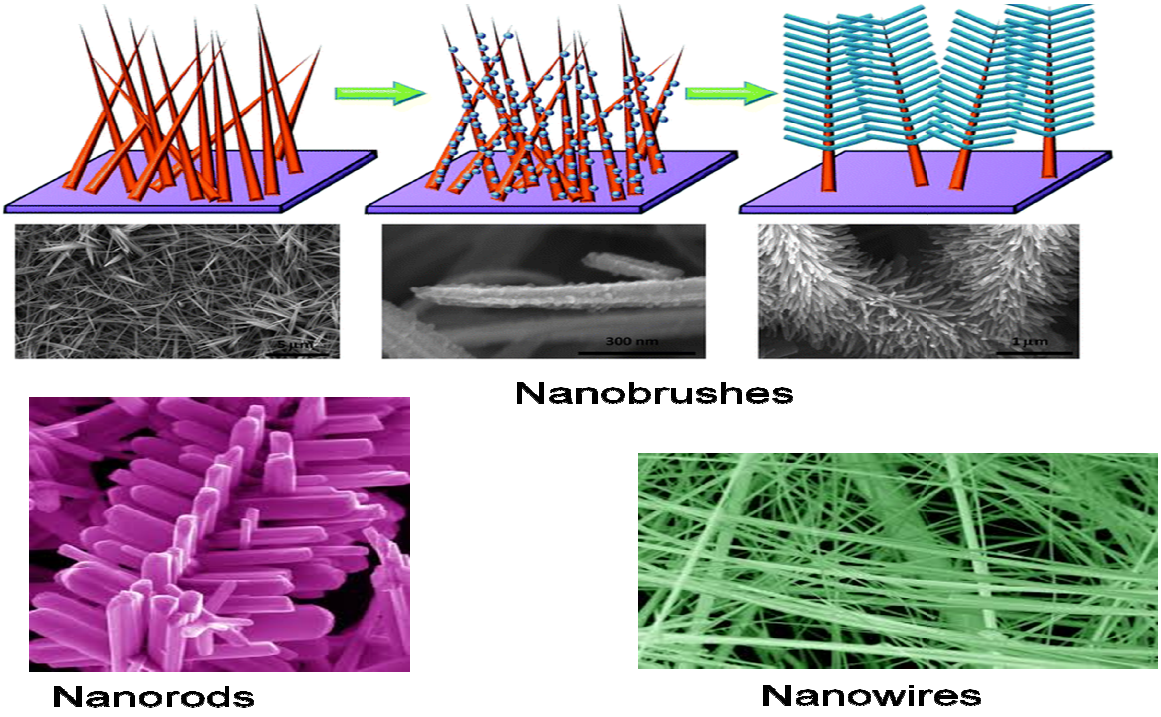

Fig-1.2: Various morphology of nanoparticles (Figure adapted from http://www.buffalo.edu/news/releases/2012/09/13667.html, http://approach.rpi.edu/2009/05/05/1-%C3%97-103-words-branched-nanorods/)

b. Effect on electronic structure:

Energy levels of crystals of larger size say micrometer range is of higher order thus there is small gap in between them. Due to the small energy gap in the orbital energy level the bulk crystals can be treated as infinite solids with continuous bands of allowed energy. Thus the bulk material has continuous energy level which seems to be unfavourable for quantum mechanical treatment. In nanoparticles, the energy levels are of lower order which makes these material having discontinuous energy and hence quantization of energy is easily observable similar to atoms and molecules. Thus, all the postulates of quantum mechanics can deal with nanoparticles having quantized energy level.

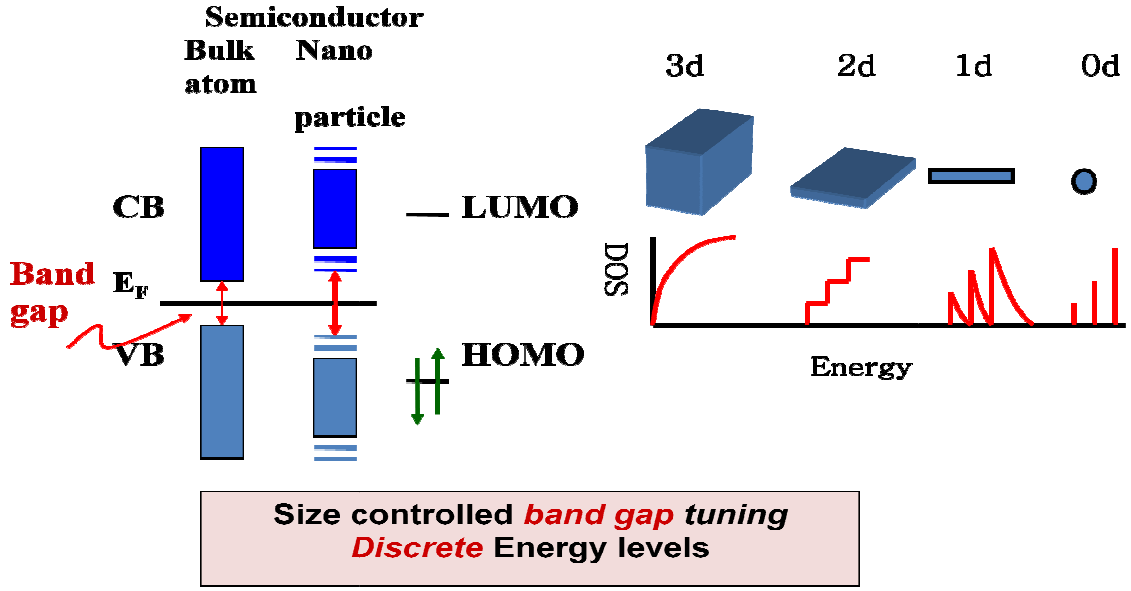

Fig- 1.3: Electronic energy level of semiconductor (adapted from Alivisatos (1996)

Band gap measurement is the difference between valence band and conduction band of the arrangement of energy level. In terms of molecular orbital theory it can be defined as difference between highest occupied energy level and lowest unoccupied energy level. The band diagram of semiconductor is shown in fig.1.3 which shows higher energy density in middle of each valence and conduction band while there is low orbital density of states at the top and bottom of the bands. Also for larger semiconductor crystal there is continuous energy level due to large number of atoms. Since, each energy level is considered as an orbital so only two electrons are possible for each energy level. When electronic transition occurs from valence band to conduction band conductivity in solids is observed. Although sufficient amount of energy is needed for such transitions. The difference between valence and conduction band is called band gap which is tabulated for some common materials in table-1.1 (Wikipedia)

Material	**Band Gap**	**Type of Band Gap**
CdS	2.42	Direct
CdSe	1.74	Direct
CdTe	1.49	Direct
ZnO	3.37	Direct
ZnS	3.54/3.91	Direct
ZnSe	2.7	Direct
ZnTe	2.25	Direct
Diamond	5.47	Indirect
Si	1.12	Indirect
Ge	0.67	Indirect

Semiconductors have middle order band gap, conductors have very low band gap while higher band gap is observed for insulators. When the size of crystal is smaller say in the range of nanosize then few atomic orbitals are available in the band region and hence discontinuous energy level is seen and quantization of energy is found similar to individual atoms and molecules. If we consider nano size crystal of a semiconductor then good agreement of the quantization is seen where variation in size of the particle changes the band energy as well, this phenomenon is called as quantum confinement effect. The smaller the particle is larger will the band gap due to very few atomic orbitals. The quantum confinement forms the basis of many tunable properties of the semiconductor nanocrystal with respect to size.

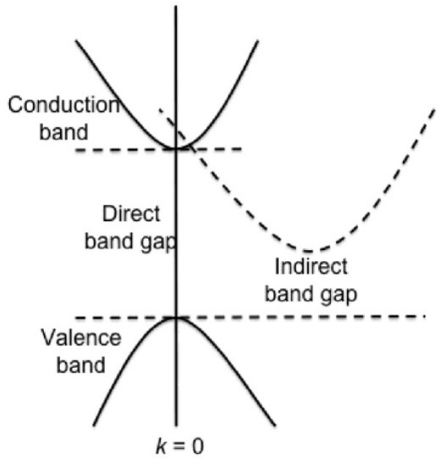

Fig-1.4 The band gap of crystals direct and indirect (Figure adapted from http://solarwiki.ucdavis.edu/The_Science_of_Solar/Solar_Basics/C._Semiconductors_and_Solar_Interactions/III._Absorption_of_Light_and_Generation/2._Direct_Semiconductors)

The nanoparticles can have nanometers dimension in any one axis or in all the three axis. The structures having nanodimension in one axis is called nanorods,quantum wells or thin fims. The structures with nanodimension in two axis is quantum wires while quantum dots have all the three spatial coordinates in nanoscale region. Density of states for all the diversified structures is depicted in Fig-1.4

The electrical conductivity in solids those which are not ionic conductors have dependency on band energy levels. Since the bands are highly quantized for nanoscale semiconductors the electric current seems to be quantized as well. Thus electric current increases step wise step and drops to zero when thermal energy is not sufficient to undergo further electronic transitions. The interaction of light with the atom results in transition of the atom to a higher energy level. The electron in atom only absorbs the photon when the wavelength of the light matches with the energy difference between the final and initial state. Also it requires some selection rules to be obeyed by the phenomenon.

Since photon has zero spin and one unit of angular momentum hence according to conservation of energy law the transition must have change spin as zero while angular momentum must have difference of 1 unit. The absorption and emission of radiation for continuous solids involve energy bands rather than atomic energy level. An electron in the valence band can undergo transition to conduction band only when both the levels have same vector k_i. In some solids the bottom of the conduction band and top of the valence band has same vector and hence this transition is allowed also called as direct band gap fig.1.4. Solids where the vectors are different for HOMO of valence band and LUMO of conduction band, transitions are not possible for top of the valence band and bottom of the conduction band. This type of transition is called as indirect band gap (Fig1.4)

1.2.2 Theory and principles: Quantum confinement

When the size of the bulk inorganic crystalline solid is in the range of 2-10 nm interesting property is found. Semiconductors having all the three dimensions in the range 1-10 nm is called quantum dot or semiconductor nanocrystals. When light of energy greater than the band gap is irradiated to the particle an electron will be promoted from lower valence band to higher conduction band. This process creates a hole in the valence band also called as exciton. Most of the semiconductors have the separation between electron and its hole as 1-10 nm range. Thus, when exciton is created in the particle of size of 1- 10 nm, the physical dimensions of the system confines the exciton in a manner similar to particle in a box. This leads to application of quantum mechanical principle of particle in a box. The energy of an electron in particle in box is described as:

$E = n^2 h^2/8\ m\ a^2$. Where

E is the energy of the particle

n is principal quantum number

h is Planks constant

m is mass of the particle in the box

a is size of the box.

Hence according to the principle of quantum mechanics, the energy of a particle following the particle in a box model is inversely proportional to the size of the box. Thus

as the size decreases, the energy difference and energy level increases resulting in various number of discrete energy levels. This results in different types of emissions for same chemical composition but with different size. The phenomenon is called quantum confinement. The quantum confinement is highly exploited for sensors development and imaging probe. The band gap of the material increases due to discrete energy levels as the size of the particle becomes smaller. Thus, one can tune the band gap and energy levels of particle by tuning the size of the material. This can be easily explained in fig.1.5.

$$\Delta E = \frac{n^2 h^2}{8ma^2}$$

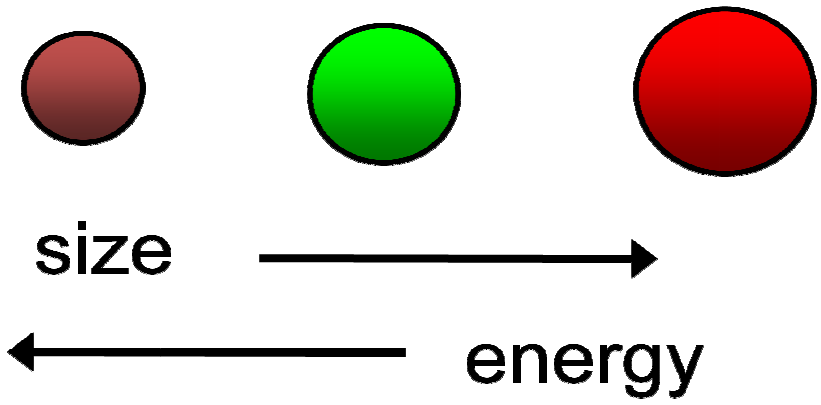

Fig-1.5 Quantum confinement effect (Figure adapted from www.elecintro.com)

1.2.3 Theory and principles: Band Gap

Larger the size of the QD smaller will be the band gap and hence larger will be the emitted wavelength. As a result larger particle will emit color near red region while smaller particle will emit color in the violet region of the visible spectrum even though the material composition is same. Fig. 1.6 shows the effect of size on band gap of QD.

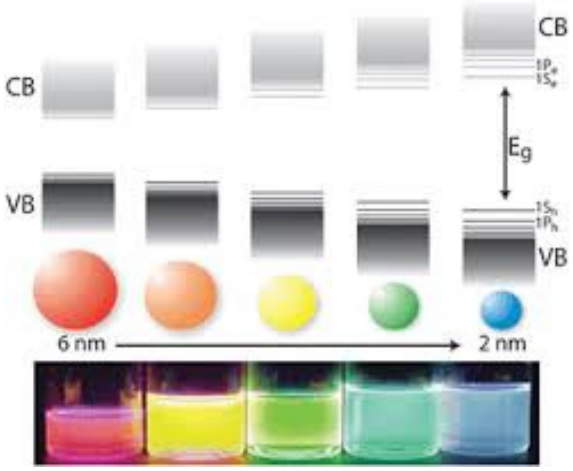

Fig-1.6.Effect of size on band gap (Figure adapted from http://pubs.rsc.org/en/content/articlehtml/2011/cs/c0cs00055h

1.2.4 Theory and principles: Stokes Shift

The difference between excited wavelength and emission wavelength is called stokes shift. Quantum dots show excellent optical property due to large stokes shift. This reduces background noise and makes the material highly efficient for imaging Purposes. The conventional organic dyes have very small stokes shift that leads to overlap of the excitation – emission spectra (Fig.1.7).

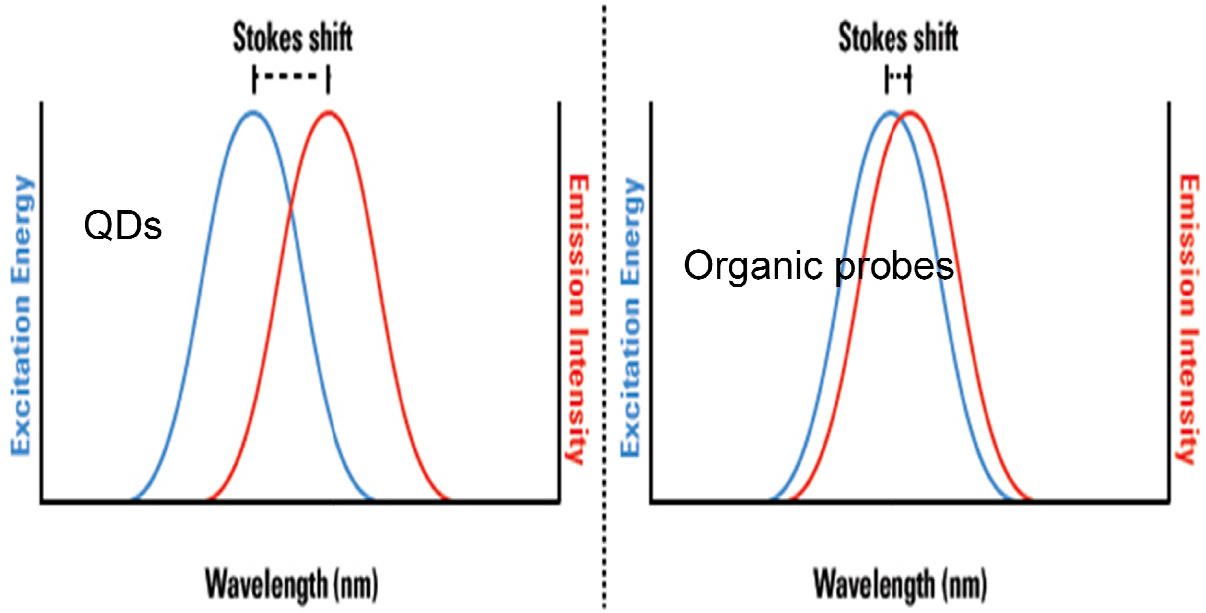

Fig- 1.7: Stoke shift variation for QD and conventional organic probe (Figure adapted from www.thermofisher.com/in/en/home/life-science/protein-biology/ protein-biology- learning- center/protein-biology-resource-library/pierce-protein-methods/fluorescent-probes.html)

The large stokes shift of QDs help them to use in multiplexing and bio-imaging. The real time imaging is easily possible for QDs due to this large Stokes shift. Resonance energy transfer is another phenomenon that is highly applicable for QDs because of large stokes shift. The donor molecule may easily transfer its energy to the acceptor molecule

as there is no overlapping of the spectra. The narrow and size tunable emission spectra of QDs which can be excited by single excitation source is highly profound application of these particles as bio-imaging probe. The low background noise can be achieved only through the large stokes shift of the particles. Thus biological imaging and cell tracking applications are highly exploited through QDs.

1.2.5 Theory and principles: luminescence

The light emitted by a source other than a hot body, incandescent body such as black body radiation is luminescence. Luminescence is explained by Jablonski diagram Fig-1.8 When external energy is applied to an atomic or molecular system the system goes to excited state and then following various pathways of loosing energy the system comes back to ground state. The transition of energy leads to emission of radiation called as emission spectra. The luminescence can be classified as:

Cathode luminescence: Source is accelerated electrons.

Photoluminescence: Source is energetic optical photons

Chemiluminescence: Source is a chemical reaction

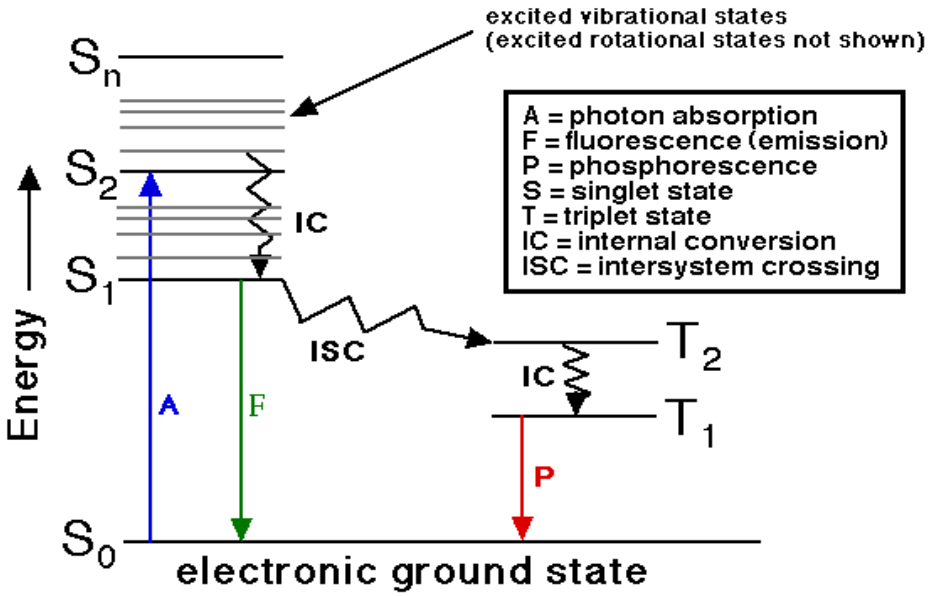

Fig-1.8: Jablonski diagram explaining the consequences of decay pathways (Figure adapted from http://www.shsu.edu/chm_tgc/chemilumdir/ JABLONSKI. html).

The luminescence where transition is caused by a photon resulting in spontaneous decay of the energy to a lower state and emitting a photon is photoluminescence. The excited electron can be trapped in an intermediate state which delays the emission.

The interaction of light with the molecule or atom changes the state of the system from ground state to excited state. As the state changes the spin does not change for spin selection rule. The emission of the photon from lowest excited state to ground state without changing the spin leads to fluorescence. But sometimes due to intersystem crossing the spin of the excited state changes. The emission from lowest triplet state to the ground state is phosphorescence. The emission that follows quantum mechanical selection rule is called allowed while emission that do not follow selection rule is not

allowed. According to spin selection rule the transition of energy is allowed for states having same spin. Thus fluorescence is spin allowed transition while phosphorescence is quantum mechanically disallowed transition. The rate of emission for fluorescence is typically 10^8 s^{-1} or 10 ns while emissive rate of phosphorescence is slow. Thus for phosphorescence life time of the material in excited state is high. When molecule gets excited by excited it relaxes to lower state by two pathways viz radiative and non-radiative decay. Radiative decay occurs by emission of photons while non-radiative decay occurs by thermal processes called as quenching. The radiative decay can occur generally by fluorescence or phosphorescence. The non-radiative decay may occur in three classical ways according to thermodynamic principles as internal conversion, external conversion and intersystem crossing. When electronic energy of the system is converted to vibrational energy of the system itself it is called internal conversion. The thermal energy is responsible for such conversions. Thus as temperature increases rate of internal conversion increases as well and luminescence intensity decreases. External conversion occurs by losing the electronic energy in the surrounding due to collision with neighboring solutes or by formation of complex. The biological environment and surrounding can be easily accounted by external quenching. The external quenching has one more aspect to deal with called as resonance energy transfer. This type of quenching is generally significant for biological systems where there is very low distance between two molecules. Transfer of energy from donor molecules excite the acceptor molecule resulting in emission of the acceptor molecule.

1.2.6 Theory and principles: Quenching

The phenomenon of decrease of luminescence intensity by decaying of the excited state of a substrate is called quenching. Quenching can be classified as internal and external quenching. The quenching that do not involve the external environment of the molecule is called internal quenching while the quenching that involves the external environment is called external quenching. There are various processes by which quenching occurs:

- Excited state reactions
- Energy transfers
- Collisional quenching also called dynamic quenching
- Complex formation also called static quenching

The quenching due to energy transfer, collisional quenching and due to complex formation are the key for the routine research work.

Dynamic quenching or collisional quenching is the process by which decrease in intensity is due to collision. The fluorescence life time decreases with increase in concentration of the quencher. Hence for dynamic quenching the quencher must be in contact when the fluorophore is in excited state. Oxygen and iodide quenches the intensity by inducing the intersystem crossing while aromatic amines donate the electrons to the excited state. This type of quenching is described by Stern-Volmer equation:

$F_O / F = 1+K_D [Q] = \Gamma_O / \Gamma =$ ratio of life time of fluorescent state.

F_O is Fluorescence intensity due to absence of quencher

F is intensity in presence of quencher

K_D is Stern-Volmer dynamic constant which is k X Γ (life time)

Q is concentration of the quencher.

Sometimes the fluorophore forms a complex with the quencher which is nonfluorescent in nature and exist at ground state such type of quenching is called as static quenching. Since in static or steady state quenching excited state is not involved the fluorescence life time is not affected by the process. The static quenching also follows the Stern-Volmer equation and is represented as:

$F_O / F = 1+K_S [Q]$

F_O is Fluorescence intensity due to absence of quencher

F is intensity in presence of quencher

K_S is Stern-Volmer static constant where life time is constant

Q is concentration of the quencher.

Static quenching decreases with increasing the temperature [*N.Ghosh et al.2015*] while dynamic quenching increases with increasing the temperature. This is due to complex formation is inversely proportional temperature while rate of diffusion and collision increases with temperature.

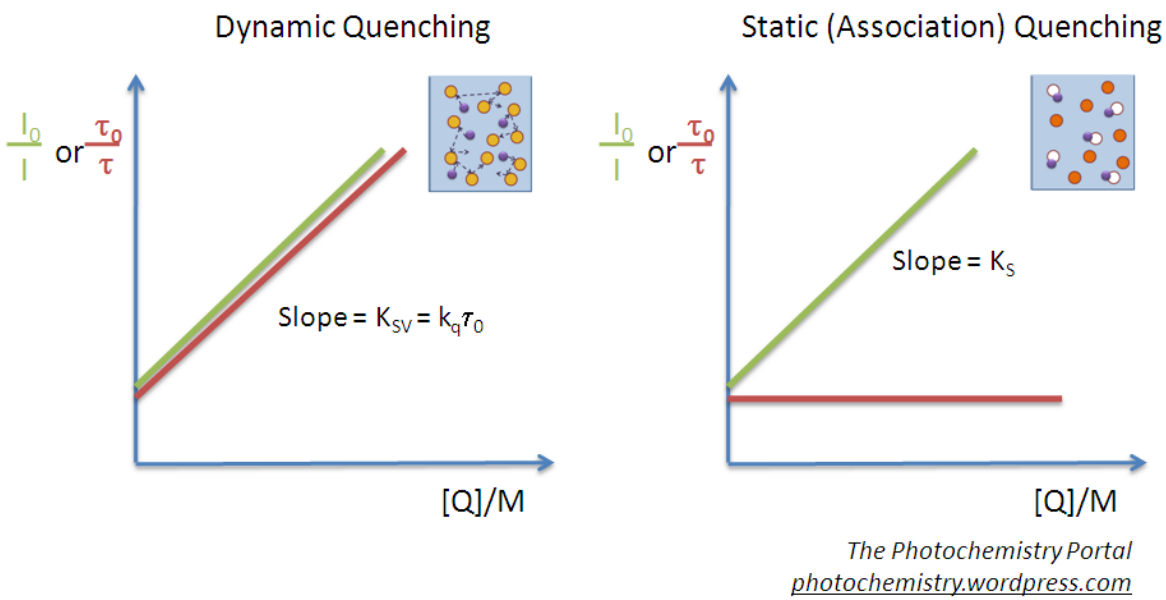

Fig-1.9: Dynamic and static quenching (Figure adapted from https:// photochemistry.wordpress.com/2009/10/30/quenching-mechanisms/)

Resonance energy transfer [*Förster, T et al. 1948*] is the third aspect of external quenching. This is commonly called as FRET (Fluorescence Resonance Energy Transfer). This type of process of non-radiative decay occurs when there are two molecules one is donor and other is acceptor. The donor transfers its energy from excited state to the acceptor molecule. The transfer of energy depends on various factors that govern the transfer of radiation from donor to acceptor. The most common factors are:

- The gap between the emission spectra of donor and excitation spectra of acceptor
- The quantum efficiency of the donor
- The orientation of transition dipoles of donor and acceptor
- The contact distance between the donor and acceptor.

1.2.7 Theory and principles: Resonance energy transfer

The resonance energy transfer is very extensively used [*Tsien, R. et al. 1998*] in studying protein-protein interaction. The transfer of energy from donor to acceptor is based on electronic coupling. The donor comes back to ground state while acceptor gets excited which may emit photon of longer wavelength as compared to the donor.

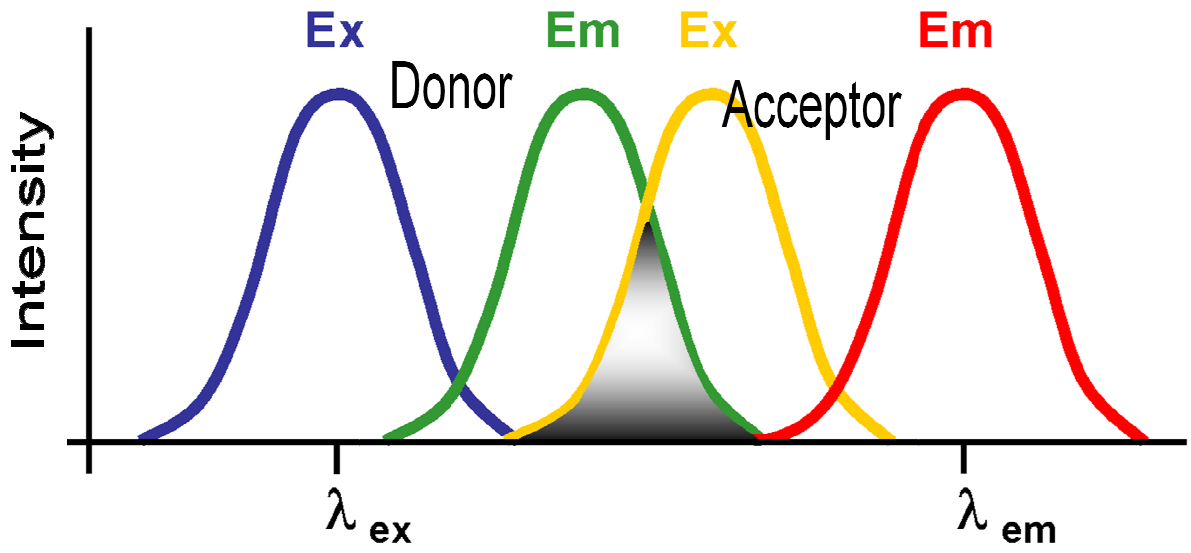

Fig-1.10: Resonance energy transfer (Figure adapted from http://bitesizebio.com/23012/you-may-not-know-theodor-forster-but-you-know-his-work-fret/)

There are various applications of resonance energy transfer

- Structure and conformation of proteins [*Jonsson T et al. 1996*]

- Spatial distribution and assembly of proteins [*Watson BS et al. 1995*]
- Receptor ligand interaction [*Berger W et al. 1994*]
- Immunoassays [*Khanna PL et al. 1980*]
- Structure and conformation of nucleic acids [*Clegg RM et al. 1994*]
- Real-time PCR assays and SNP detection [*Lee LG et al. 1999 and Myakishev MV et al. 2001*]
- Nucleic acid hybridization [*Parkhurst KM et al. 1995*]
- Distribution and transport of lipids [*Nichols JW et al. 1983*]
- Membrane fusion assays [*Uster PS et al. 1993*]
- Membrane potential sensing [*Gonzalez JE et al. 1995*]
- Fluorogenic protease assays [*Matayoshi ED et al. 1990*]
- Indicator of cyclic AMP [*Adams SR, et al. 1993]*

1.3 Quantum dots: An emerging nanomaterial

Colloidal semiconductor nanocrystals or quantum dots (QDs) can be defined as monodisperse crystalline clusters having spatial dimensions smaller than the bulk-exciton Bohr radius, i.e. the distance in an electron-hole pair. This very small size of the particle has a significant effect on the photoluminescent properties. This unique property could be understood through all spatial dimensions confinement of the exciton (*Rossetti R et al. 1984*). The spacing of the highest occupied and lowest unoccupied quantum confined orbital of QDs is determined by the size which leads to tuning ability of the energy levels. Thus, versatile luminescent particles can be tuned in a controlled way by synthesizing nanocrystals of different diameter. Although both specifically designed optical properties and the valuable feature of wide range continuous band gap tenability (*Arya H et al. 2005*) must be retained. QDs have attracted great interest during the last decades mostly due to the immense and cutting edge prospects of hybrid material. Bio-conjugates or the bio-applications especially in imaging can only be possible by exploring large number of fabricated QDs. Thus, unique electro-optical properties, which arise from the size-controlled and tunable photoluminescence (PL) and long-term photostability, made these nanomaterials emerged as advantageous alternatives to the commonly used molecular probes in biological and biomedical applications including biolabeling, bioimaging and biotargeting. A large number of QDs that have been synthesized, usually composed of atoms from groups II–VI, III–V, or IV–VI (*V. Lesnyak et al. 2013*), the emphasis been given to materials such as Mn doped ZnS and other non toxic QDs. The biocompatible QDs were obtained by using distinct synthesis routes which also ensured a strict control of the constituent material, size, shape, and surface

chemistry. Among the different physical and chemical processes for QDs preparation, the colloidal chemistry method is the best route to synthesize nanocrystals with proper surface functionality providing high luminescence efficiency, narrow size distribution and the ability to interact with selected species. Moreover, since the QDs are dispersed in a solvent, they should be stabilized in a way that prevents agglomeration. The ability to tailor QDs surface with appropriate ligands is therefore an aspect of paramount importance affecting not only nanocrystals solution properties and solubility but also their potential use as chemosensors. Selective binding on the surface of the nanocrystals, or the ligands template effect, has been frequently studied for controlling the nanocrystals shape and retaining its specificity. The ligands effects also control the size and its distribution during the QDs synthesis as well as crystal structure and nanocrystals stability. Recent advances in QDs nanotechnology have introduced these nanomaterials in analytical field mostly as chemical sensors in fluorescence-based measurements. Due to the very small size and high surface-to-volume ratio of QDs, their surface gained significant importance. Any modification of surrounding medium or interaction of given chemical species, could be modulated at distinct levels, would result in significant alteration of the photo luminescent properties. Hence optical properties specifically in terms of emission intensity are the principle of making sensor. In most of the circumstances the synthetic routes could predominantly affect the quantum yield of QDs which, defined as the ratio between emitted and absorbed photons, by influencing the efficiency of electron-hole recombination. This could also promote a spectral shift or a change in the PL decay time. To date, most commercial QDs are synthesized through the traditional organometallic method (*B. O. Dabbousi eta al. 1997)* and contain toxic

elements, such as cadmium, lead, mercury, arsenic, etc. The overall goal of this thesis study is to develop an aqueous synthesis method (*V. Lesnyak et al. 2013*) to produce nontoxic quantum dots with strong emission and good stability, suitable for biomedical imaging (*Peng Wu et al. 2013*) and analytical applications (*Peng Wu et al. 2010*). From an analytical point of view, the modulation of QDs luminescence as a selective response to a given analyte recognition could be perceived by different means: fluorescence intensity quenching or enhancing, fluorescence resonance energy transfer (FRET), direct or indirect chemiluminescence enhancing or quenching, chemiluminescence resonance energy transfer (CRET) and annihilation or co-reactant electroluminescence. These could be used alone or coupled to separation techniques like liquid chromatography or capillary electrophoresis. The characterization and quantification of chemical substances in a wide variety of matrices is still a challenge faced by scientists. Trace and ultra-trace analysis of complex samples, often rely on selective sample cleanup prior to a chromatographic separation. Affinity based separation materials, such as MIPs (*Junxiao Liu et al. 2010*), potentially offer a higher degree of sample cleanup efficiency. Molecularly imprinting is an emerging technology which enables us to synthesize the materials with highly specific receptor sites towards the target molecule. Compared with traditional sorbents, MIPs not only concentrate, but also selectively separate the target analytes from real samples, which is crucial to quantitatively determine the analytes in complex samples like urine, blood etc. MIP technique based on molecular recognition allows not only pre-concentration and cleaning of the sample but also selective extraction of the target analyte, which is important, particularly when the sample is complex and impurities can interfere with

quantification. Molecularly imprinting technique is said to be a best extraction technique in various fields. Therefore, the introduction of QDs conjugated MIPs provides a fluorescence detecting system which will enhance the selectivity and sensitivity of nanomaterials for its application in analytical or biomedical fields.

The present thesis work will explore the optical specificity, live imaging and analyte selectivity of quantum dots for its application in two major fields of science viz: biomedical and analytical chemistry.

Semiconductor and metal nanoparticles in the range of 2-10 nm have aroused great interest due to their unique size-dependent properties, which happen to also have similar dimensions to biological macromolecules (e.g. proteins and nucleic acids) (*de Mel A et al. 2012*). This has added advantage as it allows the integration of nanotechnology and biology, thus promoting great advances in cell biology, molecular biology, targeted therapeutics and medical diagnostics. Current development in this field has allowed the linking of colloidal nanoparticles to nanoparticles (e.g. QDs, CNTs) (*Pan B et al. 2006*) and to biomolecules such as proteins peptides and DNA. These nanosized bioconjugates are used in the construction of hybrid materials for the development of multicolour fluorescent probes and bioassays for ultrasensitive detection and imaging (*Dubertret, B et al. 2002 and Michalet, X et al. 2005*). QDs have broad excitation, but narrow, strong and tunable emission spectra which allows the simultaneous observation of multiple probes with different fluorescent colors using a single light source (*Gao, X et al. 2004*) with bright emission and extraordinary photostability (*Derfus, A.M et al 2004.)* QDs make the long-term real-time monitoring and tracking of molecules and cells more feasible. For example, researchers were able

to observe QDs in lymph nodes of mice for more than 4 months (*Ballou, B et al 2004*). Furthermore, QDs will enhance fluorescence lifetime significantly longer than that of organic dyes or auto-fluorescent flavin proteins. Therefore, combined with pulsed laser and time-gated detection, the use of QDs label can produce images with greatly reduced background noise (*Dahan, M, et al. 2001*).Traditionally, most colloidal quantum dots are synthesized through an organometallic method, which involves hazardous precursors, high temperature reaction, and organic solvents. Although there are some efforts to make the QDs water-soluble, many complicated post-synthesis steps have to be taken to exchange the solvent and to achieve the strong emission. There is a considerable need for a simple, economic and environment-friendly aqueous route to produce biocompatible QDs with strong emission and good stability. The synthesis of colloidal quantum dots is combination of synthetic inorganic chemistry and solid state chemistry. The use of precursors, solvents and capping agents in appropriate composition is a powerful approach in the aqueous based bottom up synthesis. Although QD-based sensing is growing in interest, FRET is still the most common mechanism for modulating QD PL.QDs are ideal donors and can be excellent acceptors when paired with appropriate donors (*B. O. Dabbousi et al. 1997*).There are mainly two ways to improve the selectivity of QDs, one way is to introduce a substance with good selectivity which can quench only the fluorescence of the aimed analyte and secondly by improving the optical properties of the QD by reducing the other non-radiative transitions with the help of capping agents and dopant concentration. Mn-doped QDs have attracted considerable attention because of the excellent properties. The doping ion acts as recombination centers for the excited electron-hole pairs and results in

strong characteristic luminescence (*Zhuang J et al. 2003*). Upon Mn^{2+} doping, an orange emission band develops around 590 nm, for the well known $^4T_1$-$^6A_1$ d-d transition of Mn^{2+} ions on Zn^{2+} sites, where the Mn^{2+} is coordinated by S^{2-} ions (*Steitz B et al. 2008*). Synthesis of QD-MIP is a strategy to combine the selectivity of MIP (molecularly imprinted polymer) and specificity of QD. This technique is used to prepare surface imprinted polymer capped Mn-Doped ZnS quantum dots and their application for detection of 4-Nitrophenol in tap water (*Junxiao Liu et al. 2010*) and for detection of Enoxacin in biological fluids (*Yu He et al. 2008*).

QDs have utility in live cell imaging and detection applications, which can be done externally, but could also require the internalization of quantum dots by cells. As demonstrated in the earlier section, internalization of quantum dots for targeting and imaging applications has been achieved using a number of different strategies, including modifications to surface coatings for passive uptake and the use of specific molecules for mediated delivery (*Kuo, Y.-C et al. 2008, Duan H et al. 2007and Bakalova R et al. 2008*). These altered surface coatings have been developed to increase the versatility and labeling efficiency of quantum dots for live cells, both prokaryotes and eukaryotes (Chang J.C et al.2008, Liu W et al. 2008). The various surface coatings will enhance the aqueous solubility, and provide varying functional groups for conjugation of antibodies, peptides, and other biomolecules, and/or reduced nonspecific binding to the cell surface (*Erogbogbo F et al 2008*). Other improvements to cellular imaging involve variations to the core composition for decreased cytotoxicity and increased biocompatibility (*Kairdolf, B.A et al 2008*). The ability to internalize quantum dot conjugates, along with the increased multiplexing capabilities, offers a major

advancement in time and cost-effectiveness over single-color experiments. Ultimately, these advantages will contribute to the detection of various cell proteins or other components of heterogeneous tumor/tissue samples, including cell mixtures, and will be critical in fields like medical/cancer diagnostics and pathogenic bacteria analysis (*Yezhelyev, M.V et al 2007, Hahn M.A et al 2008*).

1.4 Doped Quantum Dots : Synthesis and significance

The impurity in solid state is the key for its wide applications. The doped QDs although retains all the basic properties of the host lattice but also improve the optical properties by avoiding self-quenching problems. The small emission energy gap of the dopant increases the stokes shift of the material which is very profoundly used in all the optical sensors and imaging probes. Till date transition metals and lanthanide ions are used commonly as dopants such as Mn^{+2}, Co^{+2}, Ni^{+2}, Cu^{+2}, Ag^{+} , Pb^{+2}, Eu^{+2}, Ce^{+3}, Eu^{+3},Tb^{+3} etc. have been used in II-VI host QDs [*H.Hu et al. 2006, P.Reiss et al. 2007, Y.S. Yang et al. 2006, K.Jug et al. 2009, J.C. Wu et al 2011, V.Chikan et al 2011 and D. Mocatta et al 2011*]. The copper and manganese doped QDs have been extensively studied [*N.S. Karan et al 2010*]. The host for the impurity as dopant can be a large number of lattice types as Graphene, CdO, CdS, CdSe, ZnS, ZnSe, ZnO etc. Generally host having large and wide band gap is selected as ZnS [*H.Hu et al. 2006*], ZnSe [*P.Reiss et al. 2007*], ZnO [*Y.S. Wang et al. 2006, K.Jug et al. 2009*], CdS [*J.C. wu et al. 2011*], CdSe [*V.Chikan et al. 2011*]. Among all the host lattices, ZnS have been extensively studied. Trace amount of impurity creates scope of large and versatile luminescent properties. The dopant emission from transition metals and lanthanides has longer life time than their host. The longer life time creates lower background fluorescence which is useful

for bioimaging. The ZnS host lattice is non toxic in nature as compared to conventional CdS. Thus, Mn doped ZnS QDs prove to be most efficient bio-label and also due to its long tuning ability of emission makes it to be used for sensor applications. The recent areas of nano- research are based on doped QDs [*J.D. Bryan et al. 2005, and H.Hu et al.2006*]. Various synthetic routes have been used for QD synthesis but, aqueous and organic phase routes were explored in major way. The aqueous synthetic route is achieved by co-precipitation of dopant ions and cationic precursors. The capping agents or ligands play significant role in obtaining water soluble QDs. Among various ligands, thiols [*J.Q zhuang et al. 2003 and A.Aboulaich et al. 2010, 2011*], polymers [*A.A. Bol et al 2001*], phosphate [*J.F.Suyver et al. 2001*] and proteins [*W.B. Zhou et al. 2011 and A. Makhal et al. 2012*] have been commonly used as ligands. The synthesis which follows aqueous routes, the low temperature is not appropriate for creating surface defects and annealing. This results in low fluorescence intensity. Reverse micellar formation [*H.S. Yang et al. 2004*] is highly useful for doped QD synthesis. Surface dangling bonds [*H. Yang et al. 2004*] sometimes prove to decrease the luminescence intensity during synthesis and hence, other methods needed to be explored. Shell formation [*H.S. Yang et al. 2003, 2004*] increases intensity by passivation effect but increases the size of the QD. Hence, aqueous route of synthesis needed to be enhancing [*T.Q. H. Tran et al. 2011 and L.M. Gan et al. 1997*]. The most evolved aqueous synthesis is hydrothermal approach [*P.T.K. Chin et al. 2009 and P.V. Radovanovic et al. 2005*] where temperature of the aqueous solvent is increased above the boiling point of water. Although all the reported methods prove their efficacy, but synthesizing QDs at low temperature has its importance of obtaining low toxic and small size particles (Fig 1.1).

Fig-1.1. Different colors due to quantum confinement (Figure adapted from http://gizmodo.com/5514438/quantum-dots-could-make-dark-grainy-cellphone-party-pics-obsolete)

1.4 Scope and Objectives of the Thesis

As of now, it is reported that how QDs play significant role in the development of nanoscience for various applications. Various QDs are been synthesized and used till date but doped ones are ahead of all the QDs explored. Doping is the method of introducing atoms or ions in the crystal lattice to enhance the desired property of the material. The atoms or ions that is used are called as dopant and the lattice in which the dopant is added is called host. Various dopants have been studied and extensively used such as copper, iron, manganese, nickel, silver, cobalt and the lanthanides (cerium, europium etc). The common hosts that are been used are zinc sulphide, zinc oxide, cadmium sulphide, cadmium oxide etc. Manganese as dopant and Zinc Sulphide as host have thoroughly studied in the thesis. This Mn doped Zinc Sulphide QDs have been further used as optical sensors and as bio-imaging probe by reducing its toxicity through biocompatible surfactant.

1.5.1 Objectives of the thesis

- Exploring the optical properties of QDs synthesized with greener methodologies
- Synthesis and surface modification of QDs by molecularly imprinted polymer (QD-MIP) or different capping agents
- Application of QDs/QD-MIP for specific and selective detection of analytes
- Synthesis and characterization of biocompatible QDs
- Application of biocompatible QDs as tool for biomedical science

1.5.2 Methodology

a. Reagents and materials:

Several reagents, analytical standards, chemicals and consumables which are required for the synthesis of QDs have been be procured from the vendors as per the requirement and stated in the experimental section of each chapter (2-5). The surfactants and other surface modifying reagents were also procured as per the need.

b. Exploring the optical properties of QDs synthesized by aqueous routes

Wet aqueous chemical synthesis scheme adopting green synthetic routes have been employed for synthesizing number of Mn doped ZnS quantum dots and other significant quantum dots. The optical properties have been explored by varying the concentration of dopant, capping agents and other parameters in the synthesis.

c. ***Synthesis, surface modification and characterization of QDs capped with MIP***

The analytical specificity and selectivity of the QDs have been obtained by capping with MIP.The process of surface imprinting onto the QDs will be based on the reported method, except some modifications as per the requirements. All parameter should be optimized in such a way that the resultant surface modified QDs has maximum possible affinity and selectivity towards the analyte. FTIR, UV, Spectrofluorometer and XRD were used to characterize the synthesized material.

d. Application of QD-MIP for selective and specific detection of analytes

The MIP coated quantum dots has selectivity and specificity for the target analyte thus this highly efficient QD-MIP has the potential to explore it for sensors applications. Specific and highly significant analytes were chosen for the analytical validity of quantum dots. The fluorescence quenching after binding to the analyte proved be the key for the success of such analytical tool.

e. Synthesis and characterization of biocompatible QDs

The biological applications of the quantum dots depend on the toxicological profile and cellular uptake of the nanoparticles inside the cell. The common routes of uptake are endocytosis and cell transfection. Fluorescence microscope enabled the imaging of the particle inside cell. The number of QD labeled cells can be counted with flow cytometry. MTT (3-(4, 5-dimethylthiazol-2-yl)-2, 5-diphenyl tetrazolium bromide) assay was performed for the cytotoxicity profiling and obtaining minimum concentration dose for further application of QDs in biological system.

f. Application of biocompatible quantum dots as tool for biomedical science

The synthesized biocompatible QDs were used as tool for biomedical applications. Quantum Dots fabricated with coating that enable them in cell uptake, long photostability and minimum cytotoxicity have been used for the biological applications.

1.6 Possible outcomes

The result of this study outlines the applications of QDs in bioanalytical and medical sciences. Lot of work has been done in the synthesis of various capping layers to improve the biocompatibility of QDs but still its toxicity, stability, and size are the key factors for their usage in biomedical applications. In this work, we have explored simple methods of surface modification of the quantum dots for enhancing its biocompatibility. So far, analysis of biotransformed analytes with the help of QDs is not well known thus this work will speed up the integration of imprinted polymer to quantum dots as bioanalytical tool. We have explored highly green synthetic strategy for all the quantum dots synthesis hence this work will be a step to the development of nanoparticles application in various areas. The green chemistry based methods will enable low accumulation of unfriendly toxicants in environment and hence reduce the burden on society w.r.t. levels of toxicants.

Chapter-2

Chapter- 2

Synthesis and characterization of molecularly imprinted polymer by surface modification of Mn:ZnS QDs (QD-MIP): Optical sensor for detecting 3-PBA

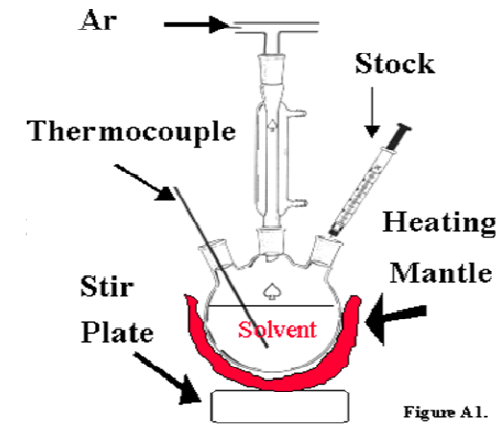

Figure A1.

QDs synthesis

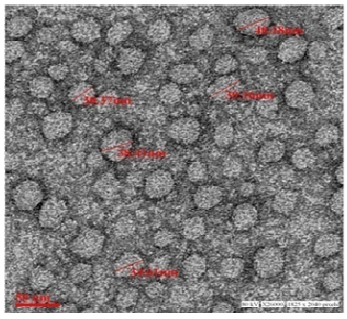

TEM Image

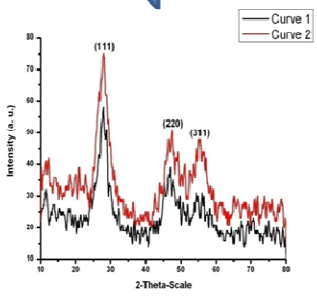

XRD Image

Spectrophotometer

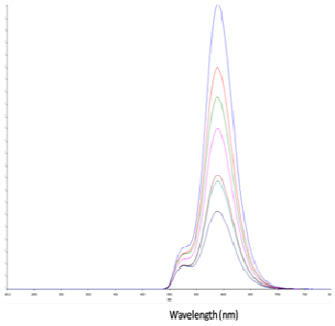

Quenching of 3PBA -QDMIPs

2.1. Introduction

Molecular imprinting polymers (MIPs) have shown wide variety of applications in the field of analytical chemistry and these synthesized MIPs will have selective binding sites for the template of interest. Molecular imprinted polymers (MIPs) are engineered cross linked polymers that can exhibit high affinity and selectivity towards a single compound or they can be intended to exhibit class selectivity for structurally related compounds.

Several advantages as given below made MIPs the target of intense investigation:

- Their high affinity and selectivity, towards the desired analytes, are similar to those of natural receptors
- Their unique physical and chemical stability which is superior to that demonstrated by natural biomolecules.
- The simplicity of their preparation and the ease of adaptation to different practical applications.

Three main approaches for the synthesis were reported, which include MIP (a) Covalent approach introduced by Wulff and co-workers (1972) (b) Non-covalent approach introduced by Mosbach and co-workers (1981) and (c) Semi-covalent approach introduced by Sellergren and Andersson (1990). Generally, non-covalent approach is applied for the synthesis of MIP because of easy removal of template through simple solvent extraction and availability of large number of monomers which interact with any kind of template. Covalent approach is restrictive since the cleavage of covalent bonds always requires harsh conditions. As we know, classical SPE sorbent retain analytes by non-selective hydrophobic interaction that leads to extraction of interfering substances but MIP technique based on molecular recognition allows not only pre-concentration and cleaning of the sample but also selective extraction of the target analyte, which is

important, particularly when the sample is complex and impurities can interfere with quantification. The selectivity mainly depends on the size and shape of the cavity and its rebinding interaction ability *(Diltemiz et al. 2008; Sellergren et al. 1994)*.

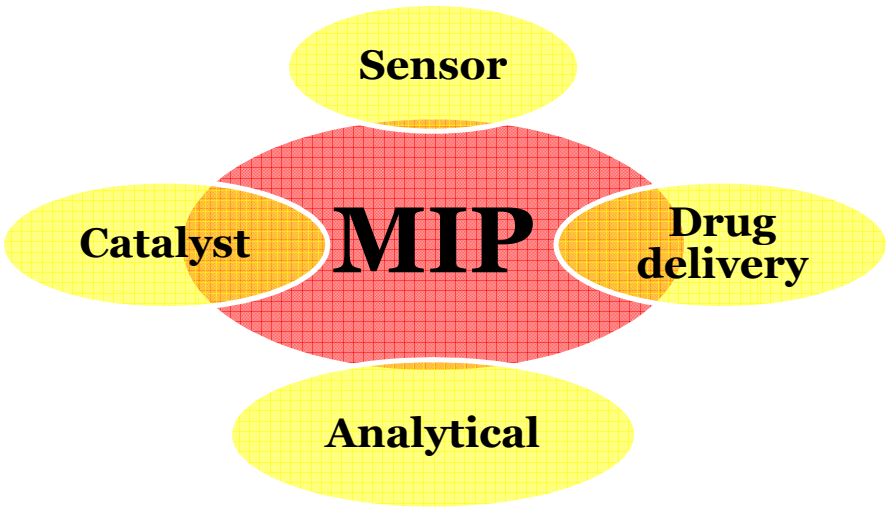

Fig-2.1. MIP application in different areas of chemical research

These MIPs has several advantages like simple to prepare, higher stability and affinity for the analyte recognition and cost-effective *(He et al.2007; He et al. 2006 and Yang et al. 2005)*. Due to these advantages, MIPs found wide applications (Fig.2.1) in the areas of bioseparations, diagnostic assays, sensors and biocatalysts *(Lin et al. 2004).*

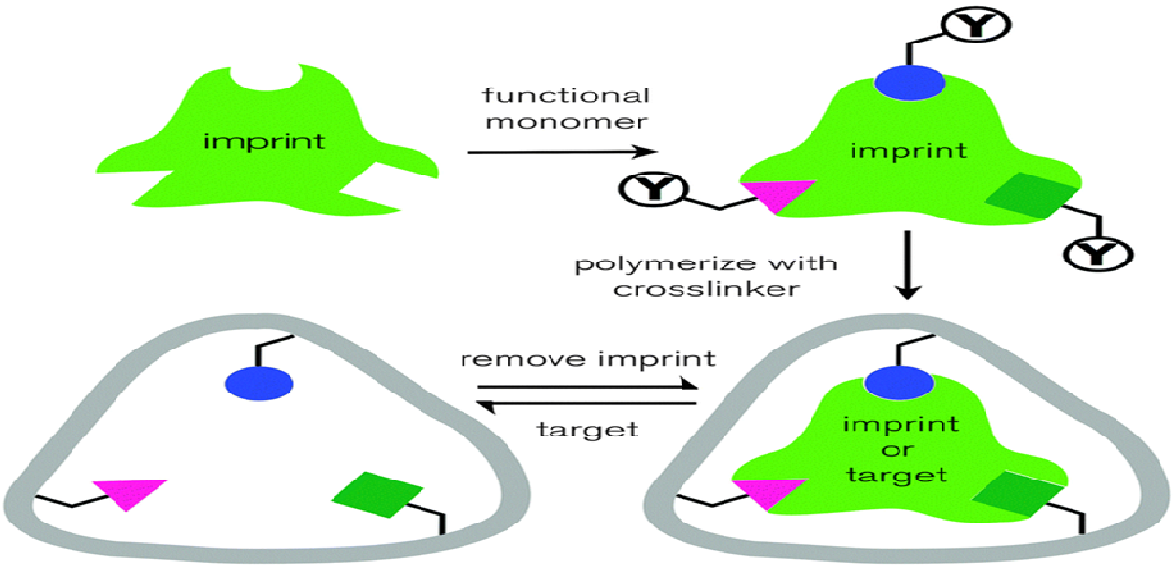

Fig-2.2 Schematic representation of MIP process (Figure adapted from Lofgreen et al.Chem.Soc.Rev.43 (2014) 911-933)

Optical sensing is found to be a straightforward method for the detection of analytes of interests and it has attracted wide attention from the researchers. Quantum dots (QDs) as optical sensors have increased in use for sensing application because of their size-dependent optical properties, large surface to volume ratios and quantum size effects *(Alivisatos et al. 1996; Chen et al. 1997; Peng et al. 2008; Xia et al. 2003; Liu et al. 2010)*. Due to high photoluminescence efficiency, size-dependent emission wavelengths and sharp emission profile, QDs are adopted for sensing of various compounds in different matrices *(Tu et al. 2008; Wang et al. 2009)*. Sensing technology is entirely based on specificity, modification of the luminescent QDs at its surface is very important for its applications in the analysis. Cadmium based quantum dots fabricated with silica have been used for optosensing of pyrethroids *(Li et al.2010)*. Surface

modification of QDs by using a molecular imprinting technique paved a way for the development of optical sensors. The MIP fabricated QD (QD-MIP) will provide the selectivity to the material due to presence of binding sites on the polymer matrix, which helps in the separation of analytes. The combination of selectivity of MIP with fluorescent characteristics of QDs provide newer applications for the detection of nonphosphorescent analytes as it will possess specific recognition ability and variable fluorescent intensity to the analytes of interest *(Zhang et al. 2012; Zhao et al. 2012)*. Thus, the surface modification of QDs of imprinted polymer leads to change in phosphorescence intensity when the target analyte is recognized by the material *(Lee et al. 2010)*. Among the various luminescent materials, Mn and Cu doped ZnS are the widely used materials in various applications as color television, radar and electroluminescence materials *(Datta et al. 2007; Romeo et al. 1999; Dimitrova et al. 2000; Chen et al. 2005; Sapra et al. 2003).* There are reports which utilize the advantages of phosphorescence of QD-MIP (Fig. 2.2). Yan and co-workers developed a method to optosense the pentachlorophenol in water by utilizing the concept of phosphorescence quenching using Mn: ZnS QDs, while; *Lin et al. 2004* has applied this for the chemiluminescence detection of 4-nitrophenol in tap water *(Liu et al. 2010).* Mn:ZnS QDs fabricated with MIP was also used for the TNT (Trinitro toluene) sensor through the fluorescence quenching by TNT *(Gao et al. 2008).* To the best of our knowledge, no application has been reported for the detection of 3-PBA in urine samples.

3-PBA (Fig.2.3.) is a non-specific and frequently detected metabolite of various pyrethroids such as cypermethrin, deltamethrin, permethrin, cyhalothrin etc. and also used as a general marker for the exposure to the pyrethroids.

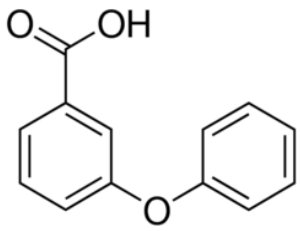

Fig-2.3.Structure of 3-PBA (Figure adapted from Wikipedia)

Due to the antiestrogenic activity, it is also considered as an endocrine disruptor chemical *(Ueyama et al. 2009; Cui et al. 2009; Perry et al. 2007)*. There is strong evidence of the role of 3-PBA in determining the exposure of pesticides in occupational workers *(*Kimata et al. 2009*).* Thus, it is necessary to detect and analyze the 3-PBA so that the implications of pesticides on human health can be known. This will provoke low applications of toxic pesticides and thus lead to minimize the ill-effects to the mankind.

3-PBA has been detected by a rapid ELISA method (*Ahn et al. 2011*), but it involves the sample preparation prior to analysis which is a tedious step. High-performance liquid chromatography (HPLC), liquid chromatography-mass spectrometry (LC-MS) *(Ding et al. 2004; Chung et al. 2012),* gas chromatography (GC), gas chromatography-mass spectrometry (GC-MS) *(Arrebola et al. 1999; Elflein et al. 2003; Schettgen et al. 2002; Corrion et al. 2005;)* and immunoassay based methods *(Chuang et al. 2011; Shan et al. 2004)* for 3-PBA analysis were also reported. Even though these methods have an advantage to quantify 3-PBA in several matrices, but they are not compatible

for on-field sensing and monitoring applications. In the present communication, an attempt has been made to form molecular recognition sites on the surface of Mn: ZnS using molecularly imprinting technique which is capable of selective extraction of 3-PBA from complex biological matrices. Hence, a simple, rapid and selective method is developed for the detection of 3-PBA in urine samples. The developed method is found to be cost effective and easy to use. Several methods were reported for the analysis of 3-PBA using various techniques of analytical and immune-analytical interest.

2.2. Experimental

Chemicals and reagents:

All the reagents used in the study were of analytical grade unless otherwise stated. $ZnSO_4.7H_2O$, $MnCl_2.4H_2O$ (97% purity), TEOS, (APTES), MPTS and 3-PBA were procured from Sigma Aldrich (St. Louis, MO, USA). All the solvents used were procured from Merck (Darmstadt, Germany) and Sd. Fine Pvt. Limited (Mumbai, India). $Na_2S.xH_2O$ was purchased from Sd. Fine Pvt. Limited (Mumbai, India). PBS of 30 mM was prepared as a stock solution by addition of 30 mM of Na_2HPO_4 and 30 mM of NaH_2PO_4.The pH of the buffer solution was maintained by 30 mM H_3PO_4 and 0.1 M NaOH solutions. Fresh aqueous solutions in milli Q water of standards and samples were prepared during experiments.

Synthesis of MPTS capped Mn:ZnS QDs:

The MPTS capped Mn: ZnS quantum dots were synthesized by following the earlier reported method with slight modification *(Wang et al. 2009)*. Briefly, to a three necked flask, $ZnSO_4$ (10 mmol), $MnCl_2$ (1 mmol), and 50 mL of water were added and the mixture was stirred under nitrogen at room temperature for 10 min. To this, 10 mL of aqueous solution containing Na_2S (10 mmol) was added drop wise and kept the mixture under stirring for 30 min. To this, MPTS (0.5 mmol) dissolved in 10 mL of ethanol was added and the reaction was kept for 20 hrs on stirring at room temperature. To ensure the purity and crystalline, the synthesized material was thoroughly washed with ethanol and water to remove unreacted parts. The material was kept in the oven at 90^0C for drying, which leads to highly crystalline QD.

Synthesis of MIP capped Mn : ZnS QDs:

To a 50 mL flask, 10 mL of alcoholic solution of 3-PBA (100 mg, template) and 250 µL of APTES (functional monomer) were added and stirred for 30 min. To the resultant mixture, 1 mL of TEOS (cross-linker) was added, and the mixture was kept stirring for 5 min. Then, MPTS capped Mn doped ZnS QDs (400 mg) and 2 mL of 6% aqueous ammonia solution was added and stirred for 16 hr. The non-imprinted polymer (NIP) was synthesized simultaneously without adding template. The resulting MIP and NIP were obtained after centrifugation and washed with ethanol followed by water and oven dried before use. The template was removed from QD-MIP through washing with methanol: acetic acid (9:1, *v/v*) several times. Finally the particles were dried for further use. Same synthetic approach was followed without template for the synthesis of QD-NIP

Instrumentation:

The size of the nanocrystal was observed using TEM, Tecnai-G2-SPIRIT FEI, Netherland. A drop of aqueous solution of QDs were placed on the copper grid to obtain images after sonication and coated with formvar. Absorbance, excitation and band gap energy were derived using a spectrophotometer, (SPECORD 210 PLUS, Analytik Jena, Germany). Fluorescence spectra of the QDs were obtained at an excitation and emission spectral wavelength of 330 and 590 nm, respectively (LS 55 photoluminescence spectrometer, Perkin Elmer, UK). The interactions of the functional group characterization of MPTS capped Mn:ZnS QDs and MIP modified QDs were performed using FTIR (Nicolet 6700,Thermo scientific, USA). The crystal lattice of the

synthesized QD was obtained by using XRD using Cu target source (SEIFERT, Germany) at ACMS Lab, IIT Kanpur.

Photoluminescence Study:

Different concentrations of 3-PBA (0.15 to 60 µM) were prepared from stock solution. An aliquot of 2.5 mL of each concentration of 3-PBA and 2 mL of PBS buffer (pH 8) was mixed with 2.5 mL of Mn: ZnS QD-MIP solution (20 mg L^{-1}) and kept stood for few minutes for interacting the analyte with QD-MIP. The complete dispersion was collected from this mixture and transferred to a cuvette for the photoluminescence study. The same procedure was followed for the QD-NIP interaction with the template (3-PBA) at the specified concentrations. The urine samples as biological matrix, used in the study were spiked at given concentrations and were diluted 50 times with water prior to be used in the analysis. The phosphorescence quenching was measured at an excitation wavelength of 330 nm by keeping the slit width of 15 nm and an emission filter at 515 nm.

Selectivity study:

The selectivity of the synthesized QD-MIP was performed by taking 2, 5-DHBA at the concentrations of (0.15 to 60 µM) using the same procedure described above. The structure of 2,5-DHBA was depicted in Fig.2.4. All other parameters for the analysis were same.

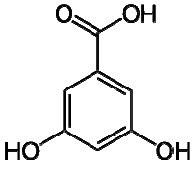

Fig-2.4. Structure of 2, 5-DHBA (Figure adapted from Wikipedia)

Method validation:

Validation assay of the developed method was performed with respect to LOD, precision, linearity and recovery. Calibration of 3-PBA in urine was drawn at five different concentrations, i.e. in the concentration range of 0.15-60 µM. LOD was calculated by determining the concentration of the analyte that quenched intensity three times the ratio of standard deviation and slope. Precision study (intra- and inter-day) was carried out at five times for 3-PBA as analyte using the synthesized QD-MIP as an optical sensor at three different concentrations (1, 30 and 60 µM) in a day and also for the five successive days. Recovery study was carried out at three different concentration levels (1, 30 and 60 µM) in urine. All the validation assays were performed in triplicate manner (n=3).

2.3. Results and Discussion

Synthesis of QD and QD-MIP:

The MPTS capped Mn:ZnS QDs were synthesized by precipitating zinc sulphide from the precursors. Zinc precursor was obtained from zinc sulphate and sulfur precursor from sodium sulphide in equimolar ratio to obtain 1:1 atomic ratio of ZnS. Doping was done instantly with nucleation so that surface defects could be obtained on the pure crystal lattice. Mn as dopant was added initially following precipitation and nucleation in parallel. Growth of the nucleated particle decides the optical properties of the material. Homogenous particle growth gives rise to similar sized nanoparticle that leads to strong photoluminescence. Growth and size of the synthesized material were controlled by using MPTS which acts as a capping agent. MPTS has very significant role in synthesizing QD-MIP as it helps not only synthesizing QDs but also acts as a linker between MIP and QD. The sol-gel approach was used for the synthesis of MIP by taking APTES as a monomer and TEOS as cross linker. The synthesis of QD-MIP not only provides selectivity to the surface by forming specific recognition sites for target analyte but also stabilizes the QD from bleaching or loss of fluorescence. The purity and crystalline nature of synthesized material are vital for sensing applications of the analytes. The interactions between template and monomer are non-covalent (H-bonding) due to which, the 3-PBA can be removed easily while retaining its imprint on the QD-MIP.

Characterization of MIP- and NIP Capped Mn-Doped ZnS QDs:

ZnS has a cubic Zinc Blende structure which is confirmed by the XRD patterns for the QD-MIP. The phase pure peaks for (111), (220), and (311) is in accordance with the JCPDS no. 05-0566. There are no other peaks in the diffraction pattern of the synthesized material which confirms the formation of pure crystalline ZnS. The diffractogram of QD and QD-MIP shows slight differences in intensity of peaks this explains that MIP capped QD is having low crystallinity as compared to pure QD (Fig-2.5).

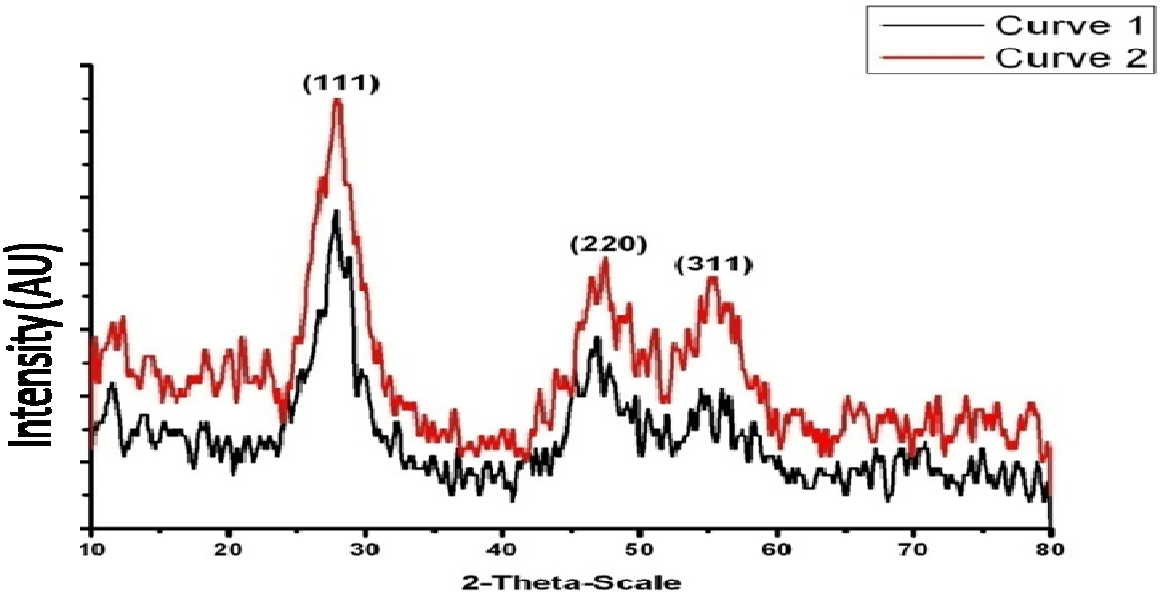

Fig-2.5. XRD of QD (curve 2) and QD-MIP (curve 1).

Further, the size for QD and QD-MIP were also calculated by XRD patterns by using scherer equation [$\beta_{1/2} = 0.94\lambda/d \cos\square$] *(Liu et al. 2010)*. Where $\beta_{1/2}$ refers to the full peak width at half maximum, λ refers to the copper target source, d refers to the size of the crystal lattice and □ refers to Braggs angle. The size of QD and QD-MIP was calculated as 10 and 13 nm respectively. So, an additional layer of 3 nm on the QD-MIP is

attributed to the formation of a MIP layer on the QD. Further, the size of the QD-MIP was also measured by TEM and the size was found to be in the range of 35-40 nm and particles are widely dispersed (Fig- 2.6). MIP layering on the surface of QDs is quite visible in the microscope. Growth of MIP is slightly controlled due to presence of template, resulting in well defined surface while the growth of NIP is uncontrolled due to absence of template resulting in highly agglomerated particles. Thus, stable and homogenous QD-MIP nanoparticles were synthesized that have imprints of template (3-PBA). The photoluminescence study of quantum dots shows excitation at 330 nm while emission at 460 nm which is characteristic peak of ZnS while at 590 nm which is the characteristic feature of Mn doped ZnS QDs (Fig-2.7).

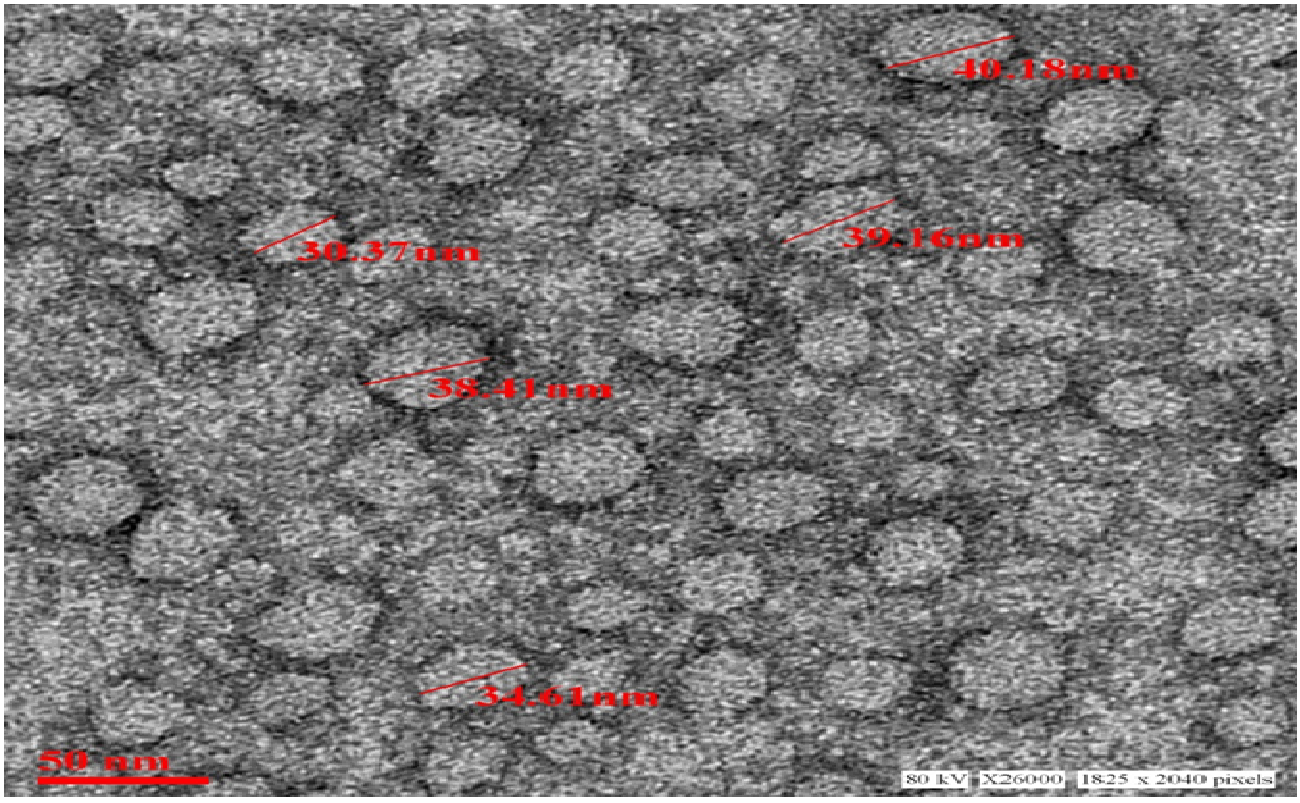

Fig-2.6. TEM image of QD-MIP.

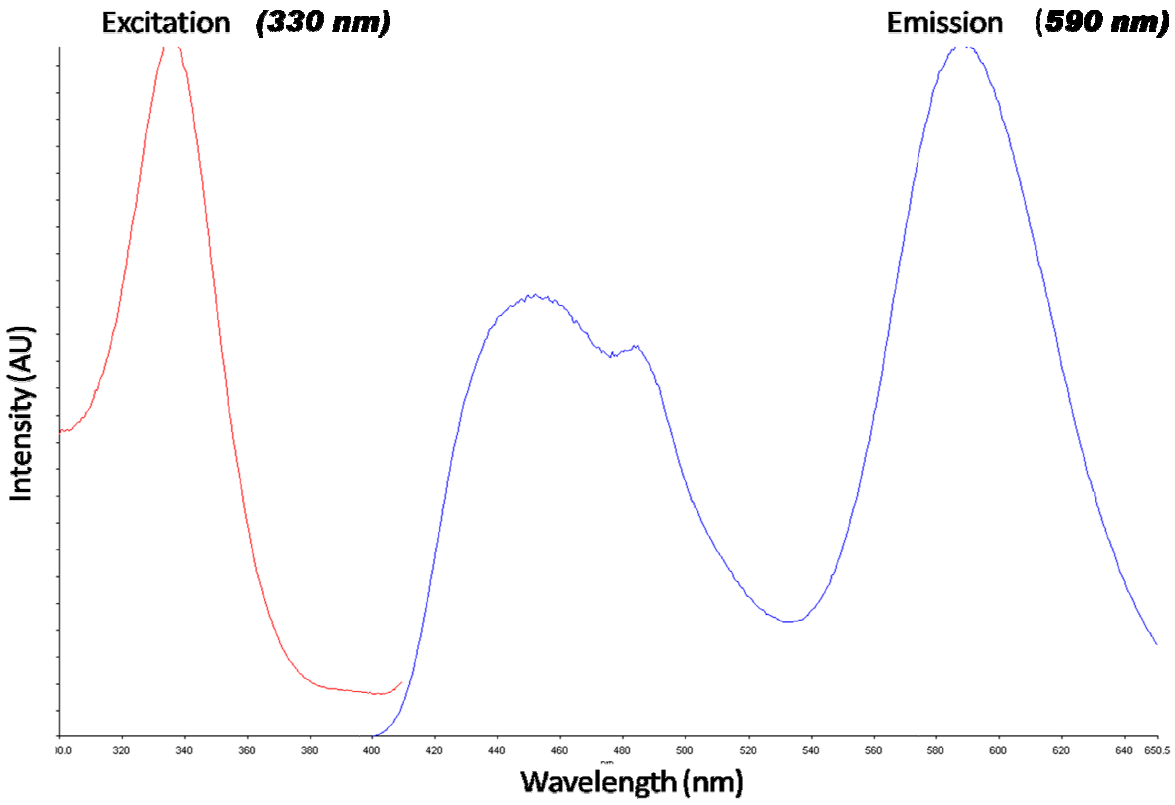

Fig-2.7. PL spectra of the Mn doped ZnS QD.

PL spectra of synthesized MPTS capped QDs shows that manganese is incorporated as dopant in the crystal lattice of zinc sulphide. The QD-MIP shows similar peak having emission at 590 nm and excitation at 330 nm, thus QD has been conjugated properly to the MIP resulting a stable). optosensing material. Further the formation of MIP has APTES as a monomer and TEOS as crosslinker is also confirmed by FTIR (Fig-2.8 a and b).

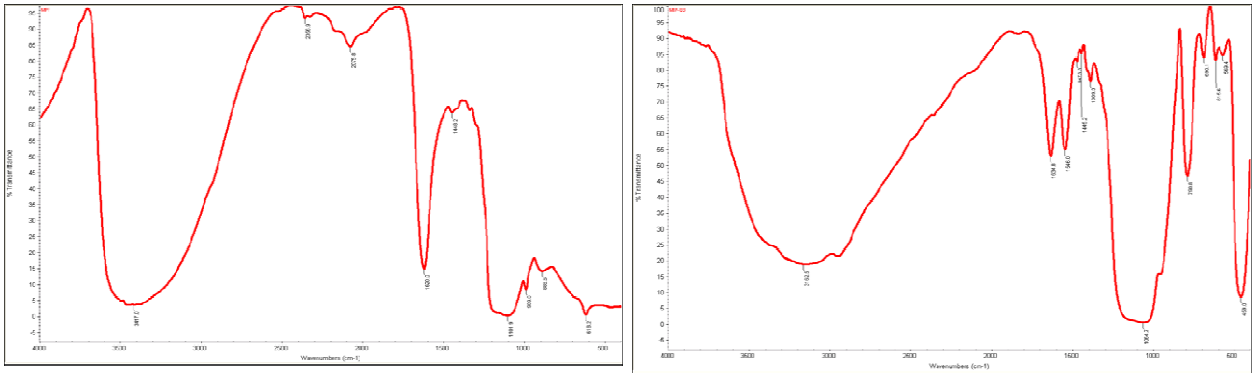

Fig-2.8. FTIR spectra of (a) QD and (b) QD-MIP

The strong and broad peak at 1101 of QD capped with MPTS was found to be shifted to 1064 after capping with MIP indicates interaction of Si-O-Si and Si-OH linkage confirms the formation of QD-MIP. The Si-O vibration at 790 and 459 in QD-MIP shows the presence of silane gel like polymeric network. This indicates that silica cross-linking plays a key role in the formation of desired polymeric material. Thus, according to all the characterization methods, it can be inferred that the particles synthesized has the properties of QD and MIP which is the prerequisite for application of nanomaterials as optical sensors.

Optimization of the pH of buffer solution used in the assay:

Luminescent property of the synthesized QD-MIP may show interaction with buffer media and can result in quenching of the phosphorescence. To obtain the suitable pH of the buffer, a 20 mg L^{-1} QD-MIP and QD was kept in PBS buffer in the pH range of 2-11 (Fig-2.9). It was found that, the phosphorescent intensity was very poor in acidic media while the intensity of the QD-MIP increases in the alkaline conditions (pH 8-11) and remains almost similar . Since the pH of urine is generally alkaline in nature, so PBS buffer of pH 8 was chosen in the study.

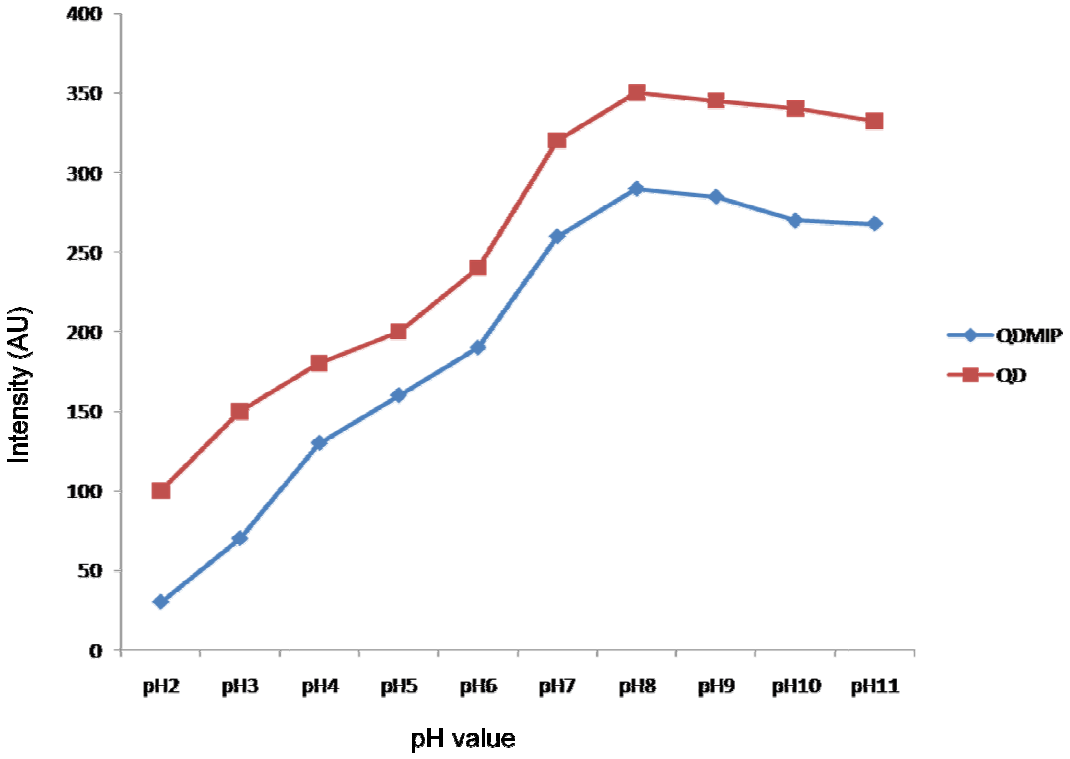

Fig-2.9. Effect of pH on photoluminescence quenching of QD-MIP at a concentration of 20 mg/mL on the addition of 30 µM 3-PBA

.

Sensing of 3-PBA by QD-MIP:

The PL study was used as a tool for selective and specific analysis of 3-PBA. The synthesized QD-MIP has phosphorescent emission at 590 nm with an excitation at 330 nm wavelength. The Mn^{2+} incorporated in the ZnS lattice is responsible for the room temperature phosphorescence at 590 nm. The coating of MIP on the surface of QDs does not interfere with the optical property of the QDs. Different concentrations of 3-PBA were interacted with a specific amount of QD-MIP & QD-NIP. Quenching of the phosphorescent intensity of the QD-MIP and QD-NIP with respect to the addition of 3-PBA (0.15-60µM) was studied (Fig. 2.10a and 2.10b). Sensing of the analyte (3-PBA) is based on the quenching of fluorescent intensity with respect to different concentrations

of quencher (3-PBA). According to Stern –Volmer equation ($P^o/P = 1 + KC$) *(Liu et al. 2010),* where P^o is initial photoluminescence intensity, P is an intensity in presence of the analyte, K is quenching constant and C is the concentration of analyte based on dynamic quenching *(Liu et al. 2010)*. The quenching constant was calculated for the QD-MIP with respect to QD-NIP and 2,5-DHBA (as quencher, analogue of 3-PBA) which is 3.4 times of QD-NIP for 3-PBA as quencher and 2 times of 2,5-DHBA as quencher respectively.

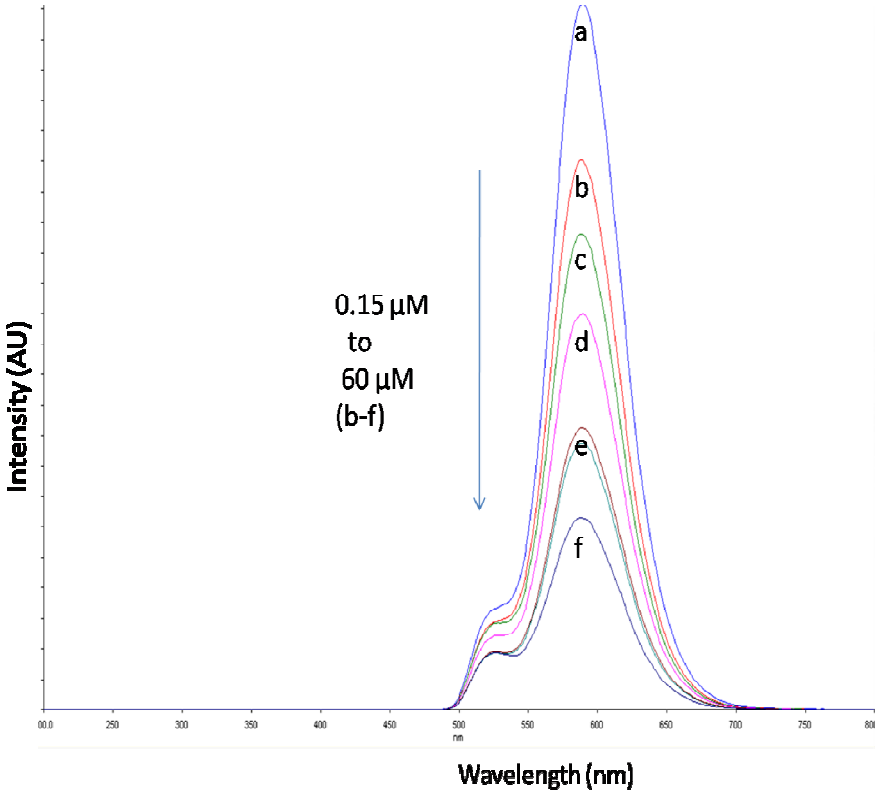

Fig-2.10. Photoluminescence quenching of QD-MIP with addition of 3-PBA (0.15 µM -60 µM, (b-f)) where a is intensity of QD-MIP

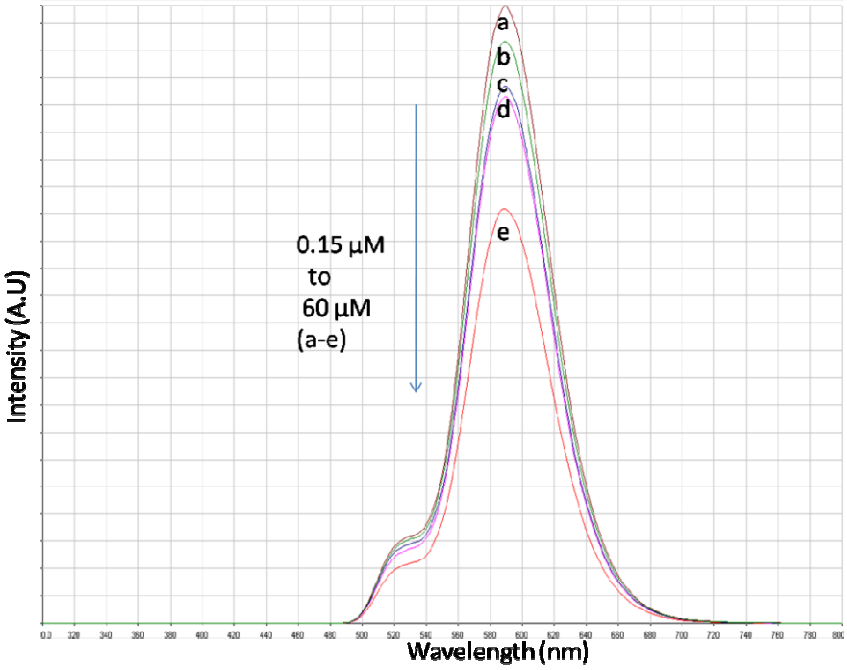

Fig-2.11. Photoluminescence quenching of QD-NIP with addition of 3-PBA at 0.15 µM -60 µM concentrations

Quenching of fluorescence intensity by 2,5-DHBA was done to check the selectivity of the imprinted polymer formed using 3-PBA as a template (Fig-2.11). The results clearly depicted the high selectivity of QD-MIP towards 3-PBA as compared to 2,5-DHBA (as an analogue).

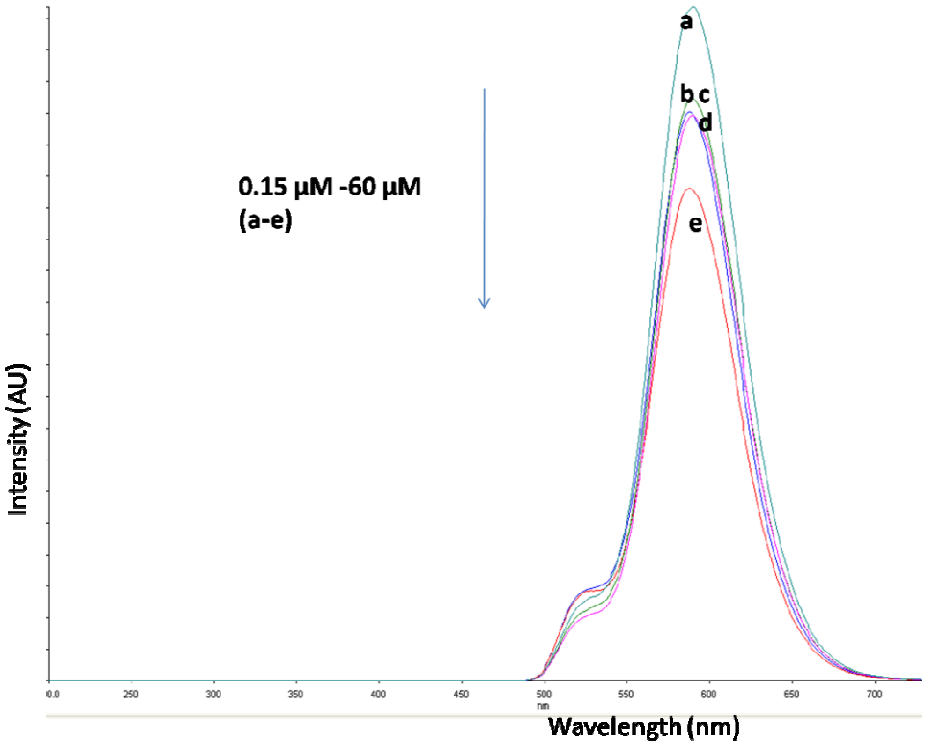

Fig-2.12. PL quenching of QD-MIP with addition of 0.15 µM -60 µM 2, 5 - DHBA

Further, the synthesized QD-MIP has been used for the detection of 3-PBA in urine (complex biological matrix) by studying the matrix effect. The matrix effect was studied by checking the quenching intensity in water and urine, while keeping all other parameters constant. It was found that, the change in phosphorescence quenching intensity on the addition of 3-PBA in urine was similar to change in phosphorescent quenching intensity of QD-MIP on addition of 3-PBA in water. Thus, the matrix effect of the material is negligible. Hence, it is inferred that the luminescence intensity of the QD-MIP and its application in sensor based assay of 3-PBA did not depend much on the components of urine matrix.

Analytical assay of the synthesized QD-MIP:

The analytical assay of the proposed method was performed with respect to linearity, LOD, recovery and precision. The synthesized MIP-capped Mn-doped ZnS QDs for 3-PBA shows good linearity with R^2 value of 0.980 for sensing 3-PBA in the concentration range of 0.15-60 µM (Fig-2.12).

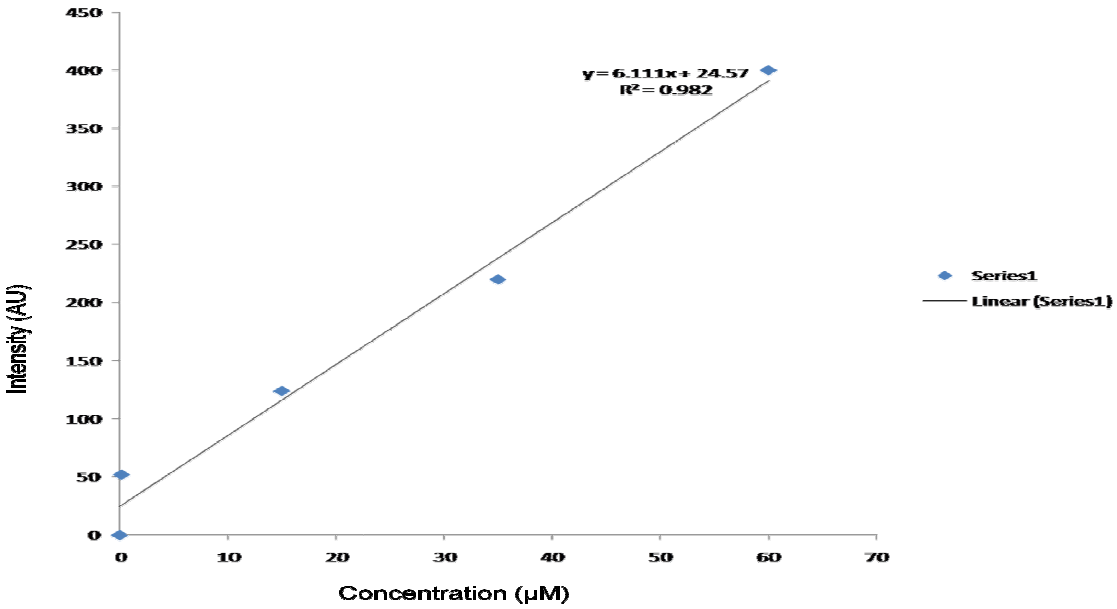

Fig-2.13. Calibration graph in the concentration range of 0.15-60 µM.

The developed method was also validated in spiked urine samples and was found to be successful in sensing 3-PBA in urine. LOD for 3-PBA was found to be 0.117 µM. Recovery study of the developed method was found to be in the range of 80-90% at three different concentrations (1, 30 and 60 µM). Precision (inter and intra-day) study was also performed at three different concentrations (1, 30 and 60 µM) and was found to be less than 8%. The percent recovery and precision values were summarized in table-2.1.

Table-2.1 Recovery and precision in spiked urine samples.

Matrices	Concentration level (µM)	% Recovery*	Precision	
			Intra-day	Inter-day
Urine	1	80.18	5.1	7.8
	30	84.28	4.1	6.9
	60	90.02	4.5	6.3

* Values based on triplicate analysis

Conclusion

In the present study, photoluminescence properties of QDs are used to sense 3-PBA in urine samples. This material acts as an optical sensor to check the exposure of pyrethroids through the analysis of 3-PBA in urine. Although the material could not quantify the analyte, but have several other advantages known and proved earlier in literature. It is highly stable and do not require any sample pre-treatment for its determination. Fabrication of the QD surface by MIP makes the material highly selective for the target analyte.

Chapter-3

Chapter- 3

Surface modification on manganese-doped zinc sulphide quantum dots by creating defects for the optical determination of methyl mercury, in river water samples

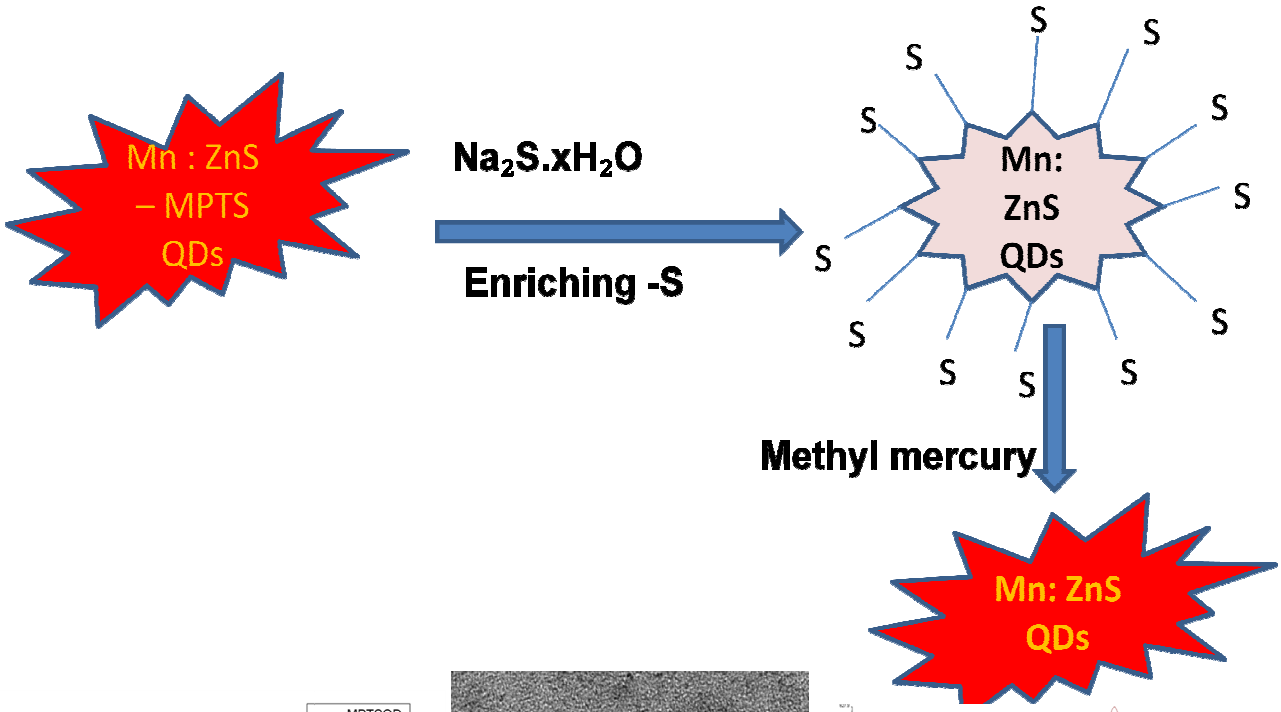

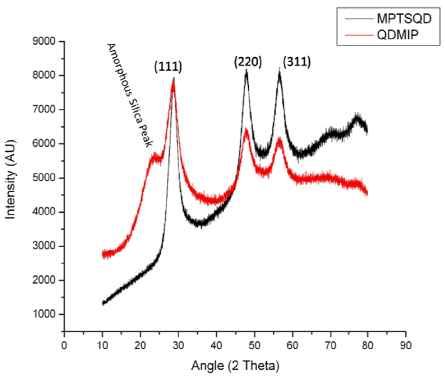

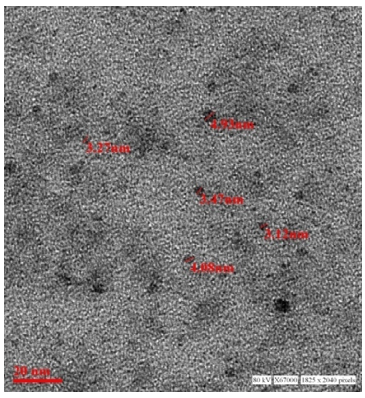

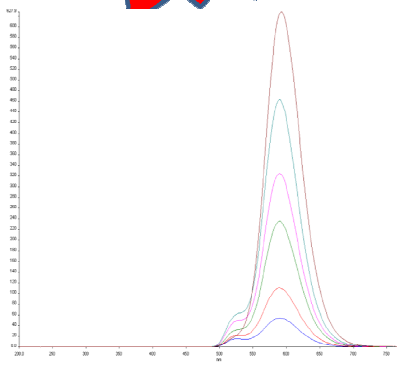

Chapter-3

3.1. Introduction

In the previous chapter, I have discussed about the surface modification of QD-MIP for enhancement of sensing and selective ability of the analyte. The imprinting technology proves the selectivity of MIP and fluorescent characteristics of QDs results in the formation of new affinity material for 3- PBA. Here, in the present chapter, turn-on approach have been used to sense methymercury in river water. The sulphur enriched Mn doped ZnS QDs as potential be a good turn-on optical sensor for methylmercury.

Now days, mercury is a big rising threat for human beings. Mercury is proved to be highly toxic element due to its accumulative and intact character in the environment. Both the inorganic and organic forms (methyl mercury) of the mercury are very fatal and being generated from different industrial activities mainly pharmaceutical, paper, electrochemical and plaguacide industries *(Uria et al. 1998)*. Various mercury containing compunds differ greatly in their physico-chemical and biological properties; among them, the methyl form is the most hazardous because of its volatility and its ability to pass through biological membranes such as the blood/brain barrier and the placenta. Accumulation of methyl mercury can cause kidney damage, irreversible central nervous system damage, paralysis, chromosomal breakage and birth defects *(Manahan et al. 1994; Craig et al. 1986; Rapsomanikis et al. 1991)*.

Human toxicity varies with the form of mercury, the dose and the rate of exposure. The target organ for inhaled mercury vapor is primarily the brain. Mercurous and mercuric salts chiefly damage the gut lining and kidney, while methyl mercury is widely

distributed throughout the body. Toxicity varies with dosage: large acute exposures to elemental mercury vapor induce severe pneumonitis, which in extreme cases can be fatal. Low-grade chronic exposure to elemental or other forms of mercury induces subtler symptoms *(Berlin et al. 2007)*. Organic mercury i.e. methyl and ethyl forms reacts with sulfahydryl (–SH) functional groups of the body hence potentially interfering the cellular and sub-cellular structure. The structures of methyl and ethyl mercury are shown in fig-3.1.

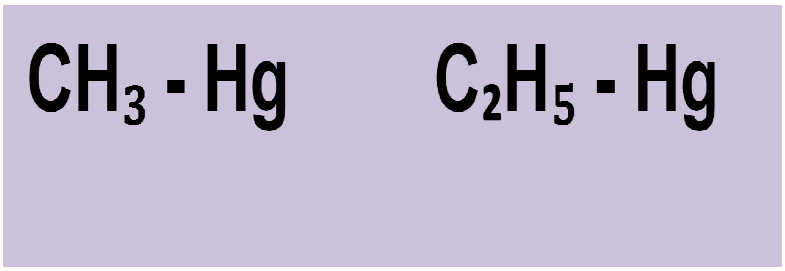

Fig-3.1. Structure of methyl and ethyl mercury

For qualitative and quantitative determination of mercury, several methods and sophisticated instruments are used along with their coupling. Generally atomic absorption spectroscopy is frequently used for the selective determination of methyl mercury. In recent years much effort have been made to develop various analytical techniques for the determination of methyl mercury in different biological and environmental matrices usually based on combination of separation techniques with elements specific detection *(Horvat et al. 2001)*. Instrumentation based techniques for separation and determination generally rely on LC and GC coupled to specific detector such as mass spectrometry. In comparison to GC, LC is generally preferred for the determination of methyl mercury. In LC, there is no need of derivatization in order to

gain volatility *(Morton et al. 2002; Rodrigues et al. 2010; Souza et al. 2010; Parsons et al. 2007)*.

In recent years, optical sensing has been explored as a straight forward method for detecting analytes present in very minute quantities. QDs serves as versatile tool to use as optical sensors. It shows increased use for sensing applications due to the size-dependent optical properties, large surface to volume ratio and quantum size effects *(Alivisatos et al. 1996; Chen et al. 1997; Peng et al. 2000; Xia et al. 2003; Liu et al. 2010)*. QDs have some very peculiar property that include high photostability and photoluminescence efficiency, sharp emission profile and size-dependent emission wavelengths which leads them to be a suitable material for sensing of various compounds in different matrices *(Tu et al. 2008; Wang et al. 2009)*.

Sensing applications can be effective based on its specificity, so modification of the luminescent QDs at its crystal lattice proves itself as a very efficient tool for its applications in the analysis. Cadmium salts were earlier used as precursor for various tailor made applications *(Li et al. 2010)*. Modification of surface of QDs by using a molecular imprinting technique paved a good approach for development of optical sensors. The MIP fabricated QD (QD-MIP) will provide the selectivity to the material due to presence of binding sites on the polymer matrix, which helps with the separation of analytes.

The combination of selectivity of MIP with fluorescent properties of QDs provides newer applications for the detection of the non phosphorescent analyte as it will possess specific recognition ability and variable intensity to the analytes of interest *(Zhang et al.*

2012; Zhao et al. 2012). To the best of our knowledge, no application has been reported for the detection of methylmercury by QD modified through S dangling bonds.

3.2. Experimental

Chemicals and reagents

All the reagents used in the study were of analytical grade unless otherwise stated. $ZnSO_4.7H_2O$, $MnCl_2.4H_2O$) (97% purity) and methyl mercury (II) chloride were procured from Sigma Aldrich (St. Louis, MO, USA). All the solvents used were procured from Merck (Darmstadt, Germany) and Sd. Fine Pvt. Limited (Mumbai, India). Sodium sulphide ($Na_2S.xH_2O$) purchased from Sd. Fine Pvt. Limited (Mumbai, India). PBS of 30 mM was prepared as a stock solution by addition of 30 mM of Na_2HPO_4 and 30 mM of NaH_2PO_4.The pH of the buffer solution was maintained by 30 mM H_3PO_4 and 0.1 M NaOH solutions. Fresh aqueous solutions in milli Q water of standards and samples were prepared during experiments.

Synthesis of MPTS capped Mn doped ZnS QD:

The MPTS capped Mn doped ZnS quantum dots were synthesized by following the earlier reported method with slight modification [10]. Briefly $ZnSO_4$ (12 mmol), $MnCl_2$ (1.2 mmol), and 70 mL of water was added in a three necked flask and the mixture was stirred under inert atmosphere in nitrogen at room temperature for 10 min. To this, 10 mL of aqueous solution containing Na_2S (12 mmol) was added drop wise and kept the mixture under stirring for 30 min. MPTS (0.5 mmol) dissolved in 10 mL of ethanol was added finally to the reaction mixture, and the reaction was kept for 20 hrs on stirring at room temperature. To ensure the purity and crystalline, the synthesized material was

thoroughly washed with ethanol and water to remove unreacted parts. The material was kept in the oven at 90℃ for drying, which leads to highly crystalline QD.

Synthesis of high sulphur containing MPTS capped Mn doped ZnS QDs :

The modified QD was prepared by earlier reported method *(Ren et al. 2011).* To a 100 mL flask, 40 mg of MPTS capped Mn doped zinc sulphide QD was dispersed in 40 mL aqueous solution which was stirred for 30 min. To the reactant mixture, 3 mL of 0.15 M of sodium sulphide solution was added. The resulting high sulphur containing material prepared was washed three to four times by water and ethanol. The final material was kept in oven drying for 24 hrs for further use.

Instrumentation:

The size of the nanocrystal was observed using transmission electron microscopy (TEM, Tecnai-G2-SPIRIT FEI, Netherland). A drop of aqueous solution of QD was placed on the copper grid to obtain images after sonication and coated with formvar. Absorbance, excitation and band gap energy were derived using a spectrophotometer, (SPECORD 210 PLUS, Analytik Jena, Germany). Fluorescence spectra of the QDs was obtained at an excitation and emission spectral wavelength of 330 and 590 nm, respectively (LS 55 photoluminescence spectrometer, Perkin Elmer, UK). The crystal lattice of the synthesized QD was obtained by using X-ray diffraction (XRD) using Cu target source (SEIFERT, Germany) at ACMS Lab, IIT Kanpur.

Photoluminescence Study:

Different concentrations of methyl mercury (0 to 25 µM) were prepared from stock solution. An amount of 2.5 mL of each concentration of the analyte and 2 mL of PBS buffer (pH 8) was mixed with 2.5 mL of high sulphur containg Mn: ZnS QD solution (30 mg L^{-1}) and kept for few minutes for interacting the analyte with QD. The complete dispersion was collected. An aliquot of 3 mL volume of the mixture was transferred to a cuvette for the photoluminescence study. The same procedure was followed for the non-modified QD interaction with the analyte at the specified concentrations. The phosphorescence quenching was measured at an excitation wavelength of 330 nm by keeping the slit width of 15 nm with an emission filter at 515 nm.

Method validation :

Validation assay of the developed method was performed with respect to limit of detection (LOD), precision, linearity and recovery. Calibration of methyl mercury was performed in the concentration range of 0-25 µM in water. LOD was calculated by determining the ratio of concentration of the analyte that increases the intensity to the standard deviation and slope (3:1). Precision study (intra- and inter-day) was carried using the synthesized high sulphur containing manganese doped zinc sulphide QD as an optical sensor at three concentration levels (5, 15 and 25 µM) in a day and also for five successive days. Recovery study was carried at three concentration levels (5, 15 and 25 µM) in urine. All the validation assays were performed in triplicate manner (n=3).

3.3. Results and Discussion

Synthesis of QD and modified QD:

The MPTS capped Mn doped ZnS quantum dots were synthesized by conventional precipitation of zinc sulphide from the precursors. The precursor for zinc was obtained from zinc sulphate and sulfur precursor from sodium sulphide in equimolar ratio to obtain ZnS in co-ordination number of 4 with atomic ratio as 1:1.The pure zinc sulphide has coordination number of 4 with respect to Zn and S which is possible only if the atomic ratio of the constituent ions remains 1:1.The doping of manganese ion in the crystal lattice of ZnS was done instantly with nucleation. Thus surface defects were obtained on the pure crystal lattice. Mn a d^8 metal having 5 unpaired electrons acts as a good luminescent centre.The properties of Mn is very much similar to zinc since both belong to 3d series and have less difference in size, hence can be easily doped in ZnS host crytal lattice. Initially, adding the dopant leads to incorporation of manganese in the nucleated particle. Growth of the formed nucleated particle decides the optico-electronic properties of the material, since variation in size governs the luminescence. Particle growth in homogenous and uniform manner was achieved by the capping agent. MPTS as capping agent used in the synthesis form covalent linkage with zinc ion through SH. Small sized QD capped with MPTS have silica networking that provides prevention of deformation in the synthesized material. Since sulphur can be easily leaked so inert silica networking is necessary. The temperature has a vital role in synthesizing small sized nanoparticles as high temperature lowers the activation energy

and fastens the rate of reaction. Here low temperature strategy was used for obtaining good quality QDs.

Characterization of modified and unmodified Mn-Doped ZnS QDs :

ZnS has a cubic Zinc Blende structure which is confirmed by the XRD pattern. The phase pure peaks for (111), (220), and (311) is in accordance with the JCPDS no. 05-0566. No other peaks in the diffraction pattern of the synthesized material was obtained in the diffractogram that confirms the formation of pure crystalline ZnS. The diffraction pattern of QD and modified QD shows slight differences in the intensity of peaks and also there is a notch in the lattice of modified QD, this explains that excess S containing QD is having low crystallinity as compared to pure QD (Fig-3.2.).

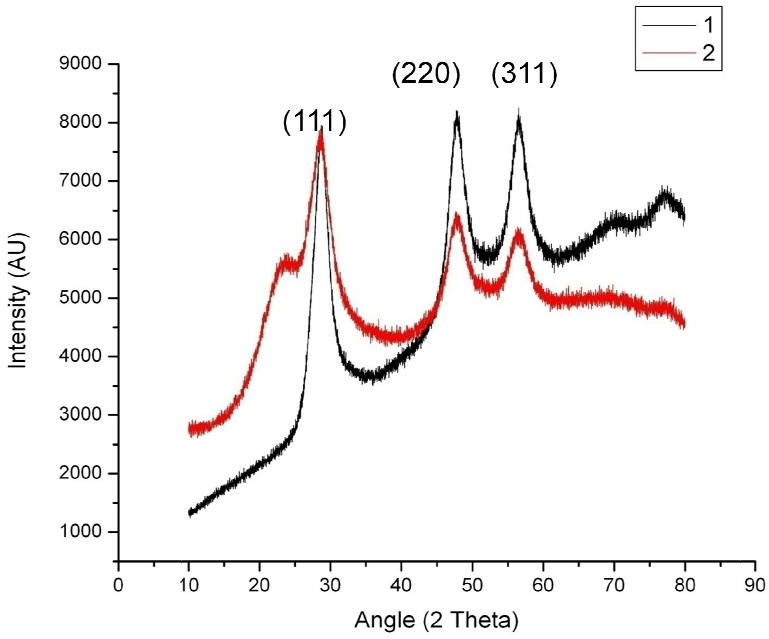

Fig-3.2. XRD analysis of enriched Sulphur-Mn:ZnS QD.

Further, the size for QD and modified QD were also calculated by XRD patterns by using scherer equation [β1/2 = 0.94λ/d cos□] *(Rodrigues et al. 2010)*. Where β1/2 refers to the full peak width at half maximum, λ refers to the copper target source, d refers to the size of the crystal lattice and □ refers to Bragg's angle. The size of QD and QD-S was calculated as 8 and 9 nm respectively. Further, the size of the modified QD was also measured by TEM, and the size was found to be in the range of 4-6 nm and particles are widely dispersed (Fig-3.3).

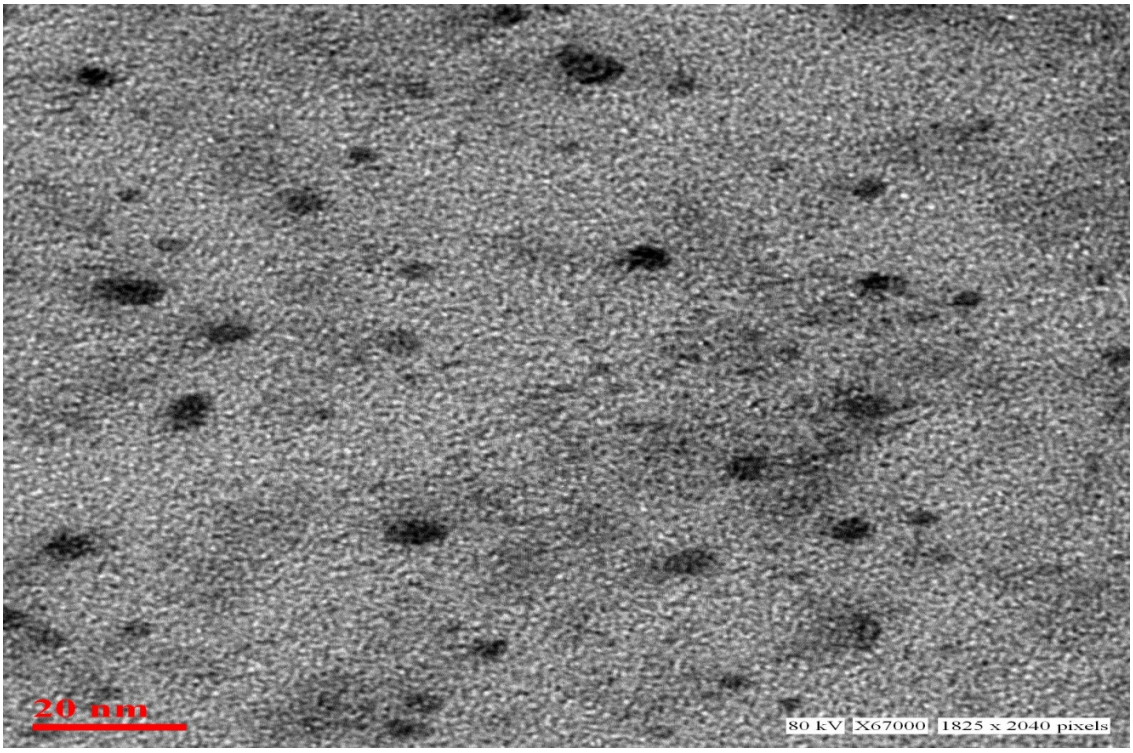

Fig-3.3. TEM Characterization of enriched S-Mn:ZnS QDs.

The luminescence study of the synthesized quantum dots shows that an excitation at 330 nm produces two effective emissions at 460 nm and 590 nm. The characteristic peak at 460 nm is of ZnS while orange emission at 590 nm gives the evidence of Mn

doping in the crytal lattice. PL spectra of synthesized MPTS capped QDs shows that manganese as dopant has been incorporated in the crystal lattice of zinc sulphide. Thus, it is confirmed that excess S containg Mn doped QD has been synthesized and is suitable for the analytical applications.

Sensing of methyl mercury by lattice modified QD :

The PL study is highly sensitive tool to analyse analytes in very minute quantities. The lattice modified Mn doped ZnS QDs has an emission in orange region at 590 nm with an excitation wavelength at 330 nm. The emission at 590 nm is attributed to the doping of Mn^{2+} ions.The deformation in the crystal lattice makes the material quite effective for analysis.The PL intensity increases as the structutre gets rid of its deformation. Since material contains high sulphur at its surface and it has been proved that Hg shows high affinity towards sulphur so as the methyl mercury gets interacted in the solution excess sulphur is removed. As the concentration of the analyte is increased, luminescence intensity gets increased, thus the sensing mechanism is a type of turn-on platform for the analysis and sensing of target analyte. The synthesized material has silica which is covering network for preventing leakage of dangled sulphur bond, which is a prerequisite for the material to act as turn-on sensor.Deformed bond has great deal of effect on luminescence intensity, thus, the increased concentration of the analyte leads to highly bright QD and hence increases the sensitivity and may detect the methyl mercury present in the matrix. Known concentrations (0-25 µM) of methyl mercury were added with a specific amount of QD & modified QD. Increase in the phosphorescent intensity of the excess S containg QD and QD with respect to the

addition of methyl mercury (0-25 µM) was studied (Fig-3.4). Sensing of the analyte is based on the effect of dangling bonds on optical properties due to defects in lattice.

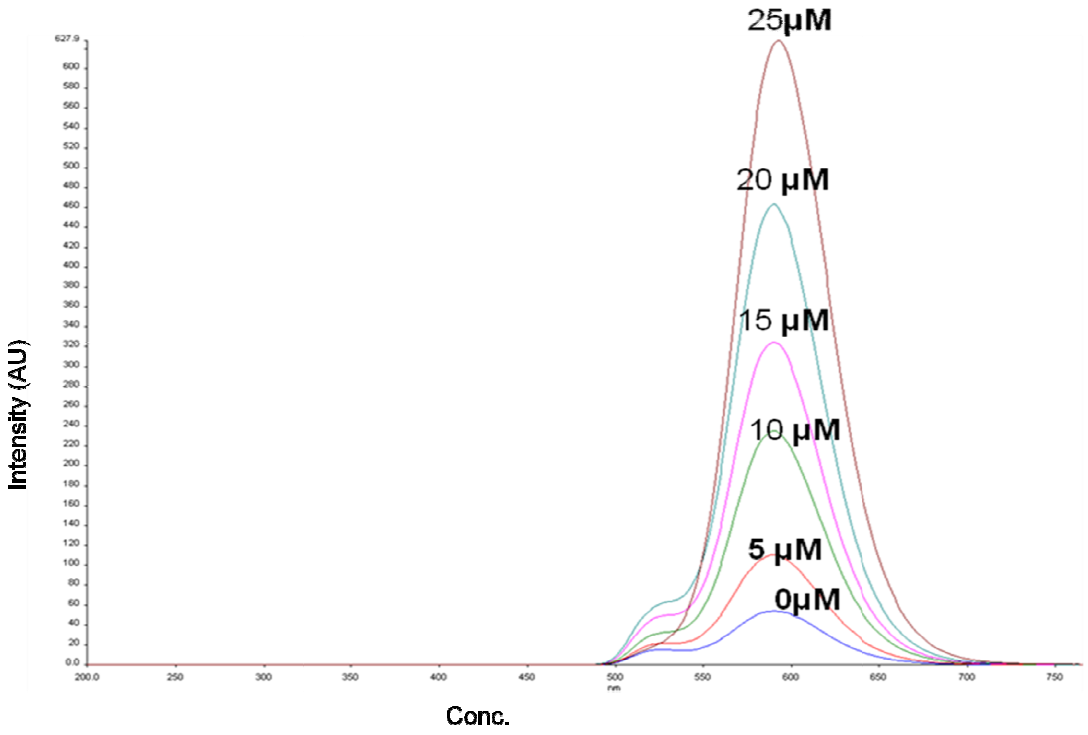

Fig-3.4. Variation in PL intensity at different concentration levels of methyl mercury.

Analytical assay of the synthesized modified QD :

The analytical assay of the proposed method was performed with respect to linearity, limit of detection (LOD), recovery and precision. The synthesized surface modified Mn-doped ZnS QDs for methyl mercury shows good linearity with a R^2 value of 0.99 for sensing methyl mercury in the concentration range of 0-25 µM (Fig-3.5)

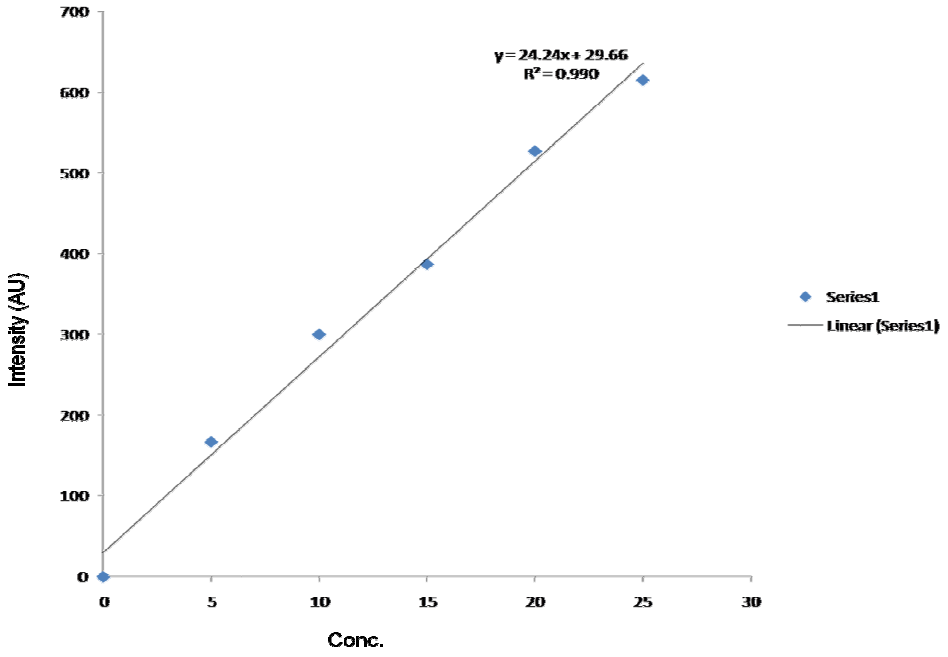

Fig- 3.5. Calibration graph in the concentration range of 0-25 µM.

The developed method was also validated in spiked water samples and was found to be successful in sensing methyl mercury in water. LOD was found to be 0.097 µM. Recovery study of the developed method was found to be in the range of 90-95% at three different concentrations (5, 15 and 25 µM). Precision (inter and intra-day) study was also performed at three different concentrations (5, 15 and 25 µM) and was found to be less than 6%. The percent recovery and precision values were summarized in table-3.1. **Table-3.1. Recovery and precision in spiked water samples**

Matrices	Concentration level (µM)	% Recovery*	Precision	
			Intra-day	Inter-day
Water	5	93.75	4.0	6.5
	15	89.47	4.1	7.9
	25	97.56	3.2	6.6

Conclusion

In the present study optoelectronic properties of QDs modified at surface are used to sense methyl mercury in water samples. This material serves as an optical sensor to determine the presence of highly toxic analyte in water samples and hence helps in checking the exposure of this highly profound toxic analyte on human health. The synthesized material could not quantify the analyte, but serve the purpose of sensing applications even in minute quantities. The synthesized material is highly stable and do not require any sample pretreatment for its determination. Fabrication of the QD surface by modification of the crystal lattice makes the material highly efficient as turn-on sensor for the target analyte.

Chapter-4

Chapter- 4

Biocompatibility evaluation of synthesized L-cysteine capped Mn:ZnS quantum dots and its biomedical application in intracellular imaging.

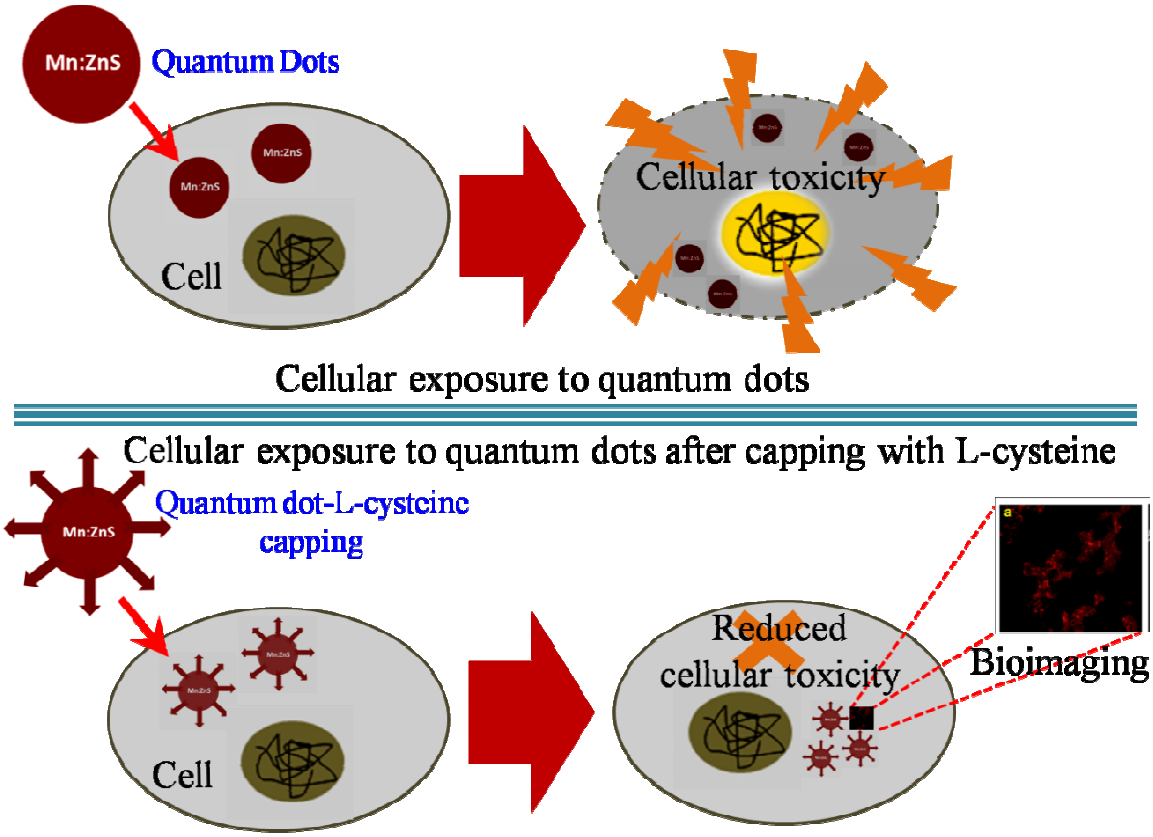

Chapter- 4

4.1. Introduction

The earlier chapters mainly deals with the applicability of Mn doped ZnS QDs for analytical applications. The quantum dots were fabricated by molecularly imprinted polymer for detection and sensing of 3-PBA while sulphur enriched material was synthesized and used for detection of methyl mercury. Here in this chapter, I have evaluated the toxicity of L-cysteine capped and uncapped Mn doped ZnS. The capping agents have enormous significance as it not only reduces the toxicity but also controls the size of the material. L-cysteine being the antioxidant has potential to act as toxicity reducer. The mercapto group of the molecule enables it to bind with the zinc metal ion and hence it is a good capping agent for zinc containing QDs. The structure of L-Cysteine is shown in Fig-4.1.

On the basis of strong quantum confinement, semiconductor nanocrystal quantum dots (QDs) are multipurpose fluorophores as compared to organic fluorophores due to their stability, broad optical property and tunable fluorescence. *(Rosetti et al. 1984; Efros et al. 1982; Klostranec et al. 2006; Pandey et al. 2013)*. The emission color of QDs (UV to visible to near infrared region) can be tuned by varying the size, chemical composition and surface chemistry of the material. Applications of QDs in various fields such as sensor development *(Frasco et al. 2009)*, drug delivery *(Dey et al. 2011)*, imaging applications *(Wang et al. 2010)*, either *in vivo* or *in vitro (Rizvi et al. 2010; Bruchez et al. 1998; Smith et al. 2008; Pinaud et al. 2006)* were explored due to the emergence of nanomedicine as an interdisciplinary area between nanotechnology and medical science. Cellular imaging has been explored using QDs for breast cancer Her2, actin,

microtubules, nuclear antigen and five tumor biomarkers *(Alivisatos et al. 2005; Gao et al. 2004; Wu et al. 2003; Yezhelyev et al. 2007)* and hence proved the importance of QD imaging in cancer research. Tracing infections, their movement and localization *(Li et al. 2009)* by cellular imaging are key areas of use of QDs in nanomedicine *(Wang et al. 2011)*. Cellular tracking by quantum dots, especially in imaging of stem cell tracking is another highly profound application of quantum dots for regenerative medicine *(Rosen et al. 2007)*. Thus, QDs have a great potential in biotechnology and medical applications *(Dubertret et al. 2002; Jaiswal et al. 2003; Zhu et al. 2004)*. Although conventional heavy metal based quantum dots like Cd have been extensively used in all aspects of technology but its release in the biological fluid causes stress, damage and cell death *(Rikans et al. 2000)* and inhibits the synthesis of DNA, RNA and proteins as well as breaking up DNA strands and mutating chromosomes *(Stohs et al. 1995; Prakash et al. 1998; Hossain et al. 2002)***.** Also the physico-chemical behaviour and cellular toxicity of nanocrystal QDs have wide dependence on the surface modification, capping agents *(Hoshino et al. 2004)* and size of QDs *(*Przybytkowski et al. 2009; Shiohara et al. 2004*)***.** Thus, synthetic strategies and capping agents are two important aspects of obtaining non-toxic and biologically applicable QDs. Aqueous synthetic strategies have been extensively used for the synthesis of various un-doped QDs containing metals such as Zn, Cd and Hg as nanocrystals as reviewed *(Lesnyak et al. 2013)*. Doping the QDs is a very important aspect of designing tailor-made material, since doping increases the stokes-shift due to very small gap in its emission energy with respect to the host material *(Kagan et al. 1996; Achermann et al. 2003)*. Thus, the doped semiconductor QDs (e.g. Mn:ZnS) have the enhanced optical performance than

the undoped counterparts, because of their low background noise. The non-toxic Mn causes large emission band gap and thus been proved to be potential dopant in various host lattices. Apart from impurity doping, suitable capping also plays a critical role in the application of QDs inside living systems. Hydroxyl group of thioglycerol, which has been used for bioconjugation in thiogycerol capped Mn:ZnS QDs, and have shown potential use for targeted *in vitro* delivery to a human cancer cell line *(Moritz et al. 2013)***.** However**,** L-cysteine has the greater potential, due to presence carboxylic and amino group, which can be used for further bioconjugation to other amino acids and proteins. Also, L-cysteine binds Zn strongly (*Shindo et al. 1965*), and hence may act as better capping agent from biocompatibility point of view *(Wang et al. 2011)***.**

In the present work, for the first time, an attempt was made to employ green, room temperature, aqueous synthetic route to obtain Mn:ZnS QDs capped with L-cysteine having a high optical response. The choice of the capping agent is based on the versatility of L-cysteine and its water solubility *(Wang et al. 2011)***.** As of our knowledge, it is the first report of the toxicological analysis of L-cysteine capped Mn: ZnS quantum dot synthesized at room temperature for imaging purpose.

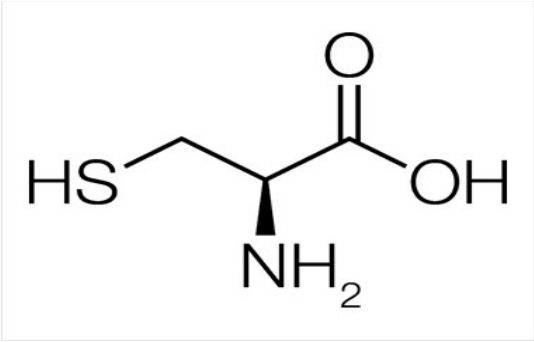

Fig - 4.1 Structure of L-Cysteine (Figure adapted from https://upload.wikimedia.org/wikipedia/commons/1/1a/L-Cystein-L-Cysteine.svg)

4.2. Experimental

Materials and methods

The chemicals and reagents used in this study were of analytical grade unless otherwise stated. Culture medium DMEM/F-12, antibiotics, foetal bovine serum and trypsin-EDTA were purchased from Gibco BRL, USA. Culture wares and other plastic wares used in the study were procured commercially from Nunc, Denmark. Milli Q water (double distilled deionized water) was used in all the experiments. Zinc sulphate heptahydrate ($ZnSO_4.7H_2O$), manganese (II) chloride tetra hydrate ($MnCl_2.4H_2O$), L-cysteine (97% purity) and ethanol were purchased from Sigma Aldrich. Sodium sulphide ($Na_2S.XH_2O$) was purchased from SD Fine Chemicals (Mumbai). The stock solutions were prepared using Milli-Q water and stored at 4^0C until their usage.

Synthesis of L-cysteine capped Mn:ZnS QDs :

To a 200 mL three necked flask, 25 mM of $ZnSO_4.7H_2O$, 2.5 mM $MnCl_2.4H_2O$ and 100 mL of water were added in presence of nitrogen gas with stirring for 20 min. Then a 10 mL aqueous alkaline solution of 15 mM L-cysteine, dissolved in Milli-Q was added. After being stirred for 2 hrs, 25 mM, Na_2S was added (dropwise) finally into the mixture. The mixture was kept stirring for 24 hours at room temperature. The synthesis yields good quality L-cysteine capped Mn:ZnS QDs which was obtained by centrifuging and washing the precipitate mixture with water for five times and finally drying in the vacuum.

Characterization of the synthesized QDs:

The size of the nanocrystal was observed using TEM, Tecnai-G2-SPIRIT FEI, Netherland. Briefly, a drop of aqueous solution of QDs was prepared after sonication and coated with formvar were placed on copper grid to obtain images. Absorbance and band gap energy was obtained and derived from spectrophotometer, SPECORD 210 PLUS, Analtik jena, Germany. A fluorescence spectrum of the QDs was obtained at 310 nm excitation using Perkin Elmer LS 55 photoluminiscence spectrometer, made in U.K. Emission maxima of 590 nm. The FTIR characterization of L-cysteine capped Mn: ZnS QDs was performed on Nicolet 6700 (U.S.A). Powder XRD pattern was computed on SEIFERT XRD, Germany in ACMS, X-Ray Lab, IIT Kanpur by the Cu target source.

In-vitro cytotoxicity assay

Cell Culture:

Human neuroblastoma cell line SH-SY5Y used in the study were procured from National Centre for Cell Sciences, Pune, India and maintained at *in-vitro* toxicology laboratory, CSIR-Indian Institute of Toxicology Research, Lucknow, India, as per the standard protocols. In brief, the cells were cultured in DMEM/F-12, supplemented with 10% foetal bovine serum (FBS), 0.2% sodium bicarbonate, 100 units/ml penicillin G sodium, 100 µg/ml streptomycin sulphate and 0.25 µg/ml amphotericin B. Cultures were maintained at 37^0C in 5% CO_2-95% atmosphere under high humid conditions. Medium was changed twice weekly and cultures were passaged at a ratio of 1:6 once in a week. Prior to use in the experiments, cells viability was ascertained by trypan blue dye exclusion assay. The culture showing viability more than 95% were used in all the

experiments. All the experiments were done on the cells with passage 18-25 only.

MTT assay:

Non-cytotoxic dose of the Mn:ZnS QDs were identified in SH-SY5Y cell line (human neuroblastoma cell line). Cytotoxicity assessment was done using standard endpoint, i.e., tetrazolium bromide MTT assay as described by *Tripathi et al. 2014***.** In brief, SH-SY5Y cells ($1x10^4$ cells/well) were seeded in 96-well tissue culture plates and incubated in the CO_2 incubator for 24 h at 37℃. Then the medium was aspirated and cells were exposed to medium containing Mn:ZnS QDs (0.1 to 2 g/L) for 24 - 96 h at 37^0C in 5%-CO_2-95% atmosphere under high humid conditions. Tetrazolium salt (10 µl/well; 5 mg/ml of stock in PBS) was added for 4 h prior to completion of respective incubation periods. At the completion of incubation period, the reaction mixture was carefully taken out and 200 µl of culture grade DMSO was added to each well. The content was mixed well by pipetting up and down several times until dissolved completely. Plates were then incubated for 10 minutes at room temperature, and color was read at 550 nm using Multiwell Microplate Reader (Synergy HT, Bio-Tek, USA). The unexposed sets were also run parallel under identical conditions that served as a basal control.

Neutral Red Uptake (NRU) assay:

The assay was carried out following the protocol described earlier by us *(Siddiqui et al. 2008)***.** Cells were exposed to Mn:ZnS QDs in identical experimental setup as to MTT assay. Upon the completion of incubation period, medium was aspirated and NRU salt (50 µM/mL in a medium) was added 100 µl per well plate and incubated for three hours.

Then, the reaction mixture was carefully taken out and plates were washed with washing solution (100 µl/ well) containing 1% $CaCl_2$ (w/v) and 0.5% HCHO (v/v) to remove unincorporated dye. Washing solution was removed and mixture of 200 µl of 1% acetic acid and 50% ethanol was added. The plates were kept on the rocker shaker for 10 minutes at room temperature and then analyzed at 540 nm using multi-well microplate reader (Synergy HT, Bio-Tek, USA). Unexposed sets were also run under identical conditions, which served as control.

Fluorescence localization:

Briefly, cells ($1x10^4$ cells/ well) were allowed to adhere on the surface of eight well chamber slides (Lab Tek, Campbell) and incubated with DMEM/F-12 medium with 10% foetal bovine serum in the CO_2 incubator for 24 h at 37°C. Cells were exposed to compound (0.2 g/L) for 24 h to uptake the compound. Following exposure, cells were washed three to four times with PBS to remove the unbound compound. The cells in the other two wells in the absence of compound were also incubated for 24 h for comparison. Cells were visualized under fluorescent microscope (Nikon Eclipse 80i equipped with Nikon DS-Ri1 12.7 megapixel camera, Japan).

4.3. Results and discussions

The fluorescent L-cysteine capped Mn:ZnS QDs were obtained by precipitation of Zn^{2+} from its sulphate and S^{2-} from sodium sulphide. Mn^{2+} ion was incorporated as a dopant in the crystal lattice by simultaneous nucleation from its chloride salt. The conventional synthesis of Mn doped QDs require addition of base in the form of hydroxide ion which

may lead to the formation of zinc hydroxide and hence would interfere with the equilibrium of ZnS precipitation. Since ZnS precipitation occurs at a definite pH, sodium sulphide aqueous solution having pH in the range of 11-13 at 25 mM strength is suitable for the successful reaction. In the present work, the reaction conditions were optimized in a new way by adding capping agent along with alkaline medium to prepare ZnS QDs. This addition process will help to reduce the probability of formation of zinc hydroxide (ZnOH) which is routinely observed when alkaline medium was added before the addition of capping agent. This will improve the optical property of the synthesized ZnS QDs. The co-precipitation of zinc and manganese is the best way of incorporating Mn ions as a dopant in the crystal structure. This will enhance the entrapment of Mn ions in the crystal lattice, which is a prerequisite for orange emission of the synthesised QDs. Low temperature is suitable for nucleation, thus the synthesis of QDs were done at room temperature as it will produce fast and homogenous nucleation. Variation of temperature was done in the range of room temperature to 80^{o}C for initial 2h after adding Zn, Mn, and water. The results show high photoluminescence at room temperature (Fig - 4.2) in comparison to the reaction conducted at other temperatures.

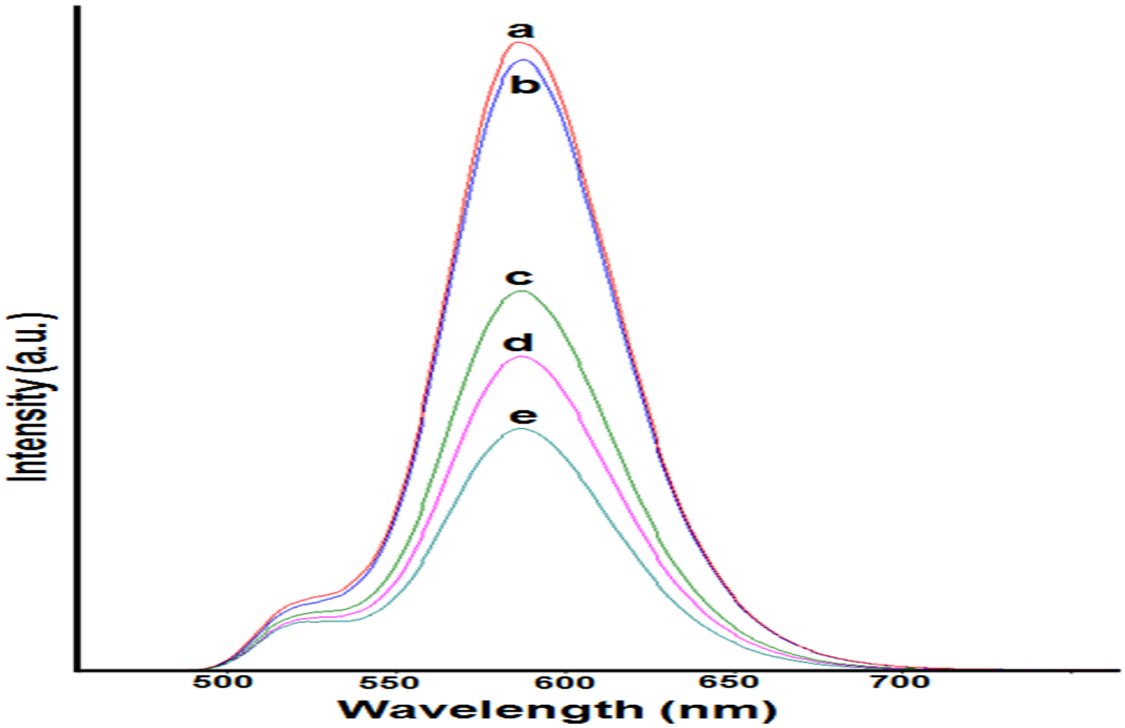

Fig-4.2. Variation of luminescence intensity at (a) room temperature, (b) 35℃, (c) 50℃, (d) 60℃ and (e) 80℃ QDs.

Thus we inferred that nucleation occurs within 1-2 h of the reaction. On addition of S^{2-} ions, a white precipitate is obtained which slowly leads to the growth of ZnS nanocrystals after being stirred for 24 h. The addition of L-cysteine as capping agent in the synthesis was done finally to arrest the particle growth so that small sized and highly energetically confined particles can be obtained. Since high temperature of reaction may lead to large size particle, we have grown the particles at room temperature for 24 h so that the rate of ostwald ripening may be reduced, and enough energy can be obtained to cross the threshold barrier.

The UV-visible absorption spectrum of synthesized QDs was recorded to prove the quantum confinement. The large blue shift is evident in the spectrum (Fig - 4.3) due to

observance of onset at 310 nm with an edge at 285 nm. The large blue shift is in agreement with the small size of the nanocrystal. The photoluminescence (PL) emission peak of Mn:ZnS QDs was observed at 590 nm, due to the well-known $^4T_1$-$^6A_1$ transition *(Erwin et al. 2005; Yan et al. 2006; Norris et al. 2008)* at 310 nm excitation wavelength (Fig- 4.4). This can be attributed to the Mn^{2+} ions caused the surface defect in the Mn:ZnS nanocrystal, which is responsible for the orange emission caused by crystal field effects *(Bhargava et al. 1994)*.

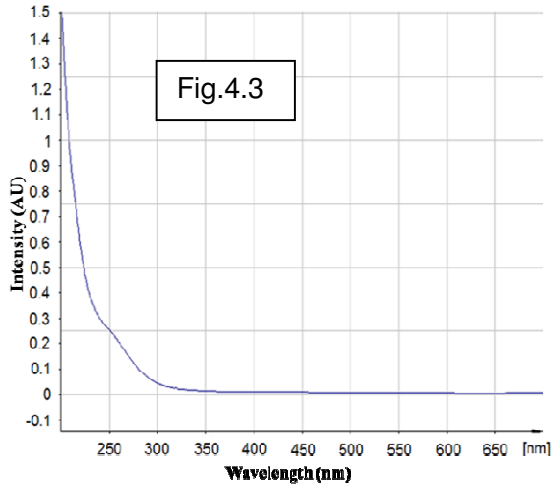

Fig-4.3. Absorption spectrum of Mn:ZnS QDs

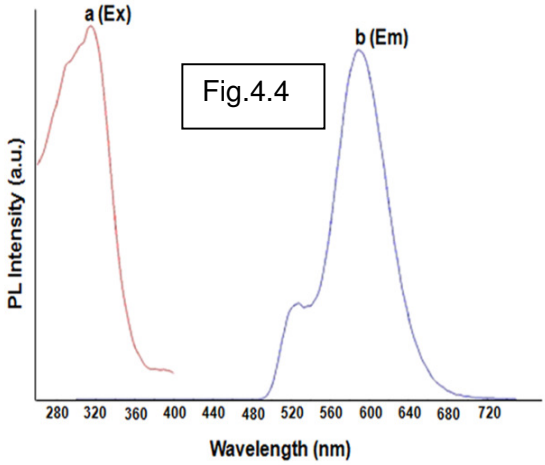

Fig- 4.4. Excitation emission spectrum of L-Cysteine capped Mn:ZnS QDs

The large stokes shift as evident in our material proves the utility of the synthesized material for low background noise imaging applications in biomedicine. The correlation of PL spectra with the UV visible spectra supports the strong quantum confinement which is in accordance with the band edge luminescence parameters. It has also been found that the QDs were stable for eight months in water in the colloidal state at room temperature without any preserving chemicals and specific environmental conditions.

The size and morphology of the nanocrystals have been observed in the TEM micrograph (Fig - 4.5).

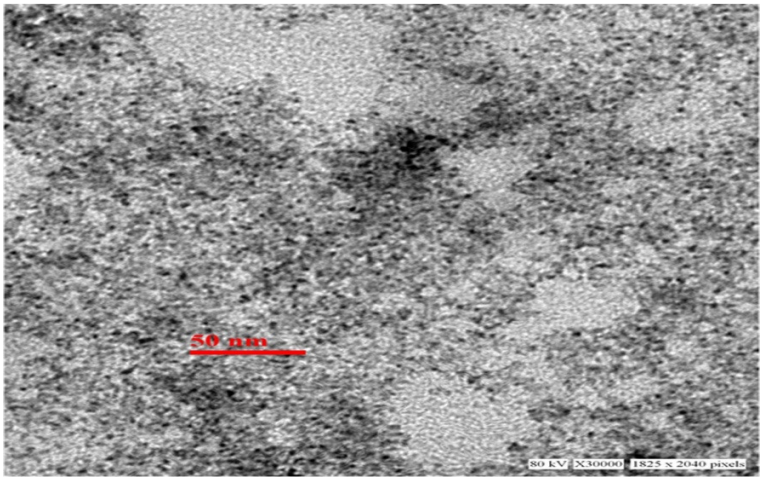

Fig- 4.5. TEM characterization of L-Cysteine capped Mn:ZnS QDs.

As evident from the above image, small sized QDs with homogenous size distribution were formed. The size of QD plays a vital role in its biological uptake and hence decides fate of the nanocrystals. Optical property of the synthesized material is in accordance with the small size effect on energy confinement, which leads to large blue shift of wavelength. Binding of the L-cysteine capping agent with Mn:ZnS QDs was confirmed by the FTIR spectra (Fig- 4.6) where strong affinity of the SH group of L-cysteine with zinc ion of the ZnS was explored. Characteristic peak at 1500-1600 cm^{-1}, and 1400 cm^{-1} correspond to the carboxyl group. The specific peak at 2550-2670 cm^{-1} represents the mercapto group of the L-cysteine. Comparing the IR spectra of QD capped with L-cysteine and spectra of L-cysteine powder, it was observed that the characteristic peak at 2550-2670 cm^{-1} found in L-cysteine was not observed in L-cysteine capped Mn:ZnS QDs.

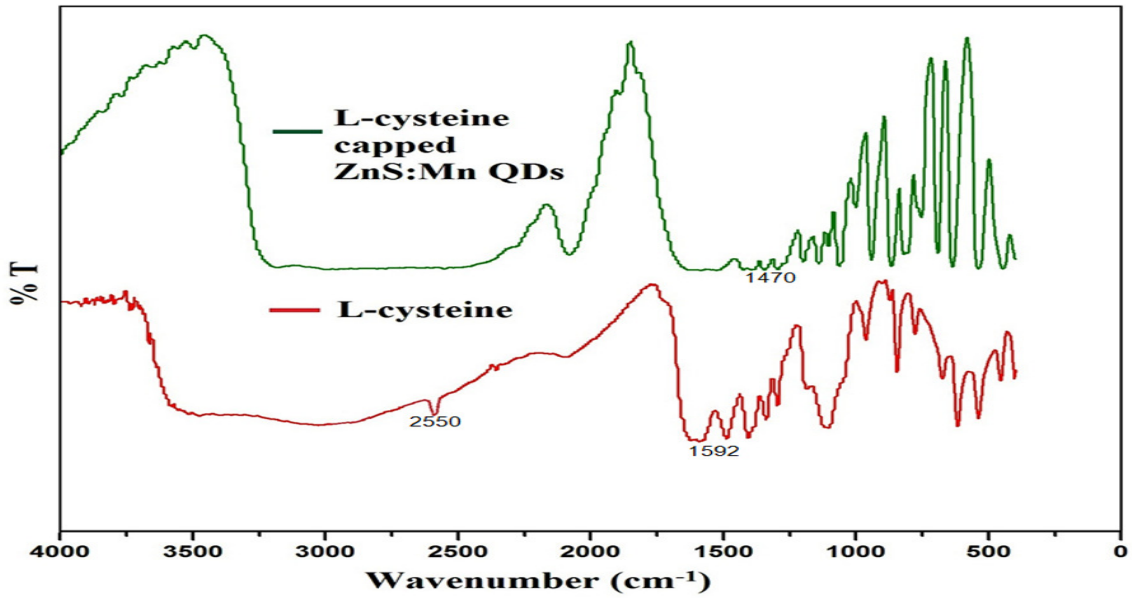

Fig- 4.6. FT-IR characterization of L-Cysteine capped Mn:ZnS QDs.

Hence the covalent interaction of zinc ion with the thiol group (SH) of the capping agent comes into play. Adsorption of L-cysteine capping agent through covalent bond between Zn ion and SH group of L-cysteine is pH dependent as the thiol group deprotonated in alkaline pH. There is competition between sulphide and thiol to bind with Zn ion, which decides the stability of the QDs. To obtain small sized QD appropriate amount of capping agent, has been used in the reaction mixture which is suitable for the formation of stable QDs.

In the XRD pattern of synthesised Mn:ZnS QDs, it was observed that the peaks have been found at 28.6, 47.7 and at 56.5°, corresponding to (111), (220) and (311) planes, which have typical miller indices for cubic zinc blende (JCPDSno.05-0566). Since ZnS exists in two forms, cubic blende and hexagonal wurtzite, due to its polymorphic property, hence the powder XRD data peaks of Mn:ZnS QDs (Fig- 4.7) confirm the evolution of cubic zinc blende structure. There is no other significant peak in the

diffraction pattern of the material was observed, indicating that the synthesized product is phase pure ZnS and the added amount of Mn in the Mn:ZnS QDs do not interfere the crystallinity of the host ZnS. The full width at half maximum (FWHM) of XRD peak are broaden, indicating formation of small sized nanocrystal QDs, as observed in TEM image and optical study.

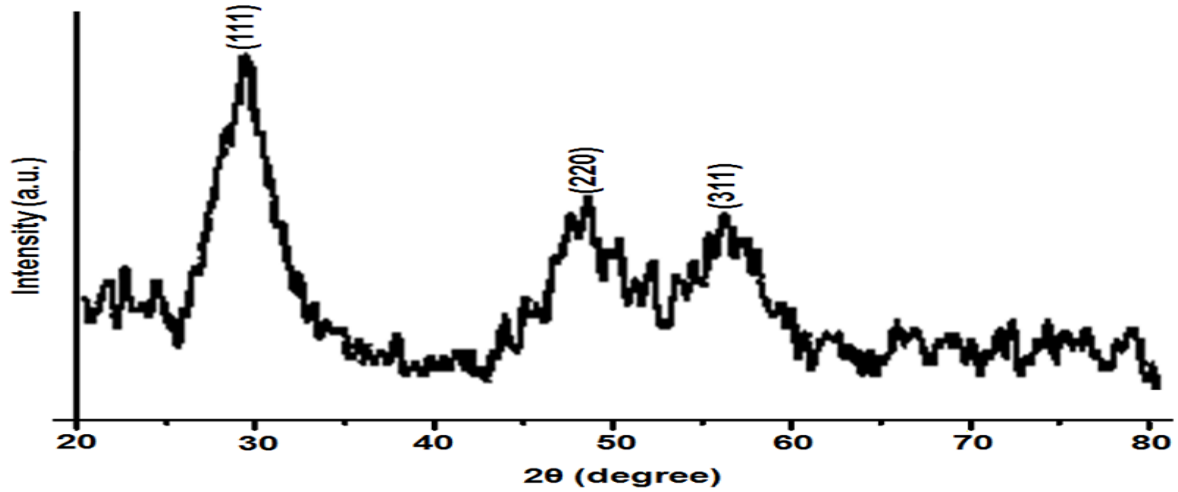

Fig- 4.7.XRD characterization of Mn:ZnS QDs

The characterization of the synthesized QDs by UV, Photoluminescence, FTIR and XRD confirms the chemical composition and structure of the material. The size and optical properties are key characterizations which enable them for imaging in biomedical science. Although the small size and homogenous nanoparticles have been synthesized but to be applicable in living cells the material has to be non-toxic and water soluble. MTT and NRU assays were used to evaluate the toxicity of the synthesized material. These assays are intracellular toxicity parameters and cell lines were used as model for the effects of the particle at various concentrations and with respect to the time in hours.

Toxicity Evaluation Studies:

The MTT assay has shown that the neuronal cells responded significantly to the L-cysteine capped Mn:ZnS QDs in a dose dependent manner. Cells exposed to QDs (0.1-1.5g/L) have shown no significant reduction in percent cell viability till 96 h. Whereas, higher concentrations of QDs i.e., 2 g/L was found to cause gradual reduction in percent cell viability, which reaches to significant levels and it shows 84±1.15, 79±1.73, 71±2.31 and 56±1.15 at 24, 48, 72 and 96 h respectively (Fig - 4.8). The dosing of Mn:ZnS QDs without capping shows toxic behaviour and cell death was observed even at very low concentration of 0.1 g/L (Fig - 4.9).

NRU assay has also shown similar results as shown by MTT assay means the QDs responds significantly. At 0.1-1.5 g/L, no significant reduction in percent cell viability were found till 96 h whereas at 2 g/L, the cell viability was reduced from 87±1.73, 81±2.31, 75±3.46 to 59±1.15 at 24, 48, 72 and 96 h respectively (Fig - 4.10). Toxicity was observed for NRU assay of uncapped QDs similar to the MTT evaluation at the dosing level of 0.1g/L (Fig - 4.11).

The MTT and NRU assay confirms that the Mn doped zinc sulphide QDs become non-toxic when they are capped with L-Cysteine as capping agent. Thus, the prepared QDs are biocompatible and have large potential to be used in living cells. The MTT and NRU confirm that the concentration of QDs capped with L-cysteine up to 1.5 g/L can be internalized by the cells. The gross toxicity was also evaluated by microscopic imaging. This will enable the applicability of synthesized material for bioimaging applications.

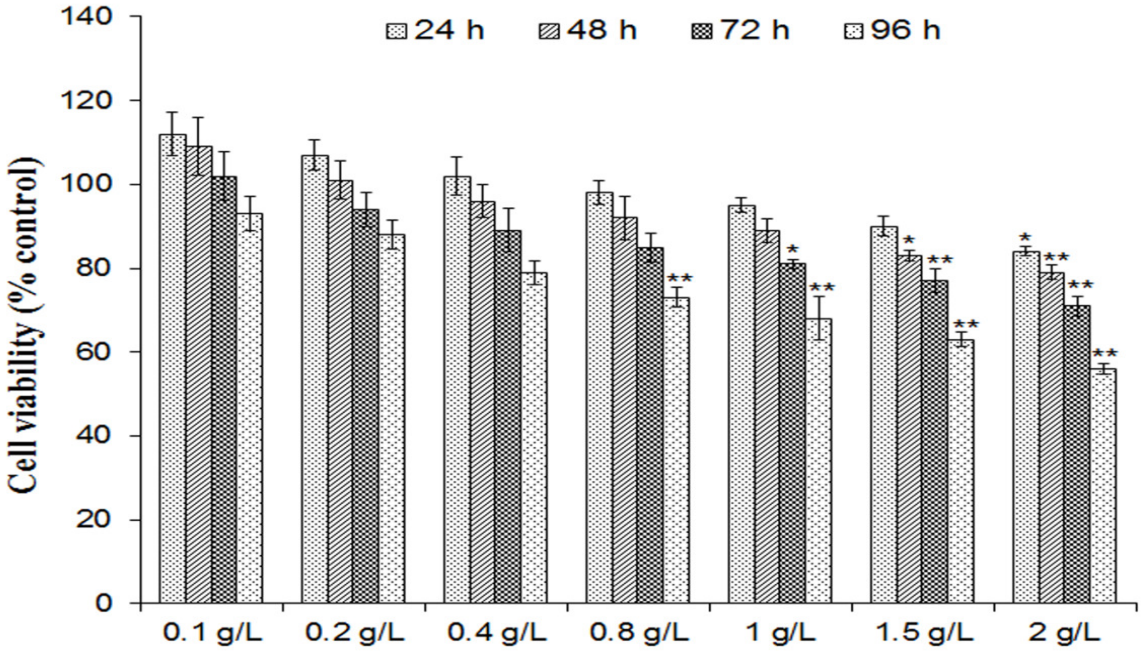

Fig-4.8. Identification of noncytotoxic doses of L-cysteine capped Mn:ZnS QDs in neuronal (SH-SY5Y) cell line. Cells were exposed to L-cysteine capped Mn:ZnS QDs (0.1-2 g/L) for 24-96 h in SH-SY5Y. The percent cell viability was assessed using MTT assay. Values are given as mean ± SE of the data obtained from three independent experiments. *p < 0.05, **p < 0.01 in comparison to unexposed controls.

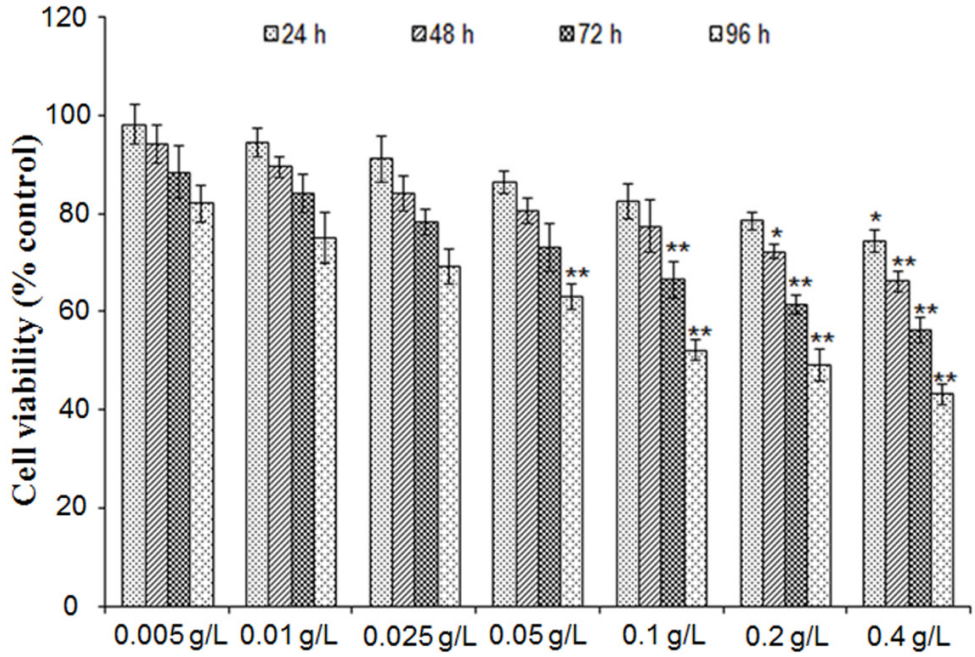

Fig- 4.9 Identification of noncytotoxic doses of uncapped Mn:ZnS QDs.in neuronal (SH-SY5Y) cell line. Cells were exposed to uncapped Mn:ZnS QDs (0.005-0.4 g/L) for 24-96 h in SH-SY5Y. The percent cell viability was assessed using MTT assay. Values are given as mean ± SE of the data obtained from three independent experiments. *p < 0.05, **p < 0.01 in comparison to unexposed controls.

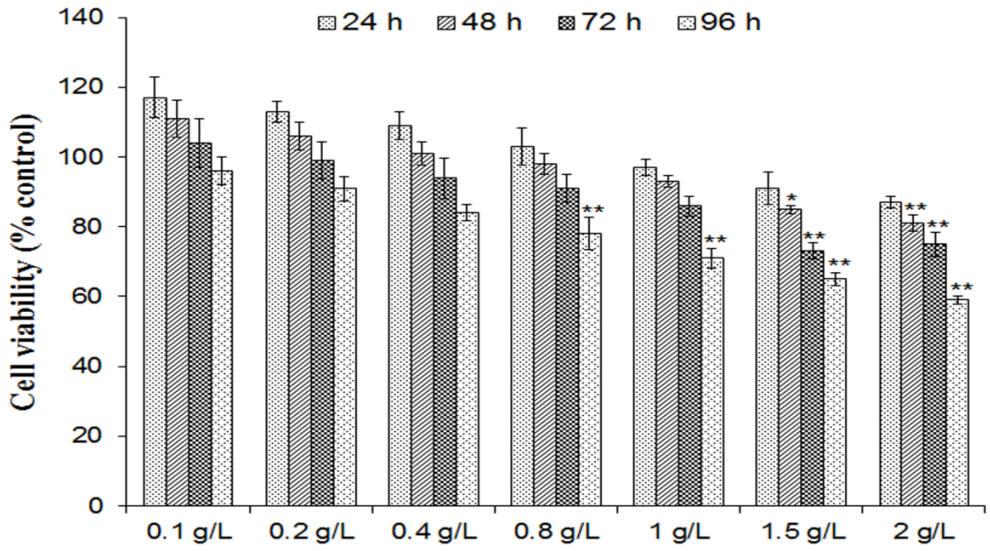

Fig - 4.10 Identification of noncytotoxic doses of L-cysteine capped Mn:ZnS QDs in neuronal (SH-SY5Y) cell line. Cells were exposed to L-cysteine capped Mn:ZnS QDs (0.1-2 g/L) for 24-96 h in SH-SY5Y. The percent cell viability was assessed using NRU assay. Values are given as mean ± SE of the data obtained from three independent experiments. *p < 0.05, **p < 0.01 in comparison to unexposed controls.

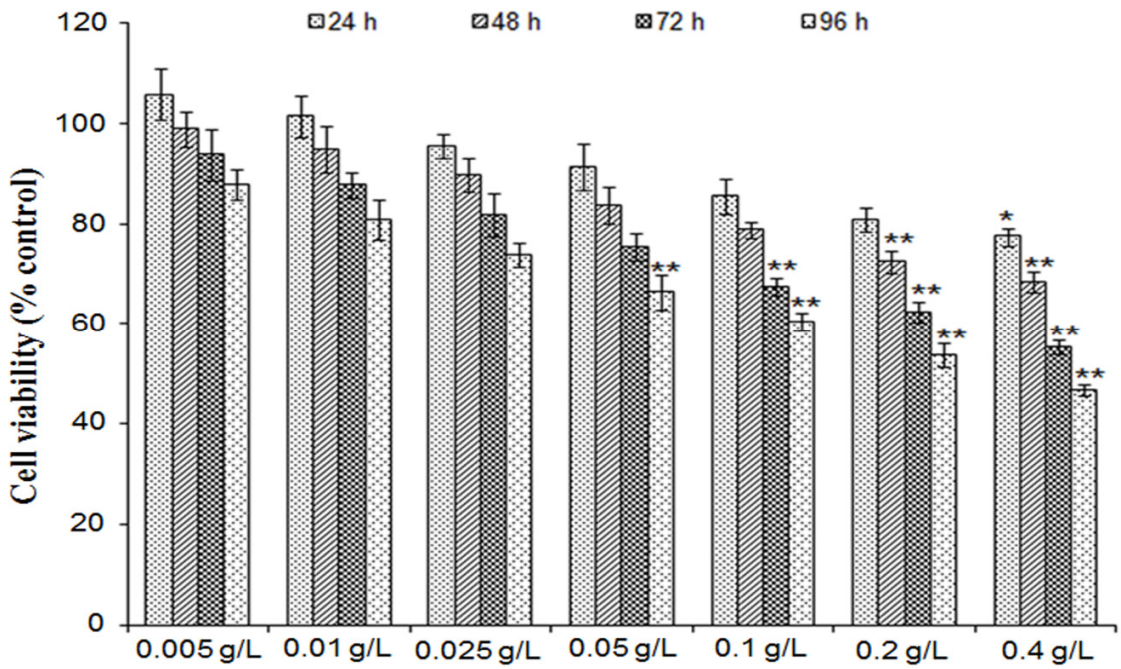

Fig - 4.11 Identification of noncytotoxic doses of un- capped Mn:ZnS QDs in neuronal (SH-SY5Y) cell line. Cells were exposed to uncapped Mn: ZnS QDs (0.005-0.4 g/L) for 24-96 h in SH-SY5Y. The percent cell viability was assessed using NRU assay. Values are given as mean ± SE of the data obtained from three independent experiments. *p < 0.05, **p < 0.01 in comparison to unexposed controls.

The applicability of the QD in biological imaging was done by incubating cells with 0.2 g/L of L-Cysteine capped Mn:ZnS and as a result of this, it was found no agglomeration of nanoparticles outside the cell membrane. The images as shown in Fig - 4.12 (a & b) gave the complete information of uptake of QDs inside the cell. Since in the process, no bioconjugation was used, therefore, it is imperative that uptake of QDs takes place through endocytosis. To demonstrate the availability of the prepared QDs for bioimaging

applications, the QDs were employed to monitor the intracellular QD in SH-SY5Y cells.

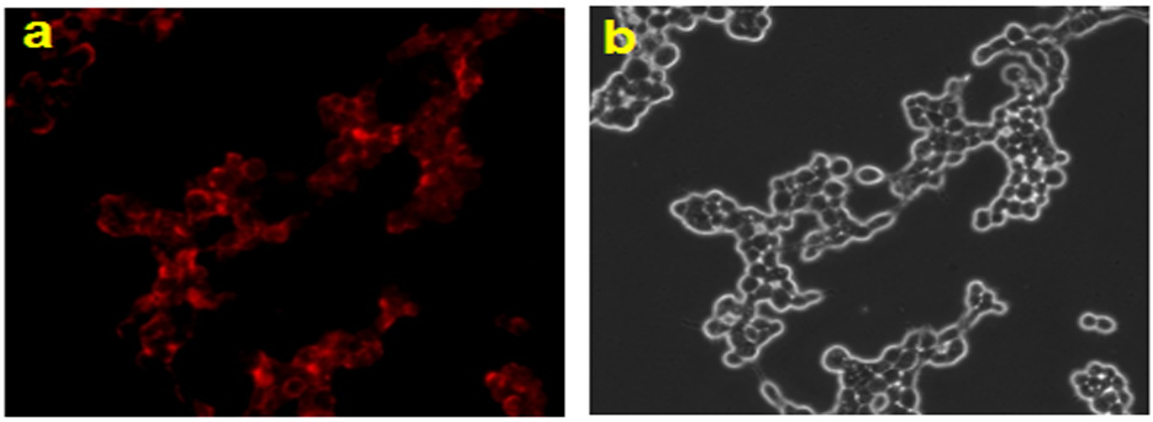

Fig - 4.12 Cellular uptake of L-Cysteine capped Mn:ZnS QDs. Fluorescence images (4.12 a) and their corresponding bright field transmission images (4.12 b). SH-SY5Y cells were cultured in 8 well chamber slide for 24 h after that, the cells were incubated with ZnS:Mn (0.2 g/L) in a fresh medium for 12 h. After that, biological imaging have been done with the help of fluorescent microscope.

Fluorescence microscopic studies showed that incubation of the SH-SY5Y cells with QD gave a photoluminescence in the red region (Fig - 4.12a). The corresponding bright-field measurements after the exposure with QDs confirm that the photoluminescence was significant in the intracellular area (Fig - 4.12b), indicating the QD was internalized into the living cells from the growth medium. The results indicate that the QD may be internalized by the process of endocytosis. Furthermore, the cytotoxicity of QDs is negligible as confirmed by the facts that no significant changes in cell morphology (Fig - 4.12a & b) and cell viability after the treatments of SH-SY5Y cells with QDs were observed.

Conclusions

Highly photoluminescent Mn:ZnS QDs capped with L-cysteine was synthesised by aqueous green synthetic methodologies at room temperature. The study establishes the fact that the nucleation of nanoparticles requires only low temperature which resulted in non-toxic, small and homogenous Mn:ZnS QDs. L-cysteine as a capping agent has reduced the toxicity of Mn:ZnS to a larger extent. Further, this will enhance the bright imaging of cells with low background emissions due to internalization of large number of QDs. Further, L-cysteine improves the biocompatibility of Mn:Zns QDs and activates endocytotic uptaking of the particles.

Chapter-5

Chapter- 5

Imidazole capped Mn: ZnS QDs: Synthesis, Characterization and Biocompatibility evaluation at cellular and genetic level

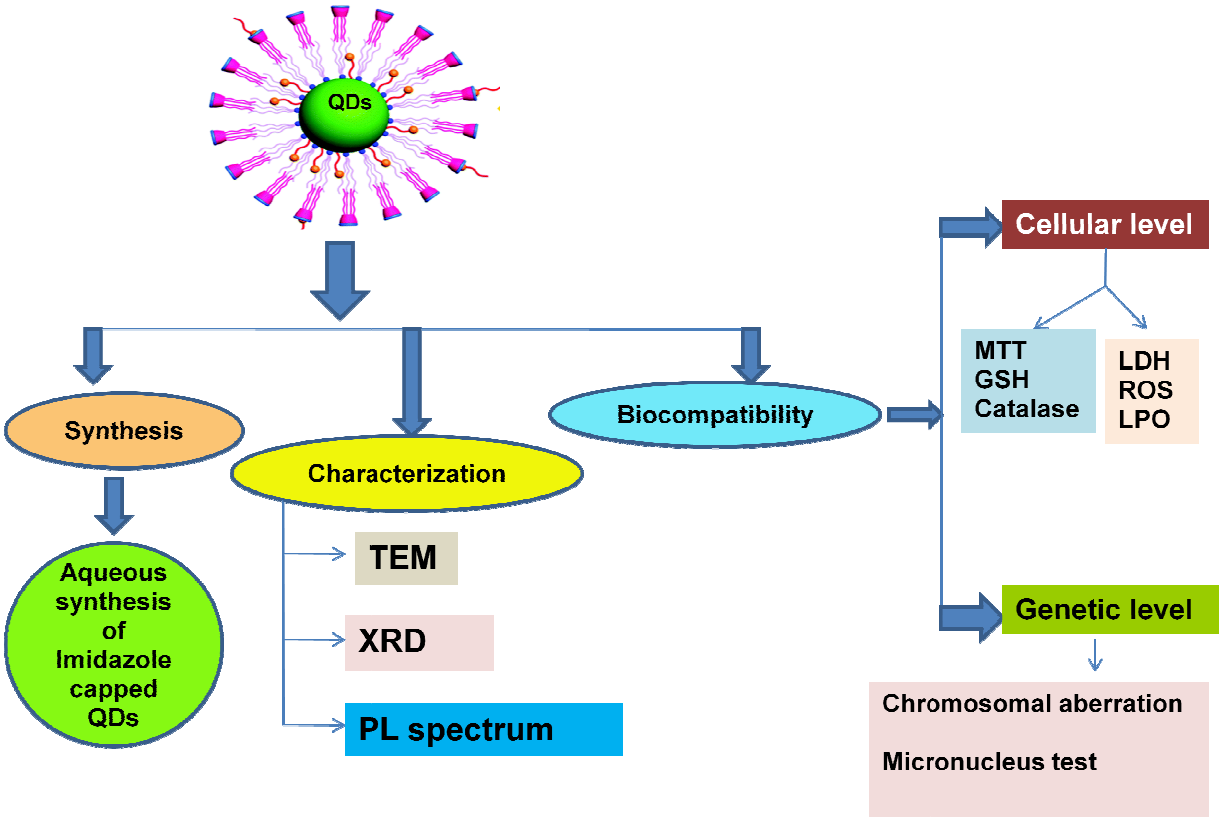

5.1 Introduction

The evolution of quantum dots (QDs) has revolutionized the nanotechnology world with its unique properties [*Bruchez et al 1998; Chan et al 1998; Coe et al, 2003*]. The small size, selectivity, stable and tunable optical properties [*Brus et al 1983; Ekimov et al 1984;Rossetti et al 1983;Bawendi et al 1992; Bawendi et al,1990*] are the key aspects that have been extensively studied for imaging and sensing applications. Various routes have been investigated to synthesize small sized and homogenous QDs, but among all the aqueous synthesis of the particle involving low temperature has various advantages over conventional routes by obtaining non-toxic and functionalized material [*Gaponik et al 2002*]. Capping agents play vital role in employing aqueous synthetic strategy as they are the only source to control the size of the material and has advantage to reduce the toxicity of QDs [*Rzigalinski et al 2009*]. In view of these, capping agents are said to be significant as they are the only part of the nanomaterial that interacts with the surface and helps in preparing tailor-made material with good quantum yield [*Reiss et al 2003*].

Various biomolecules [*Yang et al 2011*] and surfactants [*Fan et al 2005*] have been explored for the evolution of the functionalized material. The surface decorated QDs with specific molecules or surface active agents prove its efficacy both in biological [*Peng et al 2013*] and chemical fields [*Manuela et al 2009*]. For the application of nanoparticles in biological field, it has to pass through the toxicity tests so toxicity assessment is prerequisite for the QDs application in living cells. The toxicity of the QDs depends on various parameters like core material, capping agent and synthetic route [*Hardman et al 2006*]. Cadmium based QDs have shown toxicity at all levels due to leakage of the metal ion in the matrix [*Derfus et al 2004*]. Although the emergence of

zinc sulphide/cadmium sulphide core shell QDs solved many of the problems of core containing material but these also needed some more advancement in the development of biocompatible nanoparticles [*Dong et al 2014*]. The wide application of zinc sulphide crystal in optoelctronic and bioimaging applications proves how effective the lattice is in the nanoworld [*Dimitrova et al 2000*]. This helped in extending the research of obtaining non-toxic and highly applicable QDs from the zinc sulphide core. Further to enhance the optical property of the ZnS QDs doping of the zinc sulphide lattice with manganese has been routinely done which gives longer wavelength emission spectra in the orange region of the electromagnetic spectrum and found to be non-toxic [*Wup et al 2013*]. Thus, capped Mn doped ZnS QDs have paved the pathway of biologically active material in the nanotechnology research.

There are various capping agents that were explored like thioglycerol [*Rogach et al 1996; Rajh et al 1993*], L-cysteine [*Pandey et al 2015*], MPA (Mercaptopropionic acid) [*Acar et al 2009*], MPTS (Mercapto propyl trimethoxy silane) [*Pandey et al 2015*], N-acetyl L-cysteine [*Zhao et al 2009*], glutathione [*Lesnyak et al 2010*], thioglycolic acid [*Zhang et al 2006*], cysteamine [*Hoppe et al 2002*], etc. Mostly the conventional capping agents have mercapto as donor site for attachment to the metal.

Nitrogen having lone pair is also a donor ligand thus it can be used to develop capping agents having nitrogen donor atom [*Darawsheh et al 2014*]. Imidazole molecule having nitrogen in the ring can serve as ligand to donate its electron pair to the zinc atom [*Dolega et al 2009*]. Here in this thesis, we reported for the first time, imidazole capped QDs along with its toxicity profiling. The imidazoles containing molecules has major source of interest for chemist as well as for biologist as many compounds of industrial

and technological importance are having imidazole or imidazole derivatives. Imidazole-based histidine compounds play a very important role in intracellular buffering [*Hochachka et al 2002*]. There are reports for substituted imidazole derivatives in applications for treatment of many infections [*Shargel et al*]. Synthetic imidazole have many pharmacological potential [*Sun et al 2015*]. The Imidazoles have diverse synthetic properties [*Wang et al 2015*]. The molecular structure of imidazole is ring having planar 3C and 2N atom in conjugation (Fig-5.0). It is a hetero aromatic molecule, and is soluble in water and other polar solvents. Many natural products and other biological molecules (histidine) are having the imidazole ring.

Zinc has tendency to form bond with nitrogen atom of the imidazole ligand due to the basic character of imidazole and acid character of zinc ion enabling complex formation [*Appleton et al 1977*]. This feature of zinc was employed to synthesize Mn: ZnS QDs capped with imidazole. In the present work, for the first time an attempt was made to obtain biocompatible material having a high optical response. The choice of the capping agent is based on the versatility of Imidazole and its water solubility and strong connectivity with biological world. As of our knowledge, it is the first report of the synthesis and toxicological analysis of Imidazole capped Mn: ZnS quantum dot.

The synthesized QDs capped with imidazole ring containing nitrogen as heteroatom will have potential to be used in biomimicing where the carbonic anhydrase enzyme like enzymes can be mimicked having zinc as metal ion and imidazole as ligands. The synthesis is a type of typical aqueous green synthesis having water as solvent and low temperature.

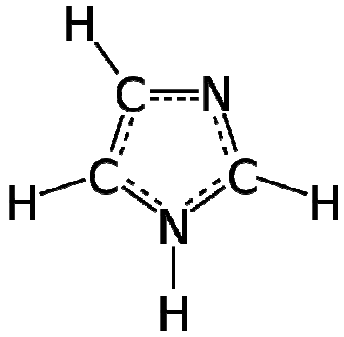

Fig-5.0: Structure of imidazole molecule (Adapted from https: // upload. wikimedia.org/ wikipedia/ commons/4/4e/ Imidazole_2D_full_aromatic.svg)

5.2 Experimental

Chemicals and Reagents

Analytical grade chemicals and reagents were used in the study unless otherwise stated. Milli Q water (double distilled deionized water) was used in all the experiments. $ZnSO_4.7H_2O$, $MnCl_2.4\ H_2O$, L-cysteine (97% purity) and ethanol were purchased from Sigma Aldrich. $Na_2S.XH_2O$ was purchased from SD Fine Chemicals (Mumbai). 2-methyl imidazole was also procured from Sigma Aldrich. The stock solutions were prepared using Milli-Q water and stored at 4^0C until their usage. All the specified biological assay chemicals and reagents were purchased from Sigma (Sigma St. Louis, MO, USA) unless otherwise stated. Culture medium Dulbecco's Modified Eagle Medium/ Nutrient Mixture F-12 (DMEM/F-12), antibiotics, fetal bovine serum (FBS) and trypsin-EDTA were purchased from Gibco BRL, USA. Culture wares and other plastic wares used in the study were procured commercially from Nunc, Denmark. Milli Q water (double distilled, deionized water) was used in all the experiments.

Cell culture

Human lung A549 cell line used in the study was procured from American Type Culture Collection (ATCC) Manassas, USA and maintained at Department of Animal Science and Biotechnology, Chonbuk National University, Jeonju, Korea Republic of, as per the standard protocols. In brief, the cells were cultured in DMEM/F-12, supplemented with 10% FBS, 0.2% sodium bicarbonate, 100 units/ml penicillin G sodium, 100 µg/ml streptomycin sulfate and 0.25 µg/ml amphotericin B. Cultures were maintained at 37℃

at 5% CO_2 - 95% atmosphere under high humid conditions. Medium was changed twice weekly and cultures were passaged at a ratio of 1:6 once in a week. Prior to use in the experiments, cell viability was ascertained by trypan blue dye exclusion assay. The culture, showing viability more than 95% were used in all the experiments. All the experiments were done on the cells with passage 18 - 25 only.

Synthesis of imidazole capped Mn:ZnS QDs

To a 100 mL of three necked flask, 10 mM of $ZnSO_4.7H_2O$, 1.5 mM $MnCl_2.4H_2O$ and 100 mL of water were added in presence of nitrogen gas with stirring for 20 min. The 10 mM of 2-methyl imidazole dissolved in water was added to control the growth. The pH of the reacting mixture was maintained at 10. After being stirred rigorously for 20 minutes, 10 mM of Na_2S was injected into the mixture. The temperature of the final reaction was maintained at 70^0 C for 1 hour. After 1 hour, the mixture was kept stirring for 18 hours at room temperature for ageing. Finally a precipitate of QD capped with imidazole was obtained which was further washed with water & ethanol through centrifugation for five times and dried under vacuum. The washed QDs were stored in water as a suspension. The synthesis yields a water dispersible, highly purified and good quality imidazole capped Mn:ZnS QDs.

Characterization of the synthesized QDs

The size of the nanocrystal was observed using TEM, Tecnai-G2-SPIRIT FEI, Netherland. A drop of aqueous solution of QDs were placed on the copper grid to obtain images after sonication and coated with formvar. Absorbance and band gap energy was derived using a spectrophotometer, spectrophotometer (SPECORD 210 PLUS, Analtika

Jena, Germany). Fluorescence spectra of the QDs were obtained at an excitation and emission spectral wavelength of 340 and 590 nm respectively (LS 55 photoluminescence spectrometer, Perkin Elmer, UK). Powder X-Ray diffraction pattern was computed using XRD by the Cu target source (SEIFERT, Germany) at ACMS Lab, IIT Kanpur, India.

Toxicity Evaluation Assay

MTT Assay

Cytotoxicity assessment was done using standard endpoint i.e., tetrazolium bromide MTT assay following the protocol of *Tripathi et al. 2014*. In brief, A549 cells (1×10^4 cells/well) were seeded in 96-well tissue culture plates and incubated in the CO_2 incubator for 24 h at 37℃. Then the medium was aspirated and cells were exposed to medium containing uncapped QDs (0.025, 0.05, 0.1, 0.2 and 0.4 g/l) and capped QDs (0.2, 0.4, 0.8, 1.0 and 2.0 g/l) for 24-96 h at 37℃ in 5% CO_2-95% atmosphere under high humid conditions. Tetrazolium salt 10 µl/ well; 5 mg/ml of stock in PBS was added 4 h prior to completion of respective incubation periods. At the completion of the incubation period, the reaction mixture was carefully taken out and 200 µl of culture grade dimethyl sulfoxide was added to each well. The content was mixed well by pipetting up and down several times until dissolved completely. Plates were then incubated for 10 min at room temperature and color was read at 550 nm using multi-well microplate reader (Synergy HT; Bio-Tek, USA). The unexposed sets were also run parallel under identical conditions that served as a basal control.

Neutral red uptake assay

The assay was carried out following the protocol described earlier by Kumar V (2015). Cells were exposed to uncapped and capped QDs in identical experimental setup as to MTT assay. Upon the completion of the incubation period, the medium was aspirated and NRU salt (50µM/ml in the medium) was added 100 µl/well plate and incubated for 3 h. Then, the reaction mixture was carefully taken out and plates were washed with washing solution (100 µl/well) containing 1% $CaCl_2$ (w/v) and 0.5% HCHO *(v/v)* to remove unincorporated dye. Washing solution was removed and a mixture of 200 µL of1% acetic acid and 50% ethanol was added. The plates were kept on rocker shaker for 10 min at room temperature and then analyzed at 540 nm using multi-well micro plate reader (Synergy HT, Bio-Tek, USA). Unexposed sets were also run under identical condition and served as controls.

Lactate dehydrogenase release assay

LDH release assay is a method to measure the membrane integrity as a function of the amount of cytoplasmic LDH released into the medium. The assay was carried out using ready-made commercially available LDH assay kit for *in vitro* cytotoxicity evaluation (TOX-7, Sigma St. Louis, MO, USA). The assay was based on the reduction of NAD by the action of LDH. The resulting reduced NAD (NADH+) was utilized in the stoichiometric conversion of a tetrazolium dye. The resulting colored compound was measured using the multi-well plate reader at wavelengths 490 and 690 nm. In brief, the cells were exposed to 0.025, 0.05, 0.1, 0.2 and 0.4 g/L of uncapped QDs and 0.2, 0.4, 0.8, 1.0 and 2.0 g/L capped QDs) for different time periods, after then the cells were

processed for LDH release assay similar to MTT assay. Culture plates were removed from CO_2 incubator as per the experimental schedule and centrifuged at 250 × g for 4 min. Then supernatant of each well was transferred to a fresh flat bottom 96 well culture plate and processed further for enzymatic analysis as per the manufacturer's instructions.

Oxidative stress studies:

Reactive oxygen species (ROS) generation

Uncapped and capped QDs induced ROS generation was assessed in A549 cells using 2', 7' diclorodihydrofluorescein di-acetate (DCFH-DA, Sigma Aldrich) dye as fluorescence agent according to method of *Kashyap et al 2011*. ROS generation was studied through fluoremetric analysis. In brief, cells ($1x10^4$ per well) were seeded in 96 well tissue culture plates (Black bottom) and allowed to adhere for 24h in CO_2 incubator at 37^0 C. The medium was then replaced with the complete medium containing different concentrations (0.025, 0.05, 0.1, 0.2 and 0.4 g/l) of uncapped QDs and (0.2, 0.4, 0.8, 1.0 and 2.0 g/l) of capped QDs for 6, 12 and 24h. At the end of incubation period, cells were washed with PBS and incubated with (10 µM) DCFH-DA for 30 min in incomplete DMEM-F12 (Stock solution 1mM in PBS). The reaction mixture was carefully aspirated and 200 µl of PBS was added to each well. The plates were kept on rocker shaker for 10 min at room temperature in the dark and the reading for fluorescence intensity were measured using multi-well micro plate reader (Synergy HT, Bio-Tek, USA) at 485-nm excitation and 528-nm emission for DCF quantification. Untreated sets run under the identical condition served as basal control. The percentage of ROS levels in exposed cells was calculated considering the controls as 100%.

Glutathione (GSH) levels

Glutathione (GSH) levels were assessed using commercially available kit (ApoGSH Glutathione Colorimetric Assay Kit, Catalog No#K261-100, Biovision, USA). In brief, the deproteinated samples were transferred to 96 well plates (50 µl/well), mixed with 150 µl freshly prepared assay cocktail and read at 405 nm using multi-well microplate reader (Synergy HT, Bio-Tek, USA) at 5 min intervals up to 30 min. Standard curve was plotted using the glutathione standard supplied in the kit and used to calculate the experimental values.

Lipid peroxidation (LPO)

Following the exposure of uncapped QDs (0.025, 0.05, 0.1, 0.2 and 0.4 g/l) and (0.2, 0.4, 0.8, 1.0 and 2.0 g/l) capped QDs for 6, 12 and 24 h, cells were harvested by centrifugation at 1000 rpm for 10 min and processed for the estimation of lipid peroxidation using commercially available kit (Lipid Peroxidation Assay Kit, catalog no. 705002; Cayman Chemicals, USA) as per the manufacturer's protocol.

Catalase (CAT) levels

The experimental setup for catalase activity was similar to the LPO. Activity was measured using commercially available kit for catalase activity (Catalog no. 707002; Cayman Chemicals, USA) following the protocol provided by manufacturer.

Genotoxicity studies:

Micronucleus (MN) assay

MN assay was carried out using protocols reported by *Kashyap MP et al. 2010*. For micronucleus (MNs) analysis, $1x10^5$ A549 - cells were seeded in each well of six well tissue culture plates (Nunc.) and allowed to adhere for 24h in CO_2 incubator at 37^0 C. The cells were exposed to uncapped and capped QDs for 24 h at different concentration (0.025, 0.05, 0.1, 0.2 and 0.4 g/l) and (0.2, 0.4, 0.8, 1.0 and 2.0 g/l) respectively then cells were washed and supplemented with cytochalasin B (3 µg/ml, Sigma) containing medium and were incubated further for another 22 hrs (Which is a doubling time for A549 cell line). Cells were then harvested by hypotonic buffer (0.075 M KCl) for 5‑10 min at 37℃ and fixed in Carnoy's fixative (methanol/acetic acid, 3:1). Finally, cells were dropped onto the slides and stained with 5% Giemsa in phosphate buffer (pH: 6.8) for 15‑20 min and mounted with DPX for microscopic examination. A minimum of 1000 binucleated cells with well‑defined cytoplasm in each slide was scored for the presence of MN using a Nikon Eclipse 80i upright microscope attached to a Nikon digital CCD cool camera (Model DS‑Ri1 of 12.7Megapixel). Data presented for MN are the mean of three slides.

Chromosomal aberration (CA) assay

CA assay was carried out using protocols reported by Kapoor E et al. 2014. A549 cells were cultured in DMEM/F‑12 medium in 25 cm^2flasks and the cells were exposed to different concentration of uncapped and capped QDs for 24 h. Colcemid (0.15 µg/ml final concentration) was added 4 h prior to harvest the cells. After the compilation of 4 h

exposure of colcemid, the medium was aspirated and the cells were washed with Hank's balanced salt solution. After that, the cells were given a hypotonic shock in potassium citrate (0.8%) for 30 min. Finally, cells were fixed in cold fixative (methanol: acetic acid, 5:2 ratios). Cells were dropped on clean slides, dried and stained in 5% Gurr's Giemsa. The cells were scored for the presence of CA using a Nikon Eclipse 80i upright microscope attached to a Nikon digital CCD cool camera (Model DS-Ri1 of 12.7 Megapixel). Data presented for CA are the mean of three slides.

Statistical analysis

The results are expressed as mean and standard error of means (Mean±SE) for at least three experiments. One way ANOVA followed by post hoc Dunnett's test was employed to detect differences between the groups of treated and control. *$p<0.05$ was taken to indicate significant differences.

5.3 Results and Discussions

The aqueous route of synthesis was involved to obtain the luminescent Mn: ZnS QDs. The precursors used in the study were zinc sulphate, manganese and sodium sulphide to provide sulphide ions for the Mn doped ZnS nanomaterial. The imidazole molecule has two nitrogen atom one having N-H bond and other having lone pair. The synthesis was performed in water and further change to pH was done with NaOH. The base attacks on the H- atom attached to the nitrogen atom and this results in the formation of nitrogen metal bond by the influence of negative charge on the first nitrogen atom. The deprotonation of 2-methyl imidazole was done to obtain highly basic anion. The capping agent was added in appropriate amount to reduce the formation of metal ligand complex. The imidazole bonded zinc was further reacted with sulphide ion. There is always a competition between capping agent and anion hence controlling this aspect is crucial. The fast addition of sulphide ion was done to form zinc sulphide precipitate immediately. After addition of sulphide ion, the temperature of the reaction mixture was increased for 1 hour. As the temperature increases, the rate of zinc sulphide formation increases as well. Synthesis of ZnS nanoparticle as a result involves another step where the formed precipitate undergoes ageing. The ageing of the nanomaterial has significant role in its crystallinity. Here room temperature was chosen for growing the particles. After 18 hrs of ageing at room temperature, the material was washed with water and ethanol several times and final mixture was kept on oven for drying. The synthesis resulted in imidazole capped Mn doped zinc sulphide quantum dots following aqueous route of synthesis.

The synthesized material obtained was characterized further by TEM for particle size determination as shown in the Fig-5.1. The particles in the size range 5.5-6.5 nm were obtained. The TEM results (Fig-5.1) show that homogenous particles have been synthesized. The typical particle size of the material is below 10 nm hence it is inferred that QD have been obtained. The dark image of the material is due to the zinc metal which is classified as heavy metal. The strong transmission of the material confirms the constituent of the material under investigation. There is no clump or cluster in the image which proves that imidazole acts as good capping agent and controls the particle size effectively.

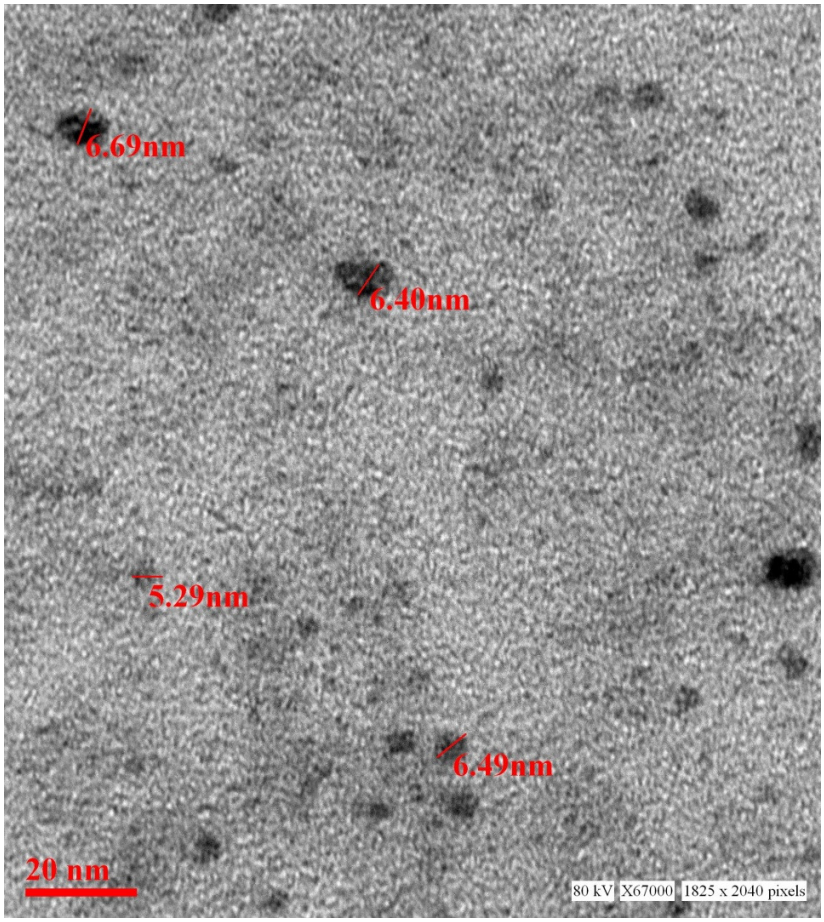

Fig-5.1: TEM image of the imidazole capped QD

The optical property of the synthesized QDs was performed by UV and spectrofluorometer. The absorbance at 310 nm and cut off at 340 nm (Fig-5.2) proves the blue shift. The cutoff at 340 nm also supports the photoluminescence spectra (Fig-5.3). The photoluminescence spectra shows that the excitation of the QD is 340 nm and emission at 590 nm. The strong quantum confinement is there in the band gap due to small sized QD. The emission at 590 nm confirms that manganese ion has been doped in the crystal lattice. The trap states created due to the manganese ion results in higher emission wavelength. Thus, the material with highly enhanced optical property has been synthesized. Both UV and photoluminescence spectra support the band gap (3.6 eV), excitation (340 nm) and emission (590 nm) parameter. Hence imidazole molecule had not altered the optical property of the synthesized quantum dots.

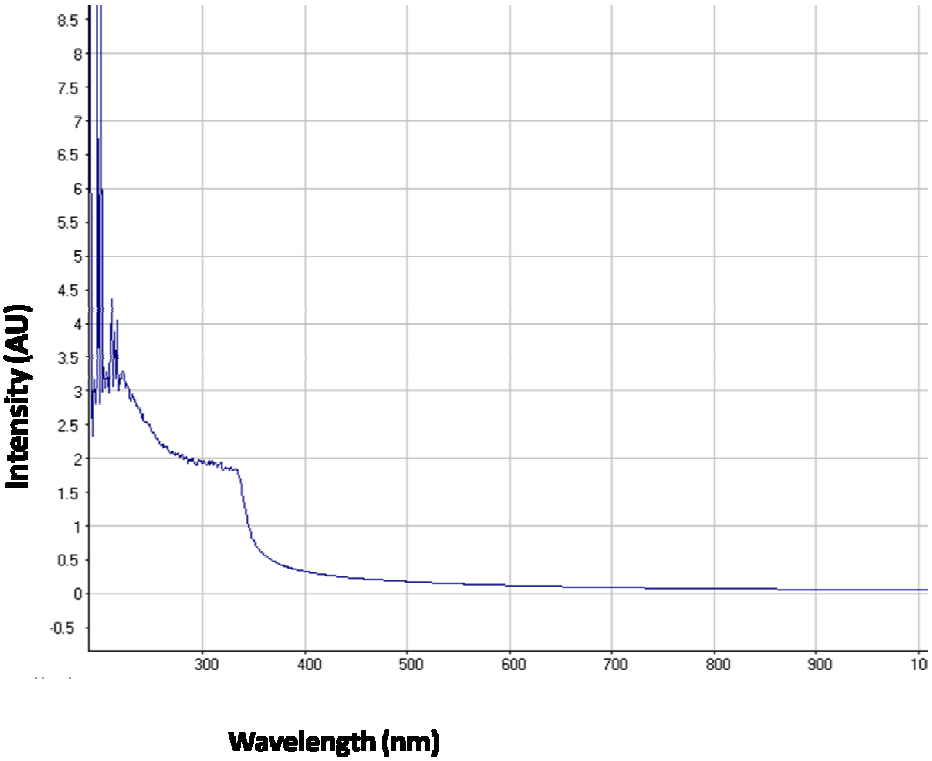

Fig-5.2 UV Spectra of the Mn: ZnS QD

The optical stability of the synthesized QD was evaluated as well. The result shows that the PL intensity of the QDs was stable till 550 seconds (Fig-5.4). Thus, the luminescence intensity of the imidazole capped QD do not decrease with respect to time and hence highly efficient probe was synthesized which can be used for a longer time in imaging.

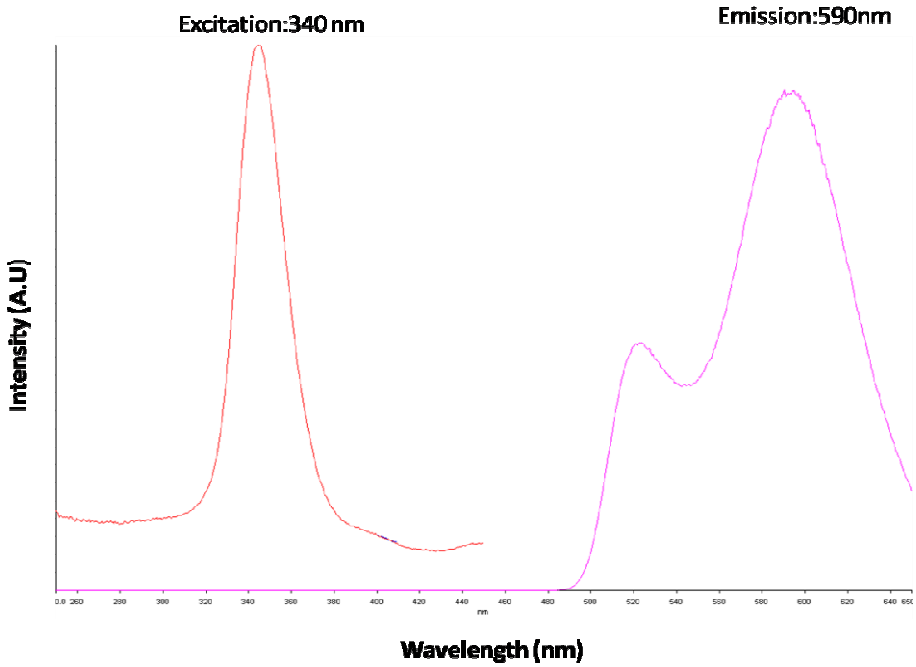

Fig-5.3 PL spectra of the Mn: ZnS QD

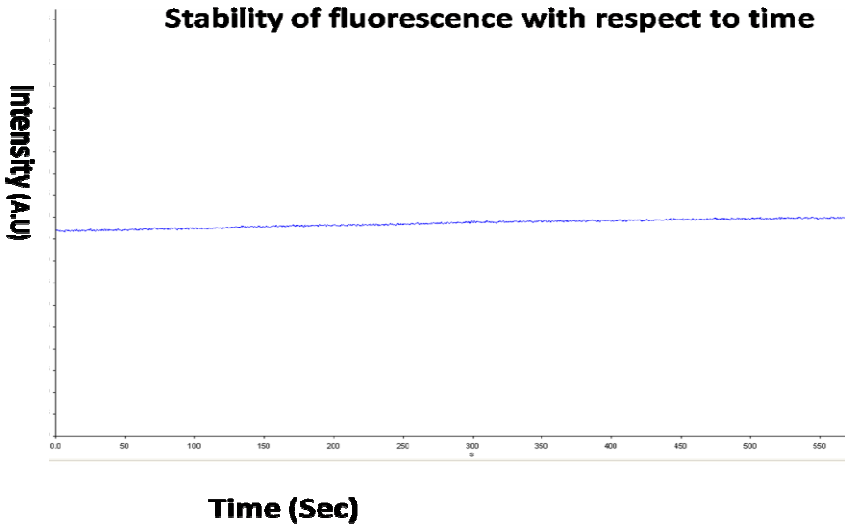

Fig-5.4 Photo stability of the imidazole capped Mn: ZnS QD

The crystal property of the material was evaluated by XRD measurement. It was observed that in the diffraction pattern, high intensity peaks were observed at 28, 47 and 56 ^{0} . The XRD pattern (Fig-5.5) shows miler planes at (111), (220) and (311) which is in accordance with JCPDS No. 05-0566. The lattice parameters of the QD synthesized and library is similar which confirms the zinc sulphide lattice of the type cubic zinc blende. The purity of the material can be acknowledged by having no other peaks in the diffraction pattern. The peaks in the diffraction pattern shows that they are of high intensity which attribute to the high crystalline property of the QDs. The smaller size has also been confirmed by the XRD data since the peaks are broaden. The size of the material was calculated by Scherer equation $\beta_{1/2} = 0.94\lambda/d \cos\theta$ *(Liu et al. 2010)*. Where $\beta_{1/2}$ refers to the full peak width at half maximum, λ refers to the copper target source, d refers to the size of the crystal lattice and θ refers to Braggs angle. The size of the imidazole capped QD was 9 nm. The peak width shows the characteristics of ZnS QDs.

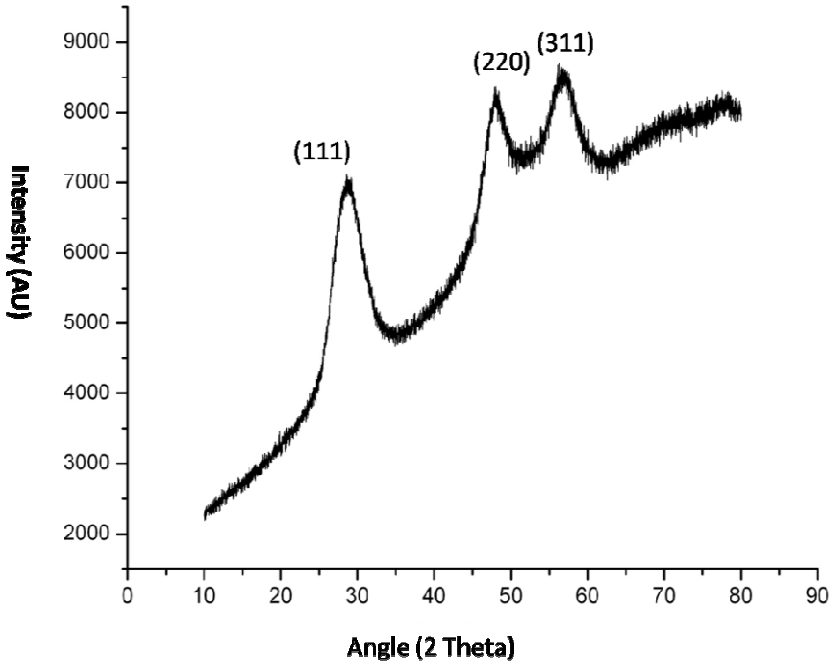

Fig-5.5 XRD Pattern of the synthesized Mn: ZnS QD

Hence high quality manganese doped zinc sulphide QD have been synthesized. It is inferred that the imidazole controls the size of the material without affecting the chemical property and material property. Here we have also evaluated the biological applicability of the capped QD with respect to uncapped one.

Invitro toxicity and genetic toxicology was evaluated by various parameters. Cellular toxicity was evaluated by MTT, NRU, LDH, ROS, Catalase, GSH and LPO as they are included in the list of abbreviations. The toxicity at genetic level was performed by chromosomal aberration and micronucleus test.

Cytotoxicity assessment

MTT Assay

Results of MTT assay are summarized in Fig-5.6. Human lung epithelium cells-A549 responded to uncapped and capped QDs in a dose and time dependent manner. There was no significant reduction in percent cell viability reported all through the exposure period, i.e., till 48 h in the used concentration i.e., 0.025-0.05 g/l of the uncapped QDs and 0.2-0.4 g/l of the capped QDs. Whereas, the concentrations of uncapped used, i.e., 0.1, 0.2 and 0.4 g/l were found to cause a gradual reduction in percent cell viability, which reaches to significant levels at and above the exposure period of 24 h. The cell viability reduces to 85.12±4.20, 76.64±3.73, 64.58±4.42 and 52.55±4.79 in the cells exposed to 0.2 g/l for a period of 24, 48, 72 and 96 h respectively. The reduction was severe in cells exposed to the highest concentration, i.e., 0.4 g/l, where the viability reduces to 68.46±1.69, 65.30±2.83, 53.27±2.60 and 41.92±3.04 at 24, 48, 72 and 96 h respectively, when compared with unexposed control cells (Fig-5.6A). Whereas capped QDs show 88.17±2.73, 82.44±3.63, 75.47±3.59 and 65.71±2.3079 in the cells exposed to 1.0 g/l for a period of 24, 48, 72 and 96 h respectively. The reduction was severe in cells exposed to the highest concentration, i.e., 2.0 g/l, where the viability reduces to 84.53±3.65, 76.51±2.86, 64.57±3.68 and 52.71±2.79 at 24, 48, 72 and 96 h respectively, when compared with unexposed control cells (Fig-5.6B).

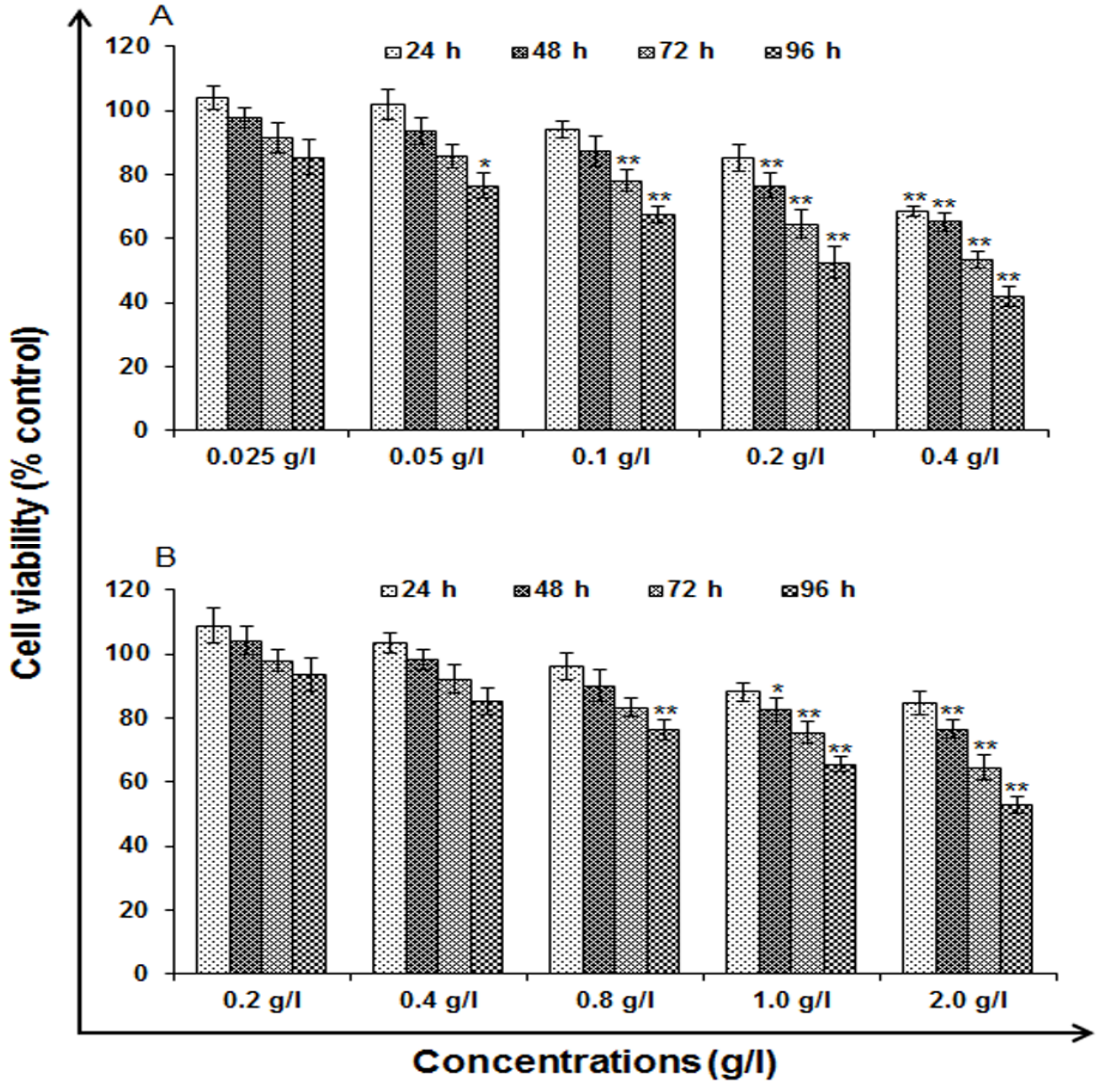

Fig-5.6 Cytotoxicity/biosafety assessment of (A) uncapped QDs and (B) capped QDs in human lung epithelium cells-A549 (3-[4, 5-dimethylthiazol-2-yl]-2,5-diphenyl tetrazolium bromide) assay. Cells were exposed to various concentrations for 24-96 h. The data presented are percent cell viability compared with unexposed control cells. Values are given as mean ± standard error of the data obtained from three independent experiments and each experiment contained at least three replicates. *P < 0.05= significant.

Neutral red uptake assay

The observations of NRU assay were having similar trends as that to the MTT assay. The lower concentration, i.e., 0.025-0.05 g/l of uncapped QDs and 0.2-0.4 g/l of capped QDs were found to induce no significant reduction in percent cell viability, while the higher concentrations, i.e., 0.1, 0.2 and 0.4 g/l of uncapped and 0.8, 1.0 and 2.0 g/l of capped QDs were able to induce a dose dependent decrease in the percent cell viability, which reaches to statistically significant levels at and beyond 24 h and exposure, when compared with unexposed control cells. The cell viability reduces to 87.31±3.18, 80.17±2.73, 74.86±2.71 and 58.14±3.65 in the cells exposed to 0.2 g/l for a period of 24, 48, 72 and 96 h respectively. The reduction was severe in cells exposed to the highest concentration, i.e., 0.4 g/l, where the viability reduces to 80.59±2.88, 72.41±3.63, 63.98±3.77 and 46.86±2.68 at 24, 48, 72 and 96 h respectively, when compared with unexposed control cells (Fig-5.7A). While the capped QDs show 90.77±4.77, 83.12±5.28, 74.83±4.23 and 65.34±4.17 in the cells exposed to 1.0 g/l for a period of 24, 48, 72 and 96 h respectively. The reduction was severe in cells exposed to the highest concentration, i.e., 2.0 g/l, where the viability reduces to 85.31±3.71, 77.65±3.19, 67.35±2.79 and 58.83±2.72 at 24, 48, 72 and 96 h respectively, when compared with unexposed control cells (Fig-5.7B).

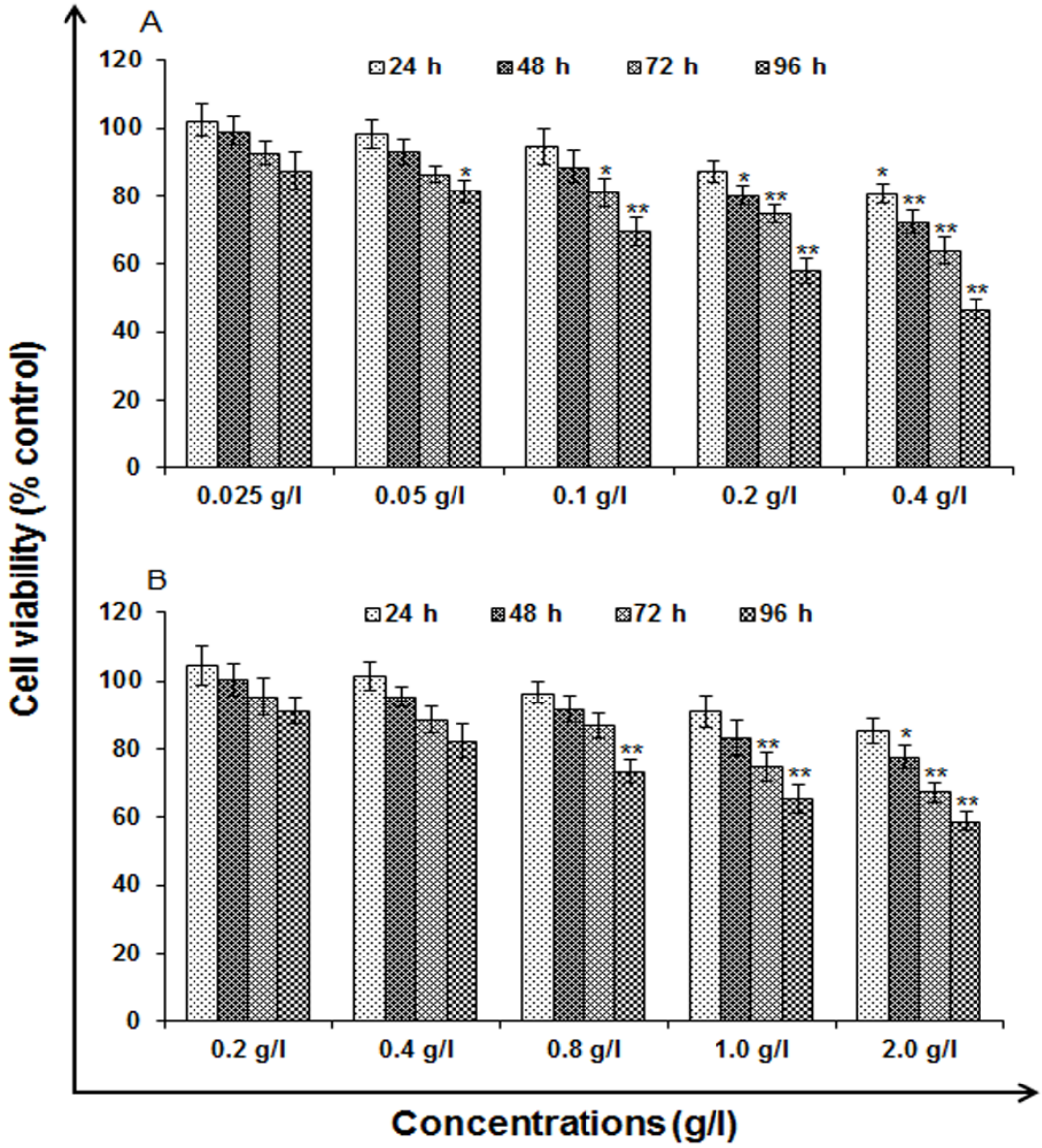

Fig-5.7: Cytotoxicity/biosafety assessment of (A) uncapped QDs and (B) capped QDs in human lung epithelium cells-A549 (neutral red uptake assay). Cells were exposed to various concentrations for 24-96 h. The data presented are percent cell viability compared with unexposed control cells. Values are given as mean ± standard error of the data obtained from three independent experiments and each experiment contained at least three replicates. *P < 0.05= significant

Lactate dehydrogenase release assay

The highlights of the results for the release of LDH following the exposure of cells to uncapped and capped QDs are presented in Fig-5.8. A significant increase in LDH release was observed in 0.1-0.4 g/l of uncapped and 0.8-2.0 g/l of capped QDs in comparison to unexposed controls. The LDH release was increased significantly to 113.54±2.85, 123.66±3.35, 133.65±5.03 and 147.22±4.34 % at 24, 48, 72 and 96 h and it reaches its maximum up to 127.25±4.70, 139.58±3.72, 162.23±5.36 and 169.47±5.85 % at 24, 48, 72 and 96 h in cells exposed to 0.1 and 0.4 g/l concentration of uncapped QDs respectively when compared with unexposed control cells (Fig-5.8A). The trends were similar after the exposure of 0.8 g/l of capped QDs and it shows 112.18±4.16, 117.39±4.46, 125.25±3.33 and 139.49±3.74 % at 24, 48, 72 and 96h which reached up to 124.67±3.71, 132.52±4.69, 144.72±3.66 and 159.16±5.32 % at 24, 48, 72 and 96h after the exposure of 2.0 g/l when compared with unexposed control cells. No significant changes were found in the cells exposed to 0.025-0.05 g/l of uncapped and 0.2-0.4 g/l of capped QDs all through the exposure (Fig-5.8B).

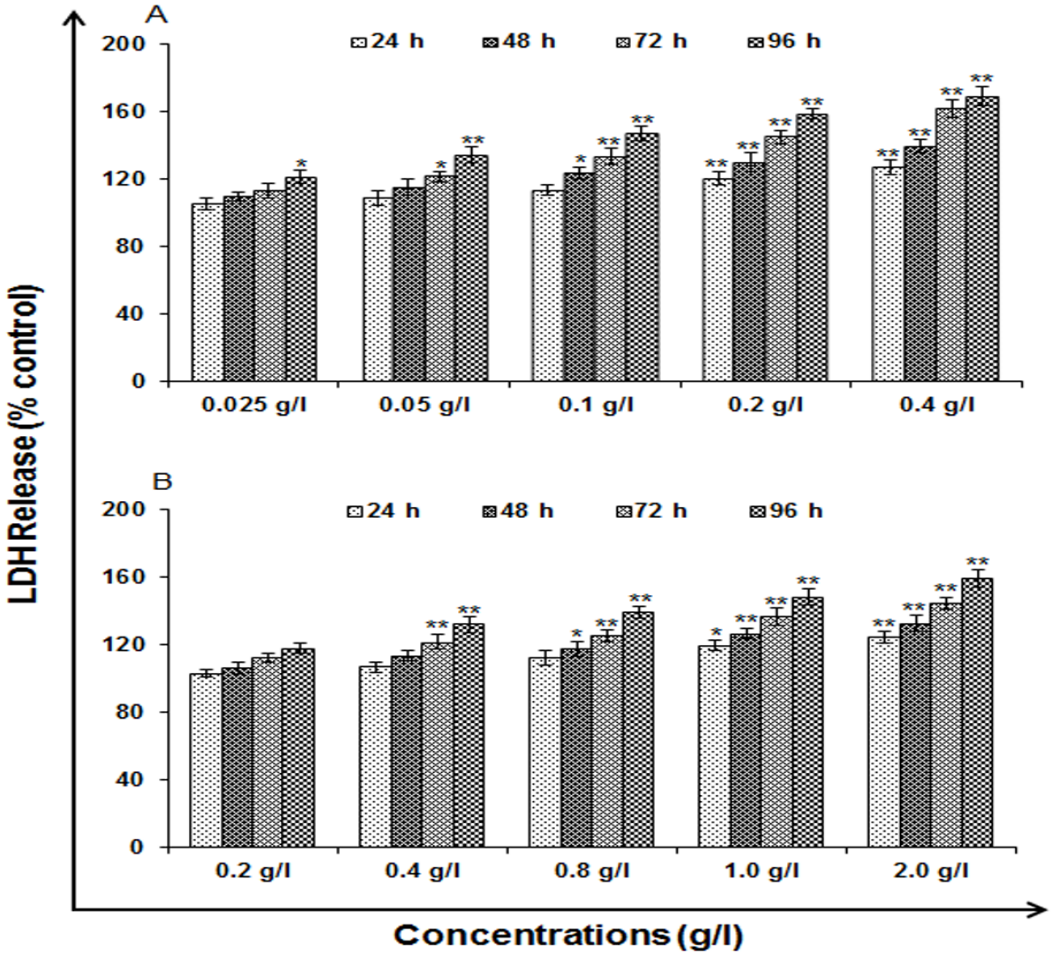

Fig-5.8 Cytotoxicity/biosafety assessment of (A) uncapped QDs and (B) capped QDs in human lung epithelium cells-A549 ((lactate dehydrogenase release assay). Cells were exposed to various concentrations for 24-96 h. The data presented are percent cell viability compared with unexposed control cells. Values are given as mean ± standard error of the data obtained from three independent experiments and each experiment contained at least three replicates. *P < 0.05= significant.

Oxidative stress studies

Reactive oxygen species (ROS) generation

The results of uncapped and capped QDs induced ROS generation are summarized in Fig-5.9. Cells show significant (*P<0.05) at 6h (119.84±3.75, 126.38±4.68), 12h (125.34±4.80%, 133.56±4.20%) and 24h (141.23±3.28%, 152.49±4.75%) of exposure (Fig-5.9B). Highest concentration of both uncapped and capped QDs used (0.4 and 2.0 g/l) was most effective at all the time points.

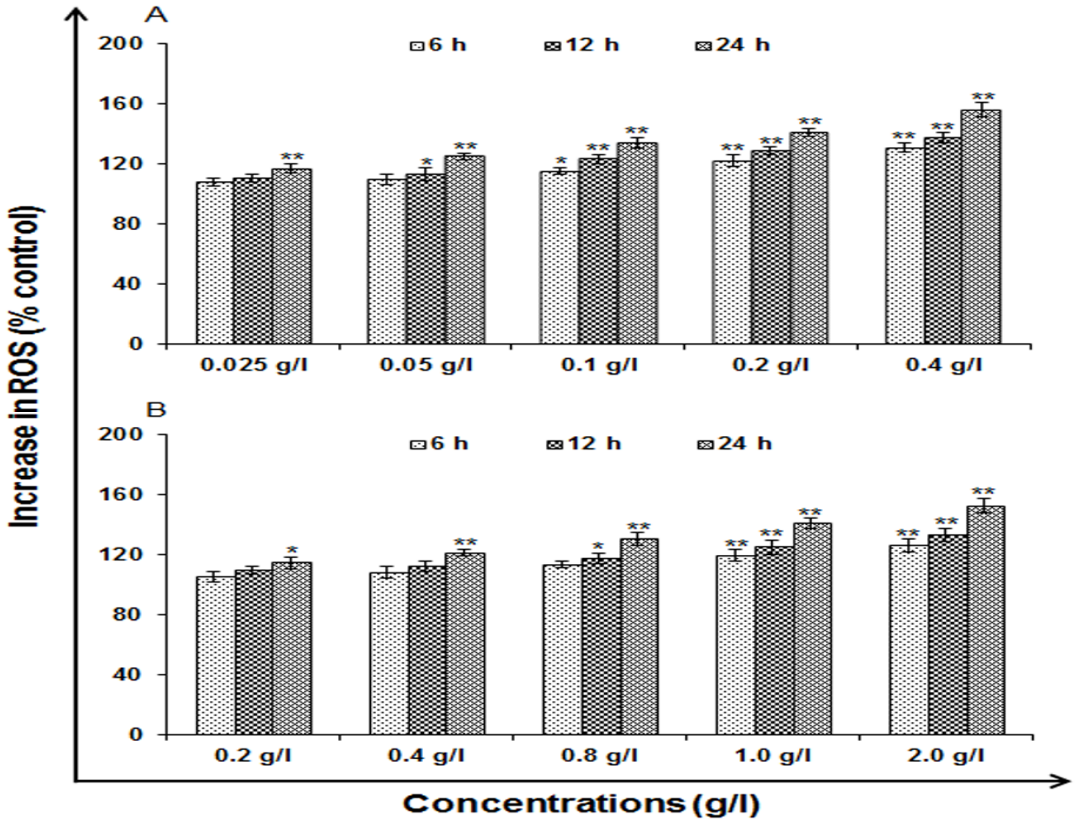

Fig-5.9 Percent change in ROS generation following 6, 12 and 24 h exposure to various concentrations of (A) uncapped QDs and (B) capped QDs in A549 cells assessed by micro plate reader. Data represented are mean±SE of three identical experiments made in three replicate. *p<0.05= significant.

Glutathione (GSH) levels

Cell exposed to uncapped QDs (0.2 and 0.4 g/l) was found to deplete the levels of GSH significantly at all the time points 6h (85.74±2.00%, 78.68±3.52%), 12h (76.62±3.23%, 67.94±2.52%) and 24h (58.98±3.35%, 45.72±2.23%) of control (Fig-5.10A). However, the capped QDs (1.0 and 2.0 g/l) show 6h (85.78±4.74%, 79.52±3.24%), 12h (76.64±2.74%, 68.96±2.09%) and 24h (65.27±4.20%, 57.63±2.84%) of control (Fig-**5.10B). While lower concentration used could not pose such severe effects.**

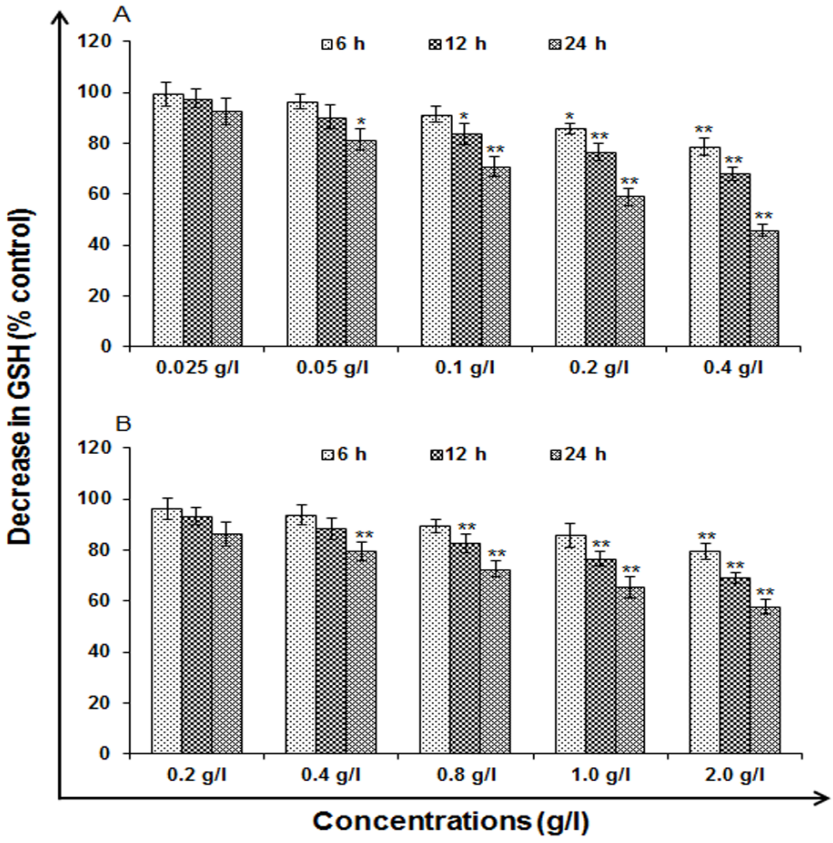

Fig-5.10 Change in levels of GSH activity in A549 cells following the exposure of (A) uncapped QDs and (B) capped QDs for 6, 12 and 24h time periods assessed by micro plate reader. Data represented are mean±SE of three identical experiments made in three replicate. *p<0.05= significant.

Lipid peroxidation (LPO)

Uncapped QDs at concentration 0.2 and 0.4 g/l induced significantly lipid per-oxidation at an exposure time of 6h (126.34±3.65%, 136.46±5.33), 12h (132.59±3.56%, 143.39±5.34%) and 24h (148.76±3.03%, 160.23±5.32%) of control (Fig-5.11A).In case of capped QDs at concentration 1.0 and 2.0 g/l significant induction of LPO was observed at 6h (120.38±3.24%, 127.63±4.68), 12h (123.64±2.61%, 131.35±3.63%) and 24h (141.24±2.76%, 153.31±2.26%) of control (Fig-5.11B).The induction of LPO was also concentration and time dependent.

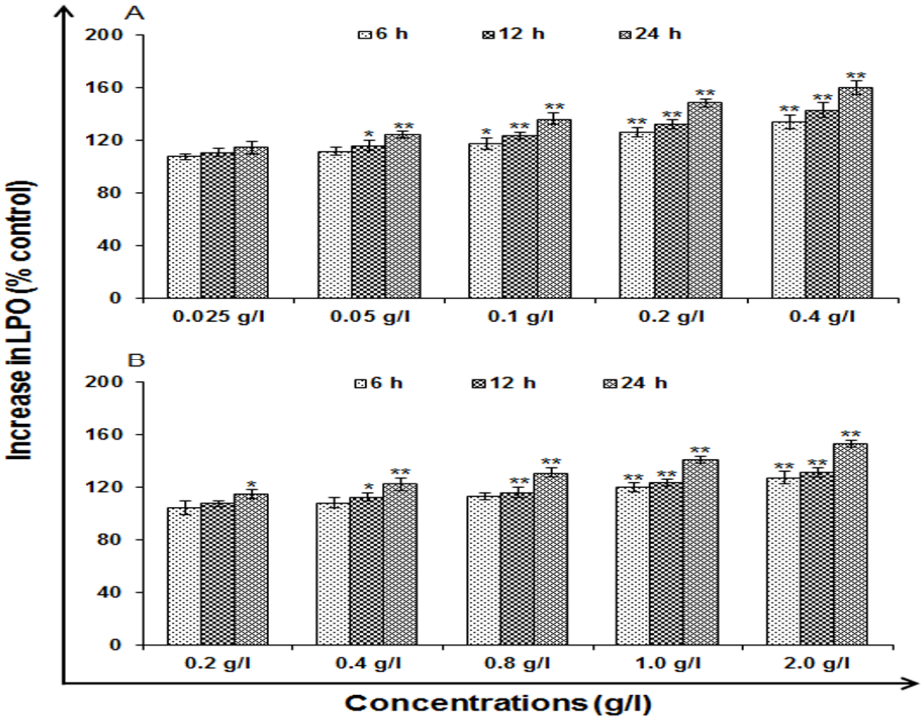

Fig-5.11 Change in levels of Lipid peroxidation in A549 cells following the exposure of (A) uncapped QDs and (B) capped QDsfor various time periods (6, 12 and 24h) assessed by micro plate reader. Data represented are mean±SE of three identical experiments made in three replicate. *p<0.05= significant.

Catalase (CAT) levels

Significant reduction in the activity of catalase was observed at 0.2 and 0.4 g/l, which was reported maximum at 24h (64.92±3.59%, 52.81±4.69%) followed by 6h (77.53±4.80%, 69.74±3.24%) and 12h (72.46±3.71%,62.59±4.69%) for uncapped QDs exposed cells (Fig-5.12A).In case of capped QDs exposed cells, decrease in the activity of catalase was observed at 1.0 and 2.0 g/l and it also show maximum at 24h 66.24±2.75%, 55.82±1.69%) followed by 6h (82.36±3.59%, 76.45±4.68%) and 12h (74.75±3.58% and 67.62±5.25) in comparison to unexposed control cells (Fig-5.12B)

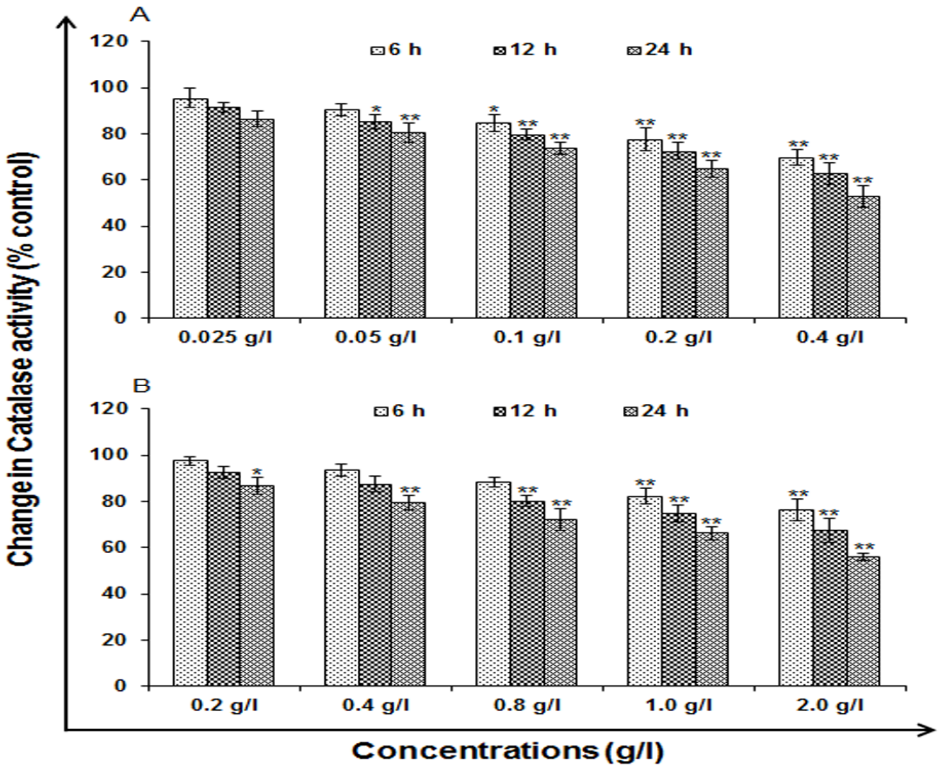

Fig-5.12 Change in levels of catalase activity in A549 cells following the exposure of (A) uncapped QDs and (B) capped QDs for various time periods (6, 12 and 24h) assessed by micro plate reader. Data represented are mean±SE of three identical experiments made in three replicate. *p<0.05= significant.

Genotoxicity studies:

Micronucleus assay

MN assay was carried out to assess the accumulation of genetic damage in the cells. The cells were grown in DMEM/F-12 medium alone served as basal control and the other set of cells exposed to different concentrations of uncapped and capped QDs for 24 h was considered as treatment group. The increase in the MN frequency was observed as compared to the cells grow in normal medium (Fig-5.13). We observed a significant increase in the induction of MN following the exposure of cells to 0.025, 0.05, 0.1, 0.2 and 0.4 g/l of uncapped QDs, i.e., 8 ±2.31, 13±0.58, 18±1.73, 26±3.46 and 34±2.89 MN/1000 cells at 24 h respectively (Fig-5.13A). However, the induction of MN following the exposure of cells to 0.2, 0.4, 0.8, 1.0 and 2.0 g/l of capped QDs, i.e., 4±0.58, 11±1.73, 16±1.15, 22±1.73 and 29±2.89 MN/1000 cells at 24 h respectively (Fig-5.13B).

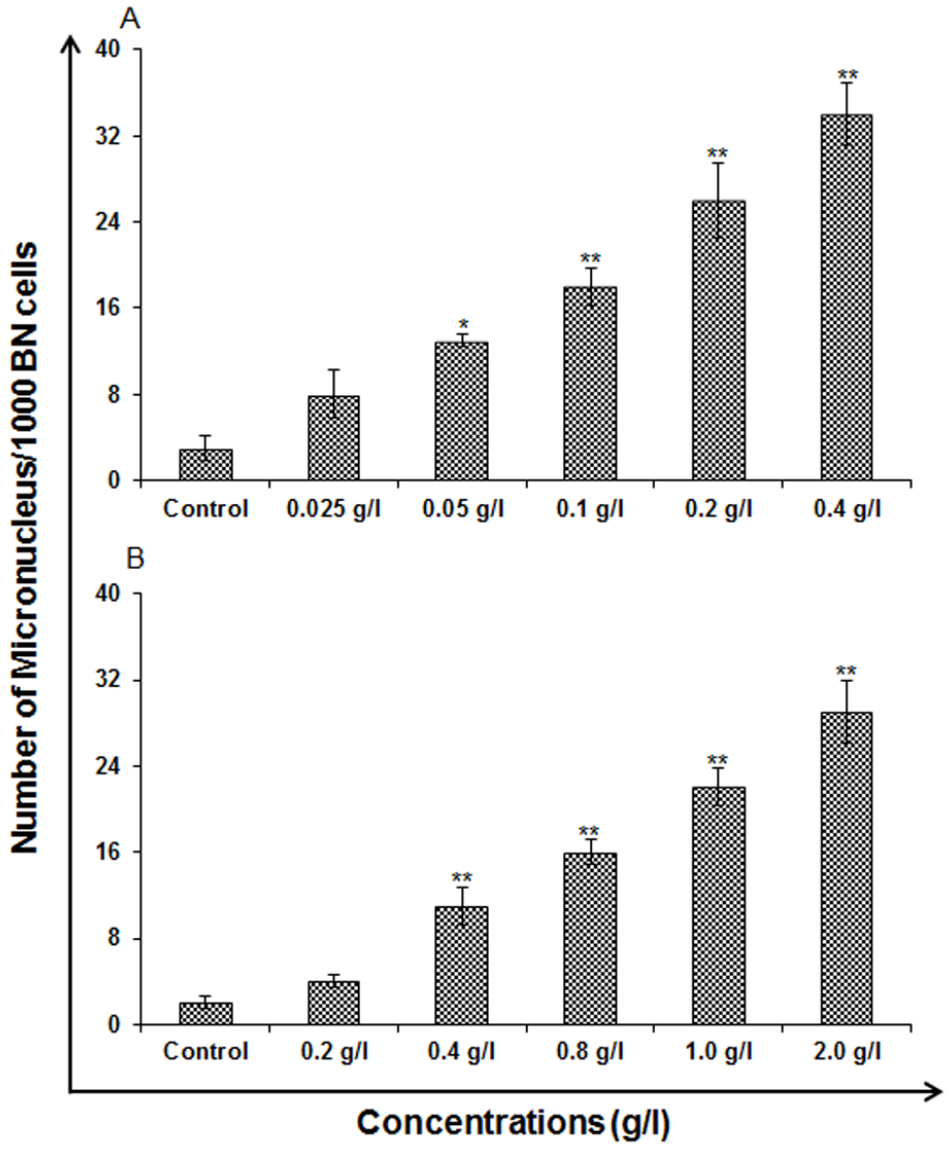

Fig-5.13 Genotoxicity/biosafety assessment of (A) uncapped QDs and (B) capped QDs in human lung epithelium cells-A549 (micronuclei assay). Cells were exposed to various concentrations for 24h. Micronuclei were calculated by scoring a minimum of 1000 cells at 24h. Values are given as mean ± standard error of the data obtained from three independent experiments and each experiment contained at least three replicates. *P < 0.05= significant.

Chromosomal aberration assay

The trends were similar as that to MN assay. The most common aberrations were found of chromatid gaps and break type, followed by higher concentrations of uncapped and capped QDs. There were occasional incidences of aneuploidy in the cells exposed to higher concentrations, i.e., 0.2 and 0.4 g/l of uncapped and 1.0 and 2.0 of capped QDs. The induction of CA was dose dependent, i.e., 8±1.15, 12±1.73, 17±2.89, 23±1.15 and 32±2.31 aberrations/100 in cells exposed to 0.025-0.4 g/l of uncapped QDs for 24 h respectively (Fig-5.14A).The capped QDs show 6±1.15, 9±1.15, 14±1.73, 20±2.89 and 27±2.31 aberrations/100 in cells exposed to 0.2-2.0 g/l for 24 h respectively (Fig-5.14B).

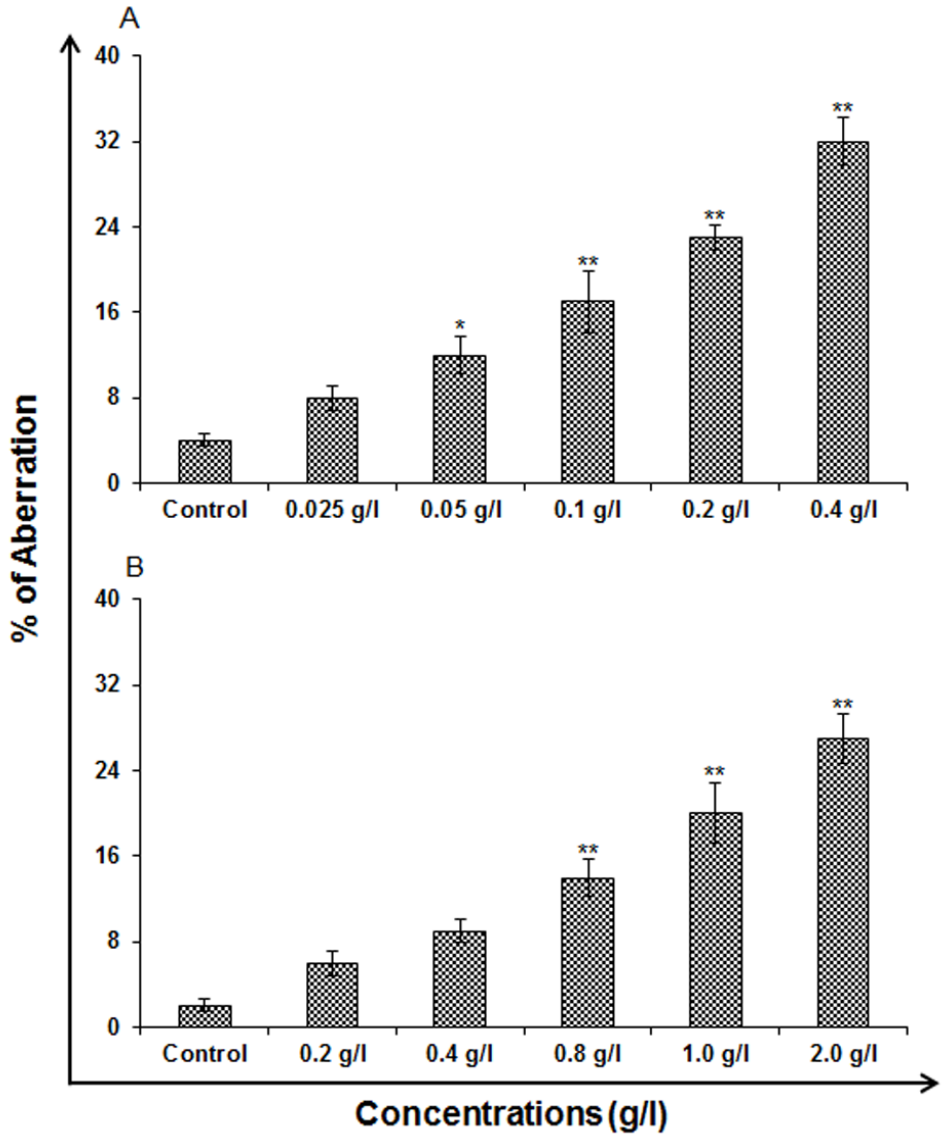

Fig-5.14 Genotoxicity/biosafety assessment of (A) uncapped QDs and (B) capped QDs in human lung epithelium cells-A549 (chromosomal aberration [CA]). Cells were exposed to various concentrations for 24h. CA wasscored at 24h in the cells exposed to uncapped and capped QDs. Values are given as mean ± standard error of the data obtained from three independent experiments and each experiment contained at least three replicates. *P < 0.05= significant.

Conclusion:

Mn doped ZnS QD is synthesized by employing aqueous route of synthesis. The imidazole is used as capping agent which do not alter the optical property or chemical structure of the synthesized material as evident by the through characterization by TEM, XRD and spectroscopy. The imidazole capped QD was further analysed and tested by toxicity parameters. As synthesized QD was undergone toxicity profiling at both cellular and genetic level. The toxicity study shows that uncapped QD very toxic as compared to imidazole capped QD.

Chapter-6

Chapter 6

General Summary and Conclusion

Nanotechnology is largely demanding due to its astonishing properties which greatly influenced the global economy and pathway from research to development leading to production and commerce. The technology of modern day is the convergence of material science and molecular biology leading to the development of substantial benefits that will have significant economic and scientific impacts, applicable to common human being. Wide areas of problem ranging from environmental remediation, healthcare, energy, transportation and routine analysis can be solved by the nano technology. Quantum dots are emerging material in area of the nanomaterial research. The unique electro-optical properties, which arise from the size-controlled, tunable photoluminescence (PL) and long-term photo stability, made these nanomaterials emerged as advantageous alternatives to the commonly used molecular probes in chemical, biological and biomedical applications including sensor, biolabeling, bioimaging and biotargeting. As nowadays interdisciplinary science is highly required for betterment of tomorrow, this research work will explore the basic knowledge of physics, chemistry, biology and mathematics to upgrade the modern science. The potential of QDs in optical specificity, bio-imaging and analyte selectivity has been extensively studied and further applied for its great application in two major fields of science viz: biomedicine and analytical chemistry. This has added advantages in that, the similarities allow integration of three major areas nanotechnology, chemistry and biology, which helps in promoting great advances in cell biology, molecular biology,

targeted therapeutics and medical diagnostics. Current development in this field has allowed the surface chemistry of colloidal nanoparticles to prepare functionalized nanomachines. There is a considerable need for a simple, economic and environment-friendly aqueous route to produce biocompatible QDs with strong emission and good stability. For the analysis of various toxicants it requires rapid, sensitive, selective, robust, economical and easy methods. Various analytical instruments such as UV-visible spectrophotometer, Photoluminescence spectrophotometer, X-ray diffraction, Fourier transform spectrophotometer, Transmission electron microscopy and scanning electron microscopy has been used enormously to characterize the synthesized material. The principles of toxicology with bioanalytical assays such as MTT, NRU, LDH, Catalase, LPO, chromosomal aberration, micronucleus test has proved the efficacy of the designed material in biomedicine. To provide specificity and selectivity, molecularly imprinting technology has been employed which involves the copolymerization of APTES as monomer and TEOS as crosslinker in the presence of the template which results in the formation of complex between template and monomer followed by sol-gel transformation. The combination of the QDs with MIP leads to development of specific and selective tailor made material. The fluorescence quenching characteristics and selectivity of imprinted polymer for target analyte results in the development of optical sensors. The long life of the optical sensors and portability makes it efficient nano-engineered on field sensor.

In the present thesis, rapid, selective and cost effective methods have been developed for the analysis of toxicants e.g. 3-PBA and methyl mercury. The biomedical

applicability was evaluated for L-Cysteine and Imidazole capped QDs. The invitro cellular and genetic toxicology was performed to obtain toxicity profiling.

6.1.2 Synthesis and characterization of molecularly imprinted polymer by surface modification of Mn:ZnS Quantum Dots (QD-MIP): Optical sensor for detecting 3-PBA

3-PBA is a non-specific and frequently detected metabolite of various pyrethroids such as cypermethrin, deltamethrin, permethrin, cyhalothrin etc. and also used as a general marker for the exposure to the pyrethroids. Due to the antiestrogenic activity, it is also considered as an endocrine disruptor chemical. There is strong evidence of the role of 3-PBA in determining the exposure of pesticides in occupational workers. Thus, it is necessary to detect and analyze the 3-PBA so that the implications of pesticides on human health can be known. 3-PBA has been detected by a rapid by ELISA method, but it involves the sample preparation prior to analysis which is a tedious step. High-performance liquid chromatography (HPLC), liquid chromatography-mass spectrometry (LC-MS), gas chromatography (GC), gas chromatography-mass spectrometry (GC-MS) and immunoassay based methods for 3-PBA analysis has been developed as well. Even though these methods have an advantage to quantify 3-PBA in several matrices, but they are not compatible for on-field sensing and monitoring applications. In the present work, we have made an attempt to form molecular recognition sites on the surface of Mn doped ZnS QDs using molecularly imprinting technique. The technique is capable of selective extraction of 3-PBA from complex biological matrices and can also sense the analyte. Hence, a simple, rapid and selective method is developed for the

detection of 3-PBA in urine samples. The developed method is found to be cost effective and easy to use.

The MPTS capped Mn doped ZnS quantum dots were synthesized by taking, $ZnSO_4$, $MnCl_2$, and water which were added and the mixture was stirred under nitrogen at room temperature for 10 min. Then aqueous solution containing Na_2S was added drop wise and kept under stirring. To this, MPTS dissolved in ethanol was added and the reaction was kept for 20 hrs on stirring at room temperature. Then synthesis for QDs capped with MIP was done, for this a 50 mL flask was taken in which alcoholic solution of 3-PBA (template) and APTES (functional monomer) were added and stirred. To the resultant mixture, TEOS (cross-linker) was added, and the mixture was kept stirring. MPTS capped Mn doped ZnS QDs and 6% aqueous ammonia solution was added and finally the reaction mixture was stirred for 16 hr. The template was removed from QD-MIP (Quantum Dot-Molecularly Imprinted Polymer) through methanol: acetic acid mixture solvent several times.

The size of the nanocrystal was found to be in the range of 35-40 nm which was observed using transmission electron microscopy. Absorbance, excitation and band gap energy were derived using a UV-spectrophotometer. Fluorescence spectra of the QDs were obtained at an excitation and emission spectral wavelength of 330 and 590 nm, respectively. The interactions of the functional group of MPTS capped Mn:ZnS QDs and MIP modified QDs were performed using Fourier transformed infrared spectroscopy. The size of the crystal lattice of QD and QD-MIP was calculated as 10 and 13 nm respectively throughXRD.

The analytical assay of the proposed method was performed with respect to linearity, limit of detection (LOD), recovery and precision. The synthesized MIP-capped Mn-doped ZnS QDs for 3-PBA shows good linearity with R^2 value of 0.980 for sensing 3-PBA in the concentration range of 0.15-60 µM. The developed method was also validated in spiked urine samples and was found to be successful in sensing 3-PBA in urine. LOD for 3-PBA was found to be 0.117 µM. Recovery study of the developed method was found to be in the range of 80-90% at three different concentrations (1, 30 and 60 µM). Precision (inter and intra-day) study was also performed at three different concentrations (1, 30 and 60 µM) and was found to be less than 8%.

Publication

Vivek Pandey[a,b], Abhishek Chauhan[a,c], Gajanan Pandey[b] and Mohana Krishna Reddy Mudiam[a,c]*. Optical sensing of 3-phenoxybenzoic acid as a pyrethroid pesticides exposure marker by surface imprinting polymer capped on manganese-doped zinc sulphide quantum dots. (*Analytical Chemistry Research, 5, page no.21–27, 2015)*

6.1.3. Surface modification on manganese-doped zinc sulphide quantum dots by creating defects for the optical determination of methylmercury in river water samples

Mercury containing compounds are now days are a big rising threat for human beings. Mercury is proved to be a highly toxic element due to its accumulative and intact character in the environment. Both the inorganic (mercury salts) and organic forms (methyl mercury) of the mercury are very fatal. They are being generated from different industrial activities mainly pharmaceutical, paper, electrochemical and plaguacide industries. Various mercury species differ greatly in their biophysico-chemical properties; among them the methyl form is the most hazardous because of its volatility and its ability to pass through biological membranes such as the blood/brain barrier and the placenta. Accumulation of methyl mercury can cause kidney damage, irreversible central nervous system damage, paralysis, chromosome breakage and birth defects. Organic mercury i.e. methyl and ethyl forms reacts with sulfahydryl (–SH) functional groups of the body hence potentially interfering the cellular and sub-cellular structure.

In the present thesis modified QD was prepared by enriching the crystal lattice with sulphur. The resulting high sulphur containing material prepared was washed three to four times by water and ethanol. The size of the nanocrystal was observed in the range of 4-6 nm using transmission electron microscopy. Absorbance, excitation and band gap energy were derived using a spectrophotometer. Fluorescence spectra of

the QDs were obtained at an excitation and emission spectral wavelength of 330 and 590 nm. The crystal lattice of the synthesized QD was obtained in the size range of 8 - 9 nm. The size of the prepared material was also calculated by XRD. The analytical assay of the proposed method was performed with respect to linearity, limit of detection (LOD), recovery and precision. The synthesized surface modified Mn:ZnS QDs for methyl mercury shows good linearity with R^2 value of 0.99 for sensing methyl mercury in the concentration range of 0-25 µM. The developed method was also validated in spiked river water samples and was found to be successful in sensing the analyte in river water. LOD was found to be 0.097 µM. Recovery study of the developed method was found to be in the range of 90-95% at three different concentrations (5, 15 and 25 µM). Precision (inter and intra-day) study was also performed at three different concentrations (5, 15 and 25 µM) and was found to be less than 6%.

This material serves as an optical sensor to determine the presence of highly toxic analyte in river water and hence helps in checking the exposure of methyl mercury on human health.

6.1.4 Biocompatibility evaluation of synthesized L-cysteine capped Mn:ZnS quantum dots and its biomedical application in intracellular imaging

Cellular imaging using QDs proved the importance of fluorescent probe in cancer research. Tracing infections, their movement and localization by cellular imaging are key areas of QDs application in nanomedicine. Thus, QDs have a great potential in biotechnology and medical applications. The applicability of nanomaterials in biological environment needs a toxicity tests to be passed. The physico-chemical behaviour and cellular toxicity of nanocrystal QDs have wide dependence on the surface modification,

capping agents and size. Thus synthetic strategies and capping agents are two important aspects of obtaining non-toxic and biologically applicable QDs. Aqueous synthetic strategies have been extensively used for the synthesis of various material containing metals such as Zn, Cd and Hg as nanocrystals. Doping the QDs is a very important part of designing tailor-made material, as it increases the stokes-shift due to very small gap in its emission energy with respect to the host material. Thus, the doped semiconductor QDs has the enhanced optical performance than the undoped counterparts, because of their low background noise. L-cysteine has the greater potential, due to presence carboxylic and amino group, which can be used for further bioconjugation to other amino acids and proteins. Also, L-cysteine binds Zn strongly and hence may act as better capping agent from biocompatibility point of view. In the present work, for the first time, an attempt was made to employ green, room temperature, aqueous synthetic route to obtain Mn:ZnS QDs capped with L-cysteine having a high optical response. The choice of the capping agent is based on the versatility of L-cysteine and its water solubility *(Wang et al. 2011)*.

Synthesis of L-cysteine capped Mn:ZnS QDs was done to modify QDs. The size of the nanocrystal was observed using transmission electron microscopy. The Fourier transformed infrared spectroscopy (FTIR) characterization of L-cysteine capped Mn : ZnS QDs was performed . Human neuroblastoma cell line SH-SY5Y, used in the study were procured from National Centre for Cell Sciences, Pune, India and maintained at *in-vitro* toxicology laboratory, CSIR-Indian Institute of Toxicology Research, Lucknow, India, as per the standard protocols. Cytotoxicity assessment was done using standard endpoint, i.e., tetrazolium bromide MTT (3-(4, 5-dimethylthiazol-2-yl)-2, 5-diphenyl tetrazolium bromide) assay. The UV-visible absorption spectrum of synthesized QDs was recorded to prove the quantum confinement. The large blue shift is evident in the spectrum due to observance of onset at 310 nm with an edge at 285 nm. The large blue shift is in agreement with the small size of the nanocrystal. The photoluminescence

(PL) emission peak of Mn:ZnS QDs was observed at 590 nm, due to the well-known $^4T_1$-$^6A_1$ transition. The correlation of PL spectra with the UV visible spectra supports the strong quantum confinement which is in accordance with the band edge luminescence parameters. Binding of the L-cysteine capping agent with the Mn:ZnS QDs was confirmed by the FTIR spectra (Fig. 5) where strong affinity of the SH group of L-cysteine with the zinc ion of the ZnS was explored. Characteristic peak at 1500-1600 cm^{-1}, and at 1400 cm^{-1} correspond to the carboxyl group. The specific peak at 2550-2670 cm^{-1} represents the mercapto group of the L-cysteine. Comparing the IR spectra of QD capped with L-cysteine and spectra of L-cysteine powder, it was observed that the characteristic peak at 2550-2670 cm^{-1} found in L-cysteine was not observed in L-cysteine capped Mn:ZnS QDs hence the covalent interaction of zinc ion with the thiol group (SH) of the capping agent has shown to be involved. Adsorption of L-cysteine capping agent through covalent bond between Zn ion and SH group of L-cysteine is pH dependent as the thiol group deprotonated in alkaline pH. There is competition between sulphide and thiol to bind with Zn ion, which decides the stability of the QDs. Amount of capping agent that has been used in the reaction mixture is suitable for the formation of stable QDs.

The MTT assay has shown that the neuronal cells responded significantly to the L-cysteine capped Mn:ZnS QDs in a dose dependent manner. Cells exposed to QDs (0.1-1.5g/L) have shown no significant reduction in percent cell viability till 96 h. Whereas, higher concentrations of QDs i.e., 2 g/L was found to cause gradual reduction in percent cell viability. The dosing of Mn:ZnS QDs without capping with L-cysteine shows toxic behaviour and cell death was observed even at very low concentration of 0.1 g/L. Toxic

results were obtained for NRU assay of uncapped QDs similar to the MTT evaluation at the dosing level of 0.1g/L. To show the applicability of the QD in biological imaging, we have incubated cells with 0.2 g/L of L-Cysteine capped Mn:ZnS and found no agglomeration of nanoparticles outside the cell membrane. Fluorescence microscopic studies showed that incubation of the SH-SY5Y cells with QD gave a photoluminescence in the red region. The corresponding bright-field measurements after the exposure with QDs confirm that the photoluminescence was significant in the intracellular area, indicating the QD was internalized into the living cells from the growth medium. The study establishes the fact that the nucleation of nanoparticles requires only low temperature which resulted in non-toxic, small and homogenous Mn:ZnS QDs. L-cysteine as a capping agent has reduced the toxicity of Mn:ZnS to a larger extent. Further, this will enhance the bright imaging of cells with low background emissions due to internalization of large number of QDs. Further, L-cysteine improves the biocompatibility of Mn:Zns QDs and activates endocytotic uptaking of the particles.

Publication

Vivek Pandey, Gajanan Pandey, Vinay Kumar Tripathi,Sapna Yadav
and Mohana Krishna Reddy Mudiama,d,e* Nucleation temperature-controlled synthesis and in vitro toxicity evaluation of L-cysteine capped Mn:ZnS quantum dots for intracellular imaging. (Luminescence, Wiley (wileyonlinelibrary.com) DOI 10.1002/bio.2965, 2015).

6.1.5. Imidazole capped Mn doped ZnS quantum dots: Synthesis, Characterization and Biocompatibility evaluation at cellular and genetic level

Capping agents are essential part of Quantum dot (QDs) applications, as they not only control the growth of the particles but also make them able to get functionalized for various applications. Synthetic routes and further surface modifications of QDs are the key factors for preparing desired material. Extensive research is going on to use biomolecules as surfactant and capping agent. Nitrogen having lone pair is also a donor ligand thus it is in need to develop capping agents having nitrogen donor atom. The efficacy of capping agent has attracted considerable interest for applications in material science and in nanotechnology. New imidazole capped QDs are synthesized as it has major source of interest for chemist and for biologist as many compounds of industrial and technological importances are having imidazole or imidazole derivatives. Synthetic imidazoles are present in many anticancer, antifungal, anti-inflammatory medications.

In the present chapter, Mn doped ZnS QD is synthesized by employing aqueous route of synthesis. The imidazole is used as capping agent which do not alter the optical property or chemical structure of the synthesized material as evident by the through characterization by TEM, XRD and spectroscopy. The imidazole capped QD was further analysed and tested by toxicity parameters. As synthesized QD was undergone toxicity profiling at both cellular and genetic level. The toxicity studya at cellular and genetic level shows that uncapped QD very toxic as compared to imidazole capped QD.

Bibliography

BIBLIOGRAPHY

Acar HY., Kas R., Yurtsever E., Ozenandl C, Lieverwirth. J.Phys. Chem. C, 113,(2009) 10005-10012

Achermann M Petruska M. A., Crooker S. A,. Klimov VI. Picosecond energy transfer in quantum dot Langmuir Blotgett Nanoassemblies. J. Phys. Chem. B. 107 (2003) 13782-13787.

Adams SR Mason WT. Optical Probes for Cyclic AMP, Fluorescent and Luminescent Probes for Biological Activity, 2nd Ed. (1993) 133-149.

Agnarsson B, Halldorsson J, Arnfinnsdottir N, Ingthorsson S, Gudjonsson T, and Leosson K, Fabrication of planar polymer waveguides for evanescent-wave sensing in aqueous environments. Microelectronics Engineering. 87(1) (2010) 56-61.

Ahn K.C., Gee S.J., Kim H.J., Aronov P.A., Vega H., Krieger R.I., Hammock B.D. Immunochemical analysis of 3-phenoxybenzoic acid, a biomarker of forestry worker exposure to pyrethroid insecticides, Anal. Bioanal.Chem. 401 (2011) 1285 -1293.

Alam M. Z. Moreno J., Aitchison S., Mojahedi M. An integrated optic hydrogen sensor for fast detection of hydrogen, Proceedings of SPIE- the International Society for Optical Engineering. (2007) 6758-67580D.

Ali E. M., Y. Zheng, H.H. Yu, and J.Y. Ying. Ultrasensitive Pb2+ detection by glutathione-capped quantum-dots. Analytical

Chemistry. 79 (24) (2007) 9452-9458.

Alivisatos A. P, Johnsson K. P, Peng X, Wilson T. E, Loweth C. J, Bruchez Jr. M. P and Schultz P. G. Organisation of nanocrystal molecules using DNA. Nature. 382 (6592) (1996) 609-611.

Alivisatos A. P Johnsson K. P, Peng X, Wilson T. E, Loweth C. J, Bruchez M. Schultz P. G. Organization of'nanocrystal molecules' using DNA, Nature. 382 (1996) 609 -611.

Anna Dołe¸ga, Aleksander Farmas, Katarzyna Baranowska, Aleksander Herman. Inorganic Chemistry Communications. 12 (2009) 823–827.

Appleton D.W. And B.Sarkar**,** StudiesofZn(II)andCo(II) complexes of imidazole N-methylimidazole with regard to the activity related ionizatic carbonic anhydrase. Bioinorganic Chemistry, 7 (1977) 211-224.

Arrebola F.J., Gutierrez A.F., Akhtar M.H. Monitoring of pyrethorid metabolites in human urine using solid-phase extraction followed by gas chromatography-tandem mass spectrometry, Anal. Chim. Acta. 401 (1999) 45 - 54.

Arya H., Kaul Z., Wdahwa R., Taira K., Hirano T., Kaul SC. Biochem Biophys Res Quantum dots in bio-imaging, Revolution by the small Commun. 329 (2005) 1173-1177.

Aslan K., Wu M., Lakowicz J. R., Geddes C. D. Fluorescence core-shell Ag@SiO2 nanocomposites for metal-enhanced fluorescence and single nanoparticle sensing platforms. Journal of the

American Chemical Society. 129 (6) (2007) 1524-1525.

Bai H., Li C., Shi G. Rapid nitroaromatic compounds sensing based on oligopyrene. Sensors and Actuators, B.Chemical. 130 (2) (2008) 777-782.

Bain C. D., E. B. Troughton, Y.T. Tao, J. Evall, G. M. Whitesides, and R. G. Nuzzo. Formation of monolayer films by the spontaneous assembly of organic thiols from solution onto gold, Journal of the American Chemical Society. 111 (1) (1989) 321-335

Bakalova R., Zhelev Z., Aoki I., Masamoto K., Mileva M., Obata T., Higuchi M., Gadjeva V., Kanno I. Multimodal silica-shelled Quantum Dots: Direct Intracellular Delivery, Photosensitization, Toxic, and Microcirculation effects, Bioconjugate Chem. 19 (2008) 1135-1142.

Ballou B, lagerholm B. C, Ernst I. A, Bruchez M. P, and Waggoner A. S, Bioconguj Chem. 15(2004) 79-86.

Banerjee S. S., Chen D.H. A multifunctional magnetic nanocarrier bearing fluorescent dye for targeted drug delivery by enhanced two-photon triggered release. Nanotechnology 20(18) 2009.

Barbe V, Bartlett C. J., Kong L, Finnie K, Lin H.Q, Larkin M, Calleja S., Bush A., and Calleja G, Silica particles: A novel drug-delivery system. Advanced Materials. 16 (21) (2004) 1959-1966.

Basabe-Desmonts L. Reinhoudt D. N., Crego-Calama M. Design of fluorescent materials for chemical sensing. Chemical Society Reviews. 36

(6) (2007) 993-1017.

Basabe-Desmonts L., Beld J., Zimmerman R. S., Hernando J., Mela P., M. F., Garcia Parajo N. F., Van Hulst,A. Van Den Berg, Reinhoudt D. N., Crego-Calama M. A simple approach to sensor discovery and fabrication on self-assembled monolayers on glass. Journal of the American Chemical Society. 126 (23) (2004) 7293-7299.

Bawendi M.G., Carroll P.J., Wilson W.L., Brus L.E. J.Chem.Phys. 96 (1992) 946-954.

Bawendi M.G., Wilson W.L., Rothberg L., Carroll P.J., Jedju T.M., Steigerwald M.L., Brus L.E, Electronic structure and photoexcited- carrier dynamics in nanometer- size CdSe clusters. Phys.Rev.Lett., 65 (1990) 1623-1626.

Beck J. S., Vartuli J. C., Roth W. J., Leonowicz M. E., Kresge C. T., Schmitt,K. D. C. T., Chu W. A new family of mesoporous molecular sieves prepared with liquid crystal templates. Journal of the American Chemical Society. 114 (27) (1992) 10834-10843

Berger W., Prinz H., Striessnig J., Kang H.C., Haugland R., Glossmann H. Complex molecular mechanism for dihydropyridine binding to L-type Ca(2+)-channels as revealed by fluorescence resonance energy transfer. Biochemistry. 33 (1994) 1875-11883.

Berlin M., Zalups R. K., Fowler A. “Mercury,” in Handbook on the

Toxicology of Metals, G. F. Nordberg, B. A. Fowler, M. Nordberg, and L. T. Friberg, Eds., chapter 33, Elsevier, New York, NY, USA, 3rd edition, 2007`

Berry C. C., and A. S. G. Curtis, Functionalisation of magnetic nanoparticles for applications in bio-medicines. Journal of Physics D-Applied Physics. 36 (13) (2003) 198-206.

Bhargava R.N., Gallagher D., Hong X., Nurmikko A. Optical properties of manganese-doped nanocrystals of ZnS. Phys. Rev. Lett. 72 (1994) 416-419.

Blanco Gomis D., D. Muro Tamayo, and J. Mangas Alonso. Determination of monosaccharides in cider by reversed-phase liquid chromatography. Analytica Chimica Acta. 436 (1) (2001) 173-180.

Botsoa J., Lysenko V., Géloën A., Marty O., Bluet J.M., Guillot G. Appl. Phys. Lett. vol. 92 (2008) N°173902.

Bottrill M., Kwok L., and Long N. J. Lanthanides in magnetic resonance imaging. Chemical Society Reviews 35 (6) (2006) 557-571.

Botzung E. Appert, V. Monnier, T. H. Duong, R. Pansu, and A. Ibanez, Polyaromatic luminescent nonocrystals for chemical and biological sensors. Chemistry of Materials. 16 (9) (2004)1609-1611.

Bruce J. I., Dickins R. S., Govenlock L. J., Gunnlaugsson T., Lopinski S., Lowe M. P., Parker D. The selectivity of reversible oxy-anion

binding in aqueous solution at a chiral europium and terbium center: Signaling of carbonate chelation by changes in the form and circular polarization of luminescence emission. Journal of the American Chemical Society. 122 (40) (2000) 9674-9684.

Bruchez M., Moronne M., Gin P., Weiss S., Alivisatos A. P. Semiconductor nanocrystals as fluorescent biological labels. Science. 281 (5385) (1998) 2013-2016.

Bruchez M., Moronne M., Gin P., Weiss S., Alivisatos A.P. Semiconductor nanocrystals as fluorescent Biological labels Science 281 (1998) 2013- 2016.

Brus L.E. A simple model for the ionization potential, electron affinity, and aqueous redox potentials of small semiconductor crystallites J.Chem. Phys, 79, (1983) 5566-5571.

Buck S. M., Koo Y.E L., Park E., Xu H., Philbert M. A., Brasuel M. A., Kopelman R. Optochemical nanosensor PEBBLEs: Photonic explorers for bioanalysis with biologically localized embedding. Current Opinion in Chemical Biology. 8 (5) (2004) 540-546.

Bulte J. W. M., Kraitchman D. L. Iron oxide MR contrast agents for molecular and cellular imaging. NMR in Biomedicine. 17 (7) (2004) 484-499.

Burns A, Ow H, and Wiesner U, Fluorescent core-shell silica nanoparticles: Towards “lab on a particle” architectures for nanobiotechnology. Chemical Society Reviews. 35 (11) (2006)

1028-1042.

Burns A, , Sengupta P Zedayk T, Baird B, and Weisner U, Core/shell fluorescent silica nanoparticles for chemical sensing: Towards single-particle laboratories. Small 2 (6) (2006) 723-726.

Busse S., Scheumann V., Menges B., Mittler S. Sensitivity studies for specific binding reactions using the biotin/streptavidin system by evanescent optical methods. Biosensors and Bioelectronics. 17 (8) (2002) 704-710.

Cai Y., Shinar R., Zhou Z., ShinarJ., Multianalyte sensor array based on an organic light emitting diode platform. Sensors and Actuators, B: Chemical 134 (2) (2008) 727-735.

Caravan P. Stratergies for increasing the sensitivity of gadolinium based MRI contrasts agents. Chemical Society Reviews 35 (6) (2006) 512-523.

Cavaliere-Jaricot S., Darbandi M., Kucur E., Nann T. Silica coated quantum dots: A new tool for electrochemical and optical glucose detection. Microchimica Acta. 160 (3) (2008) 375-383.

Chan S., Li Y., Rothberg L. J., Miller B. L., Faucet P. M. Nanoscale silicon micro cavities for bio-sensing. Materials Science and Engineering C. 15 (1-2) (2001) 277-282.

Chan W. C., Nie S. Quantum dot bioconjugates for ultrasensitive nonisotopic detection. Science. 281 (5385) (1998) 2016-2018.

Chan W.C.W., Nie S.M. Qunatum dot bioconjugates for ultrasensitive

nonisotopic detection Science. 281 (1998) 2016-2018.

Chang J.C., Su H. L., Hsu Sh. Biomaterials 29 (2008) 925-936.

Chatterjee D. K., A. J. Rufaihah, and Y. Zhang, Upconversion fluorescence imaging of cells and small animals using lanthanide doped nanocrystals. Biomaterials. 29 (7) (2008) 937-9343.

Chen C. C., A.B. Herhold, C.S. Johnson, A.P. Alivisatos, Size dependence of structural metastability in semiconductor nanocrystals, Science 276 (1997) 398 – 401.

Chen J. L., Zhu C. Q. Functionalized cadmium sulfide quantum dots as fluorescence probe for silver ion determination. Analytica Chimica Acta. 543 (2) (2005) 147-153.

Chen L. T., Weiss L. The role of the sinus wall in the passage of erythrocytes through the spleen. Blood 41 (4) (1973) 529-537.

Chen W., Bovin J.O., Wang S., Joly A.G, Wang Y., Sherwood P. Fabrication and luminescence of ZnS: Mn2+ nanoflowers, J. Nanosci. Nanotech. 5 (2005) 1309 -1322.

Cho S. H., Godin J., Lo Y.H. Optofluidic waveguides in Teflon AF- coated PDMS microfluidic channels. IEEE Photonics Technology Letters. 21 (15) (2009) 1057-1059.

Choi J. H., Nguyen F. T., Barone P. W., Heller D. A., Moll A. E., Patel D., Boppart S.A., Strano M. S. Multimodal biomedical imaging with asymmetrical single-walled carbon nanotube/iron oxide nanoparticle complexes. Nano Letters. 7 (4) (2007b) 861-867.

Choi J., Burns A. A., Williams R. M., Zhou Z., Flesken-Nikitin A., Zipfel W. R., Wiesner U., Nikitin A. Y. Core-shell silica nanoparticles as fluorescent labels for nanomedicine. Journal of Biomedical Optics. 12 (6) (2007a) 064007.

Chu B, W.-K. and V. W.-W. Yam, Sensitive single-layered oxygen-sensing systems: Polypyridyl ruthenium(II) complexes covalently attached or deposited as Langmuir-blodgett monolayer on glass surfaces. Langmuir. 22 (17) (2006) 7437-7443.

Chuang J.C., Emon J.M.V., Trejo R.M., Durnford J. Biological monitoring of 3-phenoxybenzoiic acid in urine by an enzyme-linked immunosorbent assay, Talanta. 83 (2011) 1317 -1323.

Chun A. L. Lanthanide nanoparticles: Sensing danger. Nature Nanotechnology. 2008.

Chung S.W.C., Lam C.H. Development and validation of a method for determination of residues of 15 pyrethroids and two metabolites of dithiocarbamates in foods by ultra-performance liquid chromatography tandem mass spectrometry, Analy. Bioanal. Chem. 403 (2012) 885 -896.

Clegg R.M., Murchie A.I, Lilley D.M. The solution structure of the four-way DNA junction at low-salt conditions: a fluorescence resonance energy transfer analysis. J. Biophys. 66 (1994) 99-109.

Coe S., Woo W.K., Bawendi M.G., Bulovi V. Nature. 420 (2003) 800

Cole Parmer Inc. Available from http://www.coleparmer.com. Equipment

reference: EW-75955-71. Access date: 16/07/2012.

Coradin T., Boissiere M., Livage J. Sol-gel chemistry in medicinal science. Current Medicinal Chemistry. 13 (1) (2006) 99-108.

Corot C., K. G. Petry, R. Trivedi, A. Saleh, C. Jonkmanns, J.F Le Bas, E. Blezer, Macrophage imaging in central nervous system and in carotid atherosclerotic plaque using ultrasmall superparamagnetic iron oxide in magnetic resonance imaging. Investigative Radiology. 39 (10) (2004) 619-625.

Corpuscular Inc. Fluorescent SiO2 silica nanospheres and microspheres. Available from http://www.microspheres-nanospheres.com. Access date 16/07/2012.

Corrion E.M.O.J. M .L., D.M. Bielawski, N.C. Posecion Jr., J.J. Seagraves, Detection of prenatal exposure to several classes of environmental toxicants and their metabolites by gas chromatography-mass spectrometry in maternal and umbilical cord blood., J. Chromatogr. B. 82 (2005) 221 -229.

Costa-Fernandez J. M., Pereiro R., Sanz-Medel A. The use of luminescent quantum dots for optical sensing. TrAC-Trends in Analytical Chemistry. 25 (3) (2006) 207-218.

Courty S., Luccardini C., Bellaiche Y., Cappello G., Dahan M. Tracking individual kinesin motors in living cells using single quantum-dot imaging. Nano Letters. 6 (7) (2006) 1491-1495.

Craig P.J., Craig P.J. (Ed.), Organometallic Compounds in the

Environment, Principles and Reactions, Harlow, Longman, 1986, pp. 65–101.

Crouch D. J., P. O'Brien, M. A. Malik, P. J. Skabara, and S. P. Wright, A one step synthesis of cadmium selenide quantum dots from a novel single source precursor. Chemical Communications, 9 (12) (2003) 1454-1455.

Cui W., Fang C., Zhang Q., Zhuo F. Chronic toxicity and cytotoxicity of synthetic pyrethroid insecticide cis-bifenthrin, J. Environ. Sci. 21 (2009) 1710 -1715.

Dabbousi B. O, Rodriguez-Viejo J, Mikulec F. V, Heine J. R, H. Mattoussi, R. Ober, K. F. Jensen and M. G. Bawendi, (CdSe) ZnS Core-Shell Quantum dots : Synthesis and Charaterization of a size series of highly luminescent nanocrystallites. J. Phys. Chem. B 101 (1997) 9463-9475.

Dahan M., Laurence T. Time-gated biological imaging by use of colloidal quantum dots Optics Letter. 26 (2001) 825-827.

Dai Z, Bao J, Yang X, and Ju H. A bienzyme channeling glucose sensor with a wide concentration range based on co-entrapment of enzymes in SBA-15 mesopores. Biosensors and Bioelectronics. 23 (7) 20081070-1076.

Danek M., Jensen K. F., Murray C. B., Bawendi M.G. Electrospray organometallic chemical vapor deposition- A novel technique for preparation of II-VI quantum dot composites. Applied

Physics Letters 65 (22) (1994). 2795-2797.

Darawsheh M., Abu Ali H., Abuhijleh A., Rappocciolo E., Akkawi M., Jaber S., Maloul S., Hussein Y. Eur J Med Chem. 82 (2014) 152-163.

Dasary S. S. R., Rai U. S., Yu H., Anjaneyulu Y., Dubey M., Ray P. C. Gold nanoparticle based surface enhanced fluorescence for detection of organophosphorus agents. Chemical Physics Letters. 460 (1-3) (2008) 187-190.

Datta A, Biswas S, Kar S, Chaudhuri S, Multicolor luminescence from transition metal ion (Mn2+ and Cu2+) doped ZnS nanoparticles, J. Nanosci. Nanotechnol. 7 (2007) 3670-3676.

Dave B. C, Dunn B, Valentine J. S, and Zink J. L. Sol-gel encapsulation methods for biosensors. Analytical Chemistry. 66 (22) (1994) 1120A-1127A.

de Mel A, Oh JT., Ramesh B, Seifalian AM. Regen Med. (3) (2012) 335-47

De Saja, J. A. and M. L. Rodriguez- Mendez, Sensors based on double-decker rare earth phthalocyanines. Advances in Colloid and Interface Science 116 (1-3) (2005) 1-11.

Decher G., Fuzzy nanoassemblies: Toward layered polymetric multicomposites. Science. 277 (5330) (1997) 1232-1237.

Deng Y. H., W. L. Yang, C. C. Wang, and S. K. Fu, A novel approach for preparation of thermoresponsive polymer magnetic microspheres with core-shell structure. Advance Materials 15

(20) (2003) 1729.

Deng Y., Deng C., Yang D., Wang C., Fu S., Zhang X. Preparation, characterization and application of magnetic silica nanoparticle functionalized multi-walled carbon nanotubes. Chemical Communications. (44) (2005) 5548-5550.

Deng Z, Lie F.L, Shen S, Ghosh I, Mansuripur M, and Muscat A.J. Water-based route to ligand-selective synthesis of ZnSe and cd-doped ZnSe quantum dots with tunable ultraviolet A to blue photoluminescence. Langmuir 25 (1) (2009) 434-442

Derfus A. M, Chan W. C. W and Bhatia S. N. Probing the Cytotoxicity of Semiconductor Quantum Dots Nano Lett. 4 (2004) 11.

Derfus A. M Chan W. C. W, and Bhatia S. N. Intracellular delivery of quantum dots for live cell labeling and organelle tracking. Advanced Materials. 16 (12) (2004) 961-966.

Dey N. S. Rao M. E. B, Quantum Dot: Novel Carrier for Drug DeliveryInt. J. Res. Pharm. biomedical Sci. 2 (2011) 2229-3701.

Dick L. A McFarland A. D., Haynes C. L., Van Duyne R. P. Metal film over nanosphere (MFON) electrodes for surface-enhanced raman spectroscopy (SERS): Improvements in surface nanostructure stability and suppression of irreversible loss. Journal of Physical Chemistry B. 106 (4) (2002) 853-860.

Dickert F. L., Tortschanoff M., Bulst W. E., Fischerauer G. Molecularly imprinted sensor layers for the detection of polycyclic aromatic

hydrocarbons in water. Analytical Chemistry. 71 (20) (1999) 4559-4563.

Diltemiz S.E. Say R., Buyuktiryaki S., Hur D., Denizli A., Ersoz A. Quantum dot nanocrystals having guanosine imprinted nanoshell for DNA recognition. *Talanta.* 75 (2008) 890-896.

Diltemiz S.E.S.E.D., Rıdvan Saya B, Sibel Büyüktiryakib, Deniz Hüra, Adil Denizlic, Quantum dot nanocrystals having guanosine imprinted nanoshell for DNA recognition,Talanta. 75 (2008) 890 - 896.

Dimitrova V., Tate J. Synthesis and characterization of some ZnS-based thin film phosphors for electroluminescent device applications, Thin Solid Films. 365 (2000) 134 -138.

Dimitrova V., Tate J. Synthesis and characterization of some ZnS-based thin films phosphors for electroluminescent device applications Thin Solid Films. 365 (2000) 134-138.

Ding Y., White C.A., Muralidhara S., Bruckner J.V., Bartlett M.G. Determination of deltamethrin and its metabolite 3-phenoxybenzoic acid in male rat plasma by high-performance liquid chromatography, J. Chromatogr. B. 810 (2004) 221 -227.

Doering W. E., Nie S. Spectroscopic tags using dye-embedded nanoparticles and surface-enhanced raman scattering. Analytical Chemistry. 75 (22) (2003) 6171-6176

Dong Zhu, Wei Li, Li Ma and Yu Lei, Glutathione-functionalized Mn:ZnS/ZnO core/shell quantum dots as potential time-

resolved FRET bioprobes. RSC Adv. 4 (2014) 9372.

Dosev D., M. Nichkova, R. K. Dumas, S. J. Gee, B. D. Hammock, K. Liu, and I. M. Kennedy, Magnetic/luminescent core/shell particles synthesized by spray pyrolysis and their application in immunoassays with internal standard. Nanotechnology. 18(2007)055102.

Duan H., Nie S. Cell-Penetrating Quantum dots based on multivalent and endosome disrupting surface coatings. J Am Chem Soc. 129(11) (2007). 3333–3338.

Dubertret B, Skourides P, Norris D. J, Noireaux V, Brivanlou A. H. In Vivo Imaging of Quantum Dots Encapsulated in Phospholipid Micelles. Science 298 (2002) 1759-1762.

Dubertret B, Skourides P, Norris D. J, Noireaux V, Brivanlou A. H, Libchaber A, In Vivo imaging of Quantum dots encapsulated in Phospholipid micelles Science. 298 (2002) 1759-1762.

Efros A. L Interband absorption of light in semiconductor sphere. Sov. Phys. Semicond. 16 (1982) 772-775.

Ekimov A. I. and Onushchenko A. A. Size quantization of the electron energy spectrum in a microscopic semiconductor crystal. JETP Lett. 40 (1984) 1136-1139.

Elflein E.B.P. L., A. Preiss, M. Elend, K. Levsen, G. Wunsch, Human biomonitoring of pyrethrum and pyrethroids insecticides used indoors: determination of the metabolites E-cis/trans-

chrysanthemumdicarboxylic acid in human urine by gas chromatography-mass spectrometry with negative chemical ionozation, J. Chromatogr. B. 795 (2003) 195 -207.

Erogbogbo F., Yong K.T., Roy I. Xu, G. Prasad, P.N. Swihart, M.T. Biocompatible luminescent silicon quantum dots for imaging of cancer cells. ACS Nano. 2 (2008) 873-878

Erwin S.C., Zu L., Haftel M.I., Efros A.L., Kennedy T.A. Doping semiconductor nanocrystals. Nature. 436 (2005) 91-94.

Fan H. , Leve EW., Scullin C., Gabaldon J., Tallant D., S. Bunge S., Boyle T., Wilson MC. , Brinker CJ . Nano Lett. 5 (4) (2005) 645-648.

Förster T. Intermolecular Energy Migration and Fluorescence Ann. Phys 2 (1948) 55-75.

Frasco M., Chaniotakis N. Semiconductor Quantum Dots in Chemical Sensors and Biosensors. Sensors. 9 (2009) 7266-7286.

Gao D., Z. Wang, B. Liu, L. Ni, M. Wu, Z. Zhang, Amine-capped ZnS-Mn2+ nanocrystals for fluorescence detection of trace TNT explosive, Anal. Chem. 80 (2008) 8545-8553.

Gao X., Cui Y., Levenson R M., Chung L W. Nie S. In vivo cancer targeting and imaging with semiconductor quantum dots. Nat. Biotechnol. 22 (2004) 969-976.

Gaponik N., Talapin D.V., Rogach A.L., Hoppe K., Shevchenko E.V., Kornowski A. Eychmuller and H.Weller, Thiol- capping of CdTe

nanocrystals: An alternative to organometallic synthetic routes. J.Phys. Chem. B. 106 (2002) 7177-7185.

Gonzalez J.E., Tsien R.Y. Voltage sensing by fluorescence resonance energy transfer in single cells. Biophys J. 69 (1995) 1272-1280.

Hahn M.A., Keng P.C., Krauss T.D. Flow cytometric analysis to detect pathogens in bacterial cell mixtures using semiconductor quantum dots Anal. Chem. 80, (2008) 864 872

Hardman R Environ Health Perspect. 114(2) (2006)165-72

He C, Long Y, Pan J, Li K and Liu F. Application of molecularly imprinted polymer to solid phase extraction of analyte form real sample. J.Biochem.Biophys. Methods.70 (2007) 113-150

He CY, F Liu, K A Li and H W Liu. Molecularly imprinted polymer film grafted from porous silica for selective recognition of testosterone.Anal. Lett. 39 (2006) 275-286.

He Yu, He-Fang Wang, and Xiu-Ping Yan Exploring Mn doped ZnS quantum dots for the room temperature phosphorescence detection of enoxacin in biological fluids .Anal. Chem. 80 (2008) 3832–3837.

Hochachka P.W., Somero G.N. Biochemical adaptation: mechanisms and process in physiological evolution. New York: Oxford University Press. (2002) 466 p

Hoffman R., P. Held P. BioTek Application Note.

Hoppe K., Geidel E., Weller H. Eychmuller A. Covalently bound CdTe

nanocrystals Phys.Chem.Chem.Phys.4 (2002)1704-1706.

Horvat M. Mercury do we know enough? In L. Ebdon, L. Pitts, R. Cornelis, H. Crews, O. F. X. Donart, & P. Quevauviller (Eds.), Trace Element Speciation for Environment. (2001). (pp. 127–141). RSC, UK: Food and Health.

Hoshino A, Fujioka K, Oku T, Suga M, Sasaki Y. F, Physicochemical Properties and Cellular Toxicity of Nanocrystal Quantum Dots Depend on Their Surface Modification . Nano Lett. 4 (2004) 2163-2169.

Hossain Z and Huq F. Studies on the interaction between Cd(2+) ions and DNA. J. Inorg. Biochem. 90 (2002) 85-96.

Jaiswal J. K., Mattoussi H., Mauro J. M. Simon S. M. Long-term multiple color imaging of live cells using quantum dot bioconjugates. Nat. Biotechnol. 21 (2003) 47-51.

Jonsson T., Waldburger C.D., Sauer R.T. Nonlinear free energy relationships in Arc repressor unfolding imply the existence of unstable, native-like folding intermediates."Biochemistry. 35 (1996) 4795-4802.

Junxiao Liu., Chen Hui., Zhen Lin., Jin-Ming, Preparation of surface imprinting polymer capped Mn doped ZnS quantum dots and their application for chemiluminescence detection of 4-nitrophenol in tap water Anal Chem. 82 (2010) 7380-7386.

Kagan C R, Murray C B, Nirmal M and Bawendi M G. Electronic energy

transfer in CdSe quantum dot solids. Phys. Rev. Lett. 76 (1996) 1517-1520.

Kairdolf B.A., Mancini M.C, Smith A.M, Nie S, Minimizing nonspecific cellular binding of quantum dots with hydroxyl- derivatized surface coatings. Anal. Chem. 80 (2008) 3029-3034.

Kapoor E, Tripathi V, Kumar V, Juyal V, Bhagat S, Ram V (2014). Cyto-genotoxicity Assessment of Potential Anti-tubercular Drug Candidate Molecule-trans-cyclohexane-1, 4-diamine Derivative-9u in Human Lung Epithelial Cells A549. Toxicol Int. 21(1):69-77. doi: 10.4103/0971-6580.128800.

Kashyap MP, Singh AK, Kumar V, Tripathi VK, Srivastava RK, et al. (2011) Monocrotophos Induced Apoptosis in PC12 Cells: Role of Xenobiotic Metabolizing Cytochrome P450s. PLoS ONE 6(3): e17757. doi:10.1371/journal.pone.0017757.

Kashyap MP, Singh AK, Siddiqui MA, Kumar V, Tripathi VK, Khanna VK, Yadav S, Jain SK, Pant AB (2010). Caspase cascade regulated mitochondria mediated apoptosis in monocrotophos exposed PC12 cells. Chem Res Toxicol. 23(11):1663-72. doi: 10.1021/tx100234m.

Khanna P.L Ullman E.F., 4',5'-Dimethoxy-6-carboxyfluorescein: a novel dipole-dipole coupled fluorescence energy transfer acceptor useful for fluorescence immunoassays. Anal Biochem. 108 (1980) 156-161.

Kimata A — Kondo T, Ueyama J, Yamamoto K, Mochizuki A, Asai K, Takagi K, Okamura A, Wang D, Kamijima M. Relationship between urinary pesticide metabolites and pest control operation among occupational pesticide sprayers, J. Occup. Health. 51 (2009) 100 -105.

Klostranec J.M., — Chan W.C.W. Quantum dots in biomedical applications: advances and challenges . Adv. Matter. 18 (2006) 1953-1964.

Kumar V, — Tripathi VK, Jahan S, Agrawal M, Pandey A, Khanna VK, Pant AB (2015). Lead Intoxication Synergies of the Ethanol-Induced Toxic Responses in Neuronal Cells-PC12. MolNeurobiol. 52(3):1504-20. doi: 10.1007/s12035-014-8928-x.

Kuo Y.C — Wang Q, Ruengruglikit C, Yu H, Huang Q. Antibody-conjugated CdTe Quantum dots for Escherichia coli detection J. Phys. Chem. C. 112, (2008) 4818-4824.

Lee L.G., — Livak K.J., Mullah B., Graham R.J., Vinayak RS., Woudenberg T.M. Seven-color, homogeneous detection of six PCR products." Biotechniques. 27 (1999) 342-349.

Lee M.H., — Chen Y.C., Ho M.H., Lin H.Y. Composite QDs@ MIP nanospheres for specific recognition and direct fluorescent quantification of pesticides in aqueous media, Anal. Bioanal. Chem. 397 (2010) 1457-1466

Leon Shargel. — Comprehensive Pharmacy Review (6th ed.). p. 930

Lesnyak V., — Dubavik A., Plotnikov A., Gaponik N., Eychmuller A. One-step

aqueous synthesis of blue-emitting glutathione-capped $ZnSe_{1-x}Te_x$ alloyed nanocrystal Chem.Commun. 46 (2010) 886-888.

Lesnyak V., Gaponik N., Eychmuller A. Colloidal semiconductor nanocrystal: the aqueous approach Chem.Soc.Rev. 42 (2013) 2905-2929.

Lesnyak V., Gaponik N., Eychmuller A. Colloidal semiconductor nanocrystals: the aqueous approach.Chem. Soc. Rev, 42 (2013) 2905-2929.

Li F., Zhang Z., Peng J., Cui Z., Pang D. Small, Imaging Viral Behaviors in Mammalian Cells with Self-Assembled Capsid–Quantum-Dot Hybrid Particles. 5 (2009) 718-726.

Li H., Li Y., Cheng J. Molecularly imprinted silica nanospheres embedded CdSe quantum dots for highly selective and sensitive optosensing of pyrethroids,Chem. Mater. 22 (2010) 2451-2457.

Lin C.I., A.K. Joseph, C.K. Chang, Y. Der Lee, Molecularly imprinted polymeric film on semiconductor nanoparticles: analyte detection by quantum dot photoluminescence, J. Chromatogr. A 1027 (2004) 259 - 262

Liu J., Hui Chen., Zhen Lin., Jin-Ming Lin. Preparation of surface imprinting polymer capped Mn-doped ZnS quantum dots and their application for chemiluminescence detection of 4-nitrophenol in tap water, Anal. Chem. 82 (2010) 7380 - 7386.

Liu W., Howarth M., Greytak A.B. Zheng Y., Nocera D.G., Ting A.Y., Bawendi, M.G. Biocompatible quantum dots functionalized for cellular imaging CompactJ. Am. Chem. Soc, 130 (2008) 1274-1284.

Manahan S.E. Environmental Chemistry, sixth ed., Lewis Publishers, Ann Arbor, (1994) pp. 185.

Manuela Frasco F., Nikos Chaniotakis. Semiconductor Quantum dots in chemical sensors and biosensors Sensors, 9 (2009) 7266-7286.

Matayoshi ED., GT. Wang, GA. Krafft, J. Erickson, Novel fluorogenic substrates for assaying retroviral proteases by resonance energy transfer." Science. 247 (1990) 954-958

Michalet X., Pinaud F.F., Bentolila L.A., Tsay J.M., Doose S., Li, G. Sundaresan, Wu A.M., Gambhir S.S., Weiss S. Quantum dots for Live cells, in vivo imaging and diagnostics *Science.* 307 (2005) 538-544.

Moritz M.G., Piotrowska H., Murias M., Balan L., Moritz M., Lulek J. Thioglycerol-capped Mn-doped ZnS quantum dot bioconjugates as efficient two-photon fluorescent nano-probes for bioimaging. J. Mater. Chem. B. 1(2013) 698-706.

Morton J., Carolan V.A., Gardiner J.P.H.E. The speciation of inorganic and methylmercury in human hair by high-performance liquid chromatography coupled with inductively coupled plasma mass spectrometry, J. Anal. Atom. Spectrom. 17 (2002) 377.

Mosbach K.., Arshady R. Synthesis of substrate-selective polymers by host-guest polymerization. *Macromole. Chem. Phy.* 182 (1981) 687-692.

Myakishev M.V., Khripin Y., Hu S., Hamer D.H. High-throughput SNP genotyping by allele-specific PCR with universal energy-transfer-labeled primers. Genome Res 11 (2001) 163-169.

Nichols J.W., Pagano RE. Resonance energy transfer assay of protein-mediated lipid transfer between vesicles. J Biol Chem. 258 (1983) 5368-5371.

Norris D J., A L. Efros and S C. Erwin, Doped nanocrystals. Science 319 (2008) 1776-1779.

Pan B, Cui D, Gao F, He R. Nanotechnology.17(10) (2006) 2483-2489.

Pandey G., Dixit S. Growth mechanism and optical properties determination of CdS Nanostructure . *J. Phys. Chem. C* 115 (2011) 17633-17642.

Pandey V., Chauhan A., Pandey G., Mudiam MKR. Optical sensing of 3-phenoxybenzoic acid as a pyrethroid pesticides exposure marker by surface imprinting polymer capped on manganese-doped zinc sulfide quantum dots Analytical Chemistry Research. 5 (2015) 21-27.

Pandey V., Pandey G., Tripathi V.K., Yadav S., Mudiam M.K.R. Nucleation temperature controlled synthesis and in vitro toxicity evaluation

of L-cysteine capped Mn:ZnS quantum dots for intracellular imaging doi:10.1002/bio.2965

Parkhurst K.M., Parkhurst L.J. Kinetic studies by fluorescence resonance energy transfer employing a double-labeled oligonucleotide: hybridization to the oligonucleotide complement and to single-stranded DNA. Biochemistry. 34 (1995) 285-292.

Parsons P.J., Barbosa F. Atomic spectrometry and trends in clinical laboratory medicine, Spectrochim. Acta 62 (2007) 992

Peng Wu, Ting Zhao, Yunfei Tian, Lan Wu, and Xiandeng Hou Chem. Eur. J. 19 (2013) 7473 – 7479

Peng Wu., He Yu, Fang Wang He., Xiu-Ping yan. Anal, Chem. (2010) 1427-1433.

Peng Wu., Xiu-Ping Yan. Chem Soc Rev. 42(12) (2013) 5489-521.

Peng X., Manna L.,Yang W., Wickham J., Scher E., Kadavanich A., Alivisatos A.P. Shape control of CdSe nanocrystals, Nature. 404 (2000) 59 -61.

Perry MJ, Barr DB, Xu X, Environmental pyrethroid and organophosphorus insecticide exposures and sperm concentration, Reprod. Toxicol. 23 (2007) 113 -118.

Pinaud F., Michalet X, Bentolila L. A., Tsay J. M., Doose S. Advances in fluorescence imaging with quantum dot bio-probes. Biomaterials 27 (2006) 1679-1687.

Prakash S., Rao S., Dameron C. Cadmium inhibit BPDE alkylation of DNA

in the major groove but not in the minor groove. Biochem. Biophys. Res. Commun.244 (1998) 198-203.

Przybytkowski E., M. Behrendt, D. Dubois and D. Maysinger Nanoparticles can induce changes in the intracellular metabolism of lipids without compromising cellular viability. FEBS Journal 276 (2009) 6204-6217.

Rajh T., Micic O.L., Nozik A.J. Synthesis and characterization of surface –modified colloidal cadmium telluride quantum dots J.Phys.Chem. 97 (1993)11999-12003.

Rapsomanikis S., Craig P.J. Anal. Chim. Acta. 248 (1991) 563–567.

Reisset P. "Low polydispersity core/shell nanocrystals of CdSe/ZnSe and CdSe/ZnSe/ZnS type: preparation and optical studies." Synthetic Metals. (2003) 649-652.

Rikans L.E., Yamano T. Mechanisms of cadmium-mediated acute hepatotoxicity. J. Biochem. Mol. Toxcol. 14 (2000) 110-117.

Rizvi S.B., Ghaderi S., Keshtgar M., Seifalian A.M. Semiconductor quantum dots as fluorescent probes for in vitro and in vivo bio-molecular and cellular imaging. Nano Reviews.Nano Reviews. 1 (2010) 5161-5176

Rodrigues J.L., de Souza S.S., de Oliveira Souza V.C., Barbosa Jr F. Methylmercury and inorganic mercury determination in blood by using liquid chromatography with inductively coupled plasma mass spectrometry and a fast sample preparation

procedure, Talanta. 80 (2010) 1158

Rogach A. L, Katsikas L, Kornowski A, Su D. A. Eychmuller and H. Weller, Ber. Bunsen-Ges. Synthesis and Characterization of Thiol-stabilized CdTe Nanocrystal Phys. Chem. 100 (1996) 1772-1778.

Romeo N., Cozzi S., Tedeschi R., Bosio A., Canevari V., Tagliente M.A., Penza M. High quality ZnS: Mn thin films grown by quasi-rheotaxy for electroluminescent devices, Thin Solid Films 348 (1999) 49 -55.

Rosen A. B, Kelly D.J, Schuldt A. J. T, Lu J, Potapova I. A. Finding Fluorescent Needles in the Cardiac Haystack: Tracking Human Mesenchymal Stem Cells Labeled with Quantum Dots for Quantitative In Vivo Three-Dimensional Fluorescence Analysis Stem Cells, 25 (2007) 2128-2138.

Rossetti R., Ellison J.L., Gibson J.M., Brus L.E. Size effects in the excited electronic states of small colloidal CdS crystallites. J. Chem. Phys.80 (1984) 4464-4469.

Rossetti R., Nakahara S., Brus L.E. Quantum size effects in the redox potentials, resonance raman spectra and electronic spectra of CdS crystallites in aqueous solution. J. Chem. Phys.79 (1983) 1086-1088.

Sanchez Uria J.E., Sanz-Mendel A. Inorganic and methylmercury speciation in environmental samples Talanta. 47 (1998) 509–524.

Sapra S., Nanda J., Anand A., Bhat S.V., Sarma D.D. Optical and magnetic properties of manganese-doped zinc sulfide nanoclusters, J. Nanosci. Nanotechnol. 3 (2003) 392 -400.

Schettgen K.H., Drexler T., Angerer H. New gas chromatographic-mass spectrometric method for the determination of urinary pyrethroid metabolites in environmental medicine, J. Chromatogr. B 778 (2002) 121 -131.

Sellergren B, Direct Drug Determination by Selective Sample Enrichment on an Imprinted Polymer Anal. Chem. 66 (1994) 1578 -1582.

Sellergren B, Direct drug determination by selective sample enrichment on an imprinted polymer. *Anal. Chem.* 66 (1994) 1578–1582.

Shan G1H.H., Stoutamire DW, Gee SJ, Leng G, Hammock BD, A sensitive class specific immunoassay for the detection of pyrethroid metabolites in human urine, Chem. Res. Toxicol. 17 (2004) 218 -225.

Shindo H., Brown T. L. Infrared Spectra of complexes of L-Cysteine and related compounds with Zinc, Cadmium, Mercury, Lead .J. Am. Chem. Soc. 87 (1965) 1904-1909.

Shiohara A, Hoshino A, Hanaki K, Suzukiand K and Yamamoto K. On the cyto-toxicity caused by quantum dots. Microbial. Immunol. 48 (2004) 669-675.

Siddiqui M. A., Singh G., Kashyap M.P., Khanna V.K., Yadav S. Influence of cytotoxic doses of 4-hydroxynonenal on selected

neurotransmitter receptors in PC-12 cells. Toxicol. in Vitro. 22 (2008) 1681-1688.

Smith A. M, Duan H, Mohs A. M and Nie S, Bioconjugated quantum dot for in vivo molecular and cellular imaging Adv. Drug. Deliv. Rev. 60 (2008) 1226-1240.

Souza S.S., Rodrigues J.L., Oliveira Souza V.C., Barbosa F. A fast sample preparation procedure for mercury speciation in hair samples by high-performance liquid chromatography coupled to ICP-MS, J. Anal. Atom. Spectrom. 25 (2010) 79.

Steitz B, Axmann Y., Hofmann H., Pe tri-Fink, A. Optical properties of annealed Mn^{2+}-doped ZnS nanoparticles J. Lumin.128 (2008) 92–98.

Stohs S.J., Bagchi D. Oxidative mechanisms in the toxicity of metal ions. Free Radical Biol.Med.18 (1995) 321-336.

Sun B, Liu K Han J, Zhao L. Y, Su X., Lin B. Zhao D.M., and Cheng M.S. Bio org Med Chem. 23(20) (2015) 6763-73.

Tripathi V. K., Kumar V., Singh A K., Kashyap M P., Jahan S. Monocrotophos induces the expression and activity of xenobiotic metabolizing enzymes in pre-sensitized cultured human brain cells.PLoS One. 9 (2014) e91946.

Tripathi VK, Kumar V, Singh AK, Kashyap MP, Jahan S, et al. (2014) Monocrotophos Induces the Expression and Activity of Xenobiotic Metabolizing Enzymes in Pre-Sensitized Cultured

Human Brain Cells. PLoS ONE 9(3): e91946. doi:10.1371/journal.pone.0091946.

Tsien R. Ann. Review Biochem, 67 (1998) 509-544.

Tu R., Liu B., Wang Z., Gao D., Wang F., Fang Q., Zhang Z. Amine-capped ZnS-Mn2+ nanocrystals for fluorescence detection of trace TNT explosive, Anal. Chem. 80 (2008) 3458 -3465.

Ueyama J., Kimata A., Kamijima M., Hamajima N., Ito Y., Suzuki K., Inoue T., Yamamoto K., Takagi K., Saito I. Urinary excretion of 3-phenoxybenzoic acid in middle-aged and elderly general population of Japan, Environ. Res. 109 (2009) 175-180.

Uster PS. In situ resonance energy transfer microscopy: monitoring membrane fusion in living cells. Methods Enzymol. 221 (1993) 239-246.

Wang C., X. Gao, X. Su, In vitro and in vivo imaging with quantum dots . Anal. Bioanal. Chem. 397 (2010) 1397-1415.

Wang H.F., He Y., Ji T.R., Yan X.P. Surface molecular imprinting on Mn-doped ZnS quantum dots for room-temperature phosphorescence optosensing of pentachlorophenol in water, Anal. Chem. 81 (2009) 1615 -1621

Wang Q., Ye F., Liu P., Min X. Li X. Conjugation and fluorescence quenching between bovine serum albumin and L-cysteine capped CdSe/CdS quantum dots. Protein Pept. Lett. 18 (2011) 410-414.

Wang R, Chemistry. (2015) doi: 10.1002/chem.201503105.

Wang Y, and Chen L. Quantum dots, lighting up the research and development of nanomedicine. Nanomedicine. 7 (2011) 385-402.

Watson B.S., TL. Hazlett, J.F. Eccleston, C. Davis, DM. Jameson, AE. Johnson. Macromolecular arrangement in the aminoacyl-tRNA.elongation factor Tu.GTP ternary complex. A fluorescence energy transfer study. Biochemistry. 34 (1995) 7904-7912

Wu P., Yan XP. Chem Soc Rev. 42(12) (2013) 5489-521

Wu X. Y., Liu J. H., Liu J. Q., Haley K. N, Treadway J. A. Immunofluorescent labeling of cancer marker Her2 and other cellular targets with semiconductor quantum dots. Nat. Biotechnol. 21(2003) 41-46.

Wulff G., Sarhan A. The use of polymers with enzyme analogous structures for the resolution of racemates. *Angew. Chem. Int. Ed.* 11 (1972) 341-344.

Xia Y, Yang P, Sun Y, Wu Y, Mayers B, Gates B, Yin Y, Kim F, Yan H, One dimensional nanostructures: synthesis, characterization, and applications, Adv. Matter. 15 (2003) 353 - 389.

Yan Y, Chen O, Angerhoferand A, Cao Y C, Radial –Position – Controlled Doping in CdS/ZnS Core/Shell Nanocrystals J. Am.

Chem. Soc. 128 (2006) 12428-12429.

Yang H.H, Zang S Q, Tan F, Zhuang Z. X., Wang X. R. Surface molecularly imprinted nanowires for biorecognition. J.Am.Chem.Soc. 127 (2005) 1378-1379

Yang P., Zhou G. Phase transfer of hydrophobic QDs for water-soluble and biocompatible nature through silanization. Mater Res Bull. 46(12) (2011) 2367–72.

Yezhelyev V., Al-Hajj A., Morris C., MarcusA.I., Liu T. In Situ Molecular Profiling of Breast Cancer Biomarkers with Multicolor Quantum Dots Adv. Matter.19 (2007) 3146-3151.

Zhang H., Wang D., Mohwald H. Angew. Chem.Int.Ed. 45 (2006) 748-751.

Zhang K. Ai., Lu L. Europium-based fluorescence nanoparticle sensor for rapid and ultrasensitive detection of an anthrax biomarker. Angewandte Chemie-International Edition. 48 (2) (2009) 304-308.

Zhang W., He X.W., Chen Y., Li W.Y., Zhang Y.K. Molecularly imprinted polymer anchored on the surface of denatured bovine serum albumin modified CdTe quantum dots as fluorescent artificial receptor for recognition of target protein, Biosens. Bioelectron. 31 (2012) 84-89.

Zhao D., Z. He, W.H. Chan and M.M. F. Chi, Synthesis and Characterization of high quality water soluble near infrared-

emitting CdTe/CdS Quantum dots capped by N-acetyl-L-cysteine via hydrothermal method. J.Phys.Chem.C, 113 (2009) 1293-1300

Zhao Y, Ma Y, Li H, Wang L, Composite QDs@ MIP nanospheres for specific recognition and direct fluorescent quantification of pesticides in aqueous media, Anal. Chemistry. 84 (2012) 386-395.

Zhu L., Ang S., Liu W T. Quantum dots as a novel immunofluorescent detection system for Cryptosporidium parvum and Giardia lamblia. Appl. Environ. Microbiol. 70 (2004) 597-598.

Zhuang J., Zhang X., Wang G., Li D., Yang W., Wensheng Yang., Li T.J. Matter. Chem. 13 (2003) 1953–1857.

Zigalinski R., BeverlyA., Jeannine Strobl S. "Cadmium-containing nanoparticles: Perspectives on pharmacology and toxicology of quantum dots." Toxicology and Applied Pharmocology. (2009) 280-288.

List of Publications

List of Publications

1. **Vivek Pandey**, Gajanan Pandey Vinay Kumar Tripathi Sapna Yadav and Mohana Krishna Reddy Mudiam*. Nucleation temperature-controlled synthesis and in vitro toxicity evaluation of L-cysteine capped Mn:ZnS quantum dots for intracellular imaging. (*Luminescence, Wiley, DOI 10.1002/bio.2965, 2015).*

2. **Vivek Pandey**, Abhishek Chauhan, Gajanan Pandey and Mohana Krishna Reddy Mudiam*. Optical sensing of 3-phenoxybenzoic acid as a pyrethroid pesticides exposure marker by surface imprinting polymer capped on manganese-doped zinc sulphide quantum dots. (*Analytical Chemistry Research, 5, page no.21–27, 2015)*

3. **Vivek Pandey**, Vinay Kumar Tripathi, Gajanan Pandey, Inho Hwang and Mohana Krishna Reddy Mudiam* A new Imidazole capped Mn doped ZnS quantum dots: Synthesis, Characterization and Biocompatibility evaluation at cellular and genetic level (Under Communication)

4. Tejasvi Bhatia ,Abhishek Chauhan, Manoj K Gupta, Pathya Pandey, **Vivek Pandey**, Prem N Saxena, Mohana Krishna Reddy Mudiam*. Imprinted nanospheres based on precipitation polymerization for the simultaneous extraction of six urinary benzene metabolites from urine followed by injector port silylation and gas chromatography-tandem mass spectrometric analysis. (Journal of Chromatography B, 2015 Sep 15; 1001:66-74. doi: 10.1016/j.jchromb.2015.07.027.)

5. Rajeev Jain, Manoj Kumar Gupta, Abhishek Chauhan, **Vivek Pandey**, Mohana Krishna Reddy Mudiam*, Ultrasound assisted DLLME followed by GC-MS/MS analysis for the determination of valproic acid in urine samples .(Bioanalysis, 2015, Future Science Group)

CONFERENCES

1) Optical Determination of Methyl Mercury A Highly Profound Toxic Analyte By Surface modification on Manganese-Doped Zinc Sulphide Quantum Dots **Vivek Pandey**, Gajanan Pandey and Mohana Krishna Reddy Mudiam. International Conference on Biochemistry, Nutrition and Pharmacy, Hyderabad, September 3-5, 2015. **(Awarded Best Oral Presentation)**

2) Luminiscence sensing study of 3-phenoxy benzoic acid in urine through surface imprinting polymer capped ZnS:Mn quantum dots **Vivek Pandey**, M.K.R Mudiam and Gajanan Pandey, *National Conference on Recent Trends in Environmental Science***,** Gwalior, February, 2014. (Oral Presentation)

3) Biochemical analysis in serum of rat after acute oral exposure to ZnO nanoparticles, fabricated in aqueous phase **Vivek Pandey** and Gajanan Pandey *International Symposium on Drug Development for Orphan/Neglected Diseases*, Lucknow, February, 2013. (Poster Presentation)